Scheduling and Power Allocation in Full-Duplex Wireless Networks

Hassan Fawaz

SAINT JOSEPH UNIVERSITY OF BEIRUT
FACULTY OF ENGINEERING

This dissertation is submitted in partial fulfillment of the requirements for the degree of
Doctor of Philosophy

Hassan Fawaz

Scheduling and Power Allocation in Full-Duplex Wireless Networks

Defended on the 13th of November 2019

Joumana Farah *Lebanese University, Lebanon*	**Jury President**
Zaher Dawi *American University of Beirut, Lebanon*	**Reviewer**
Xavier Lagrange *IMT Atlantique, France*	**Reviewer**
Sanaa Sharafeddine *Lebanese American University, Lebanon*	**Jury Member**
Jad Nasreddine *Rafik Hariri University, Lebanon*	**Jury Member**
Samer Lahoud *ESIB, Saint Joseph University of Beirut, Lebanon*	**Supervisor**
Melhem El Helou *ESIB, Saint Joseph University of Beirut, Lebanon*	**Co-Supervisor**
Marc Ibrahim *ESIB, Saint Joseph University of Beirut, Lebanon*	**Co-Supervisor**

N° d'ordre 32

To my loving parents . . .

Declaration

I hereby declare that except where specific reference is made to the work of others, the contents of this dissertation are original and have not been submitted in whole or in part for consideration for any other degree or qualification in this, or any other university. This dissertation is my own work and contains nothing which is the outcome of work done in collaboration with others, except as specified in the text. This dissertation contains about 190 pages including appendices, bibliography, footnotes, tables and equations and has fewer than 70 figures.

Thesis by: Hassan Fawaz
Defended on the 13^{th} of November, 2019

Acknowledgements

I would like to start by acknowledging the National Council for Scientific Research of Lebanon (CNRS-L) for awarding me a doctoral fellowship, as well as the Research Council at Saint Joseph University of Beirut for granting me a doctoral scholarship. Without their support, my work on this dissertation would not have been possible.

I am profoundly grateful to my thesis supervisor Dr. Samer Lahoud for his continuous support of my Ph.D. study and research, for his patience, motivation, enthusiasm, continuous encouragements, as well as immense contributions to my work. His guidance helped me all the time in my research and in the writing of this dissertation as well. His ability to efficiently conduct research in countless areas like networking, wireless communications, IoT systems, and others continues to astonish me. He saw the possible reaches of full-duplex wireless communications and presented the idea on which my thesis was based. I would like to thank him for ever so generously giving me the most valuable resource, time.

My heartfelt thanks go to my thesis co-supervisor Dr. Melhem El Helou for his help, encouragement, and both technical and moral support. Ever the optimist, his immense contributions were necessary for the success of my work on this thesis. The code guru in our small team, he never hesitated to help me with even the smallest details.

My sincere thanks to Dr. Marc Ibrahim for all his contributions to my research. His valuable and constructive proposals helped improve the quality of my work. As head of the CIMTI laboratory at ESIB-USJ, he spared no resources assisting me and my fellow Ph.D. students with our work.

I am grateful to all of those with whom I had the pleasure to work during the past years, especially Dr. Kinda Khawam. She helped me venture into new domains all the while providing continuous support.

I would like to extend my sincere thanks to all the members of the CIMTI laboratory, professors, staff, and doctoral students alike. In addition to their assistance, comments, and critiques of my work, their daily presence around the halls made CIMTI feel like home. I would especially like to thank Youssef El Bakouny with whom I've shared a cubicle for the past three years. He was my first friend at ESIB and has always been there for me for both

moral and technical support. Many thanks to Joanna, Hussein, Karen and the rest of the crew!

Finally, I would love to express my profound gratitude to my family. My loving mom and dad, my brothers, and my sister for their continuous support and endless encouragements throughout.

Abstract

With over 5.7 billion global mobile users, and an excess of 12 billion mobile-ready devices expected by the year 2022 [1], the availability of reliable and fast wireless connectivity is more necessary than ever before. Today, in order to satisfy the need for bidirectional wireless communications, networks implement either time division duplexing (TDD) or frequency division duplexing (FDD). In TDD, the transmitted and received signals at a wireless device are sent on the same frequency but at different times. In FDD, the transmitted and received signals at a wireless device are sent at the same time but on different frequencies. This separation, whether in the time or the frequency domain, has always been deemed necessary. If a wireless device were to transmit and receive, at the same time and on the same radio resource $i.e.$, operate in full-duplex, the transmitted signal–which is typically multiple times stronger at the device–would interfere on the signal being received making its proper reception and decoding infeasible. This is known as self-interference. For decades of wireless communications, it was believed to be a permanent obstacle in the face of full-duplex wireless transmissions.

At the turn of the decade, self-interference cancellation (SIC) technologies came into effect. SIC defines a set of analog and digital cancellation techniques that enable the mitigation of self-interference at a full-duplex node. The existence and continuous development of these technologies have made full-duplex wireless communications possible. With the capability of simultaneously transmitting and receiving on the same radio resources, a theoretical doubling of the bandwidth efficiency can be achieved. This could count for more connected users and higher connection speeds.

Nonetheless, self-interference is not the only interference problem facing full-duplex wireless communications. With users utilizing the same radio resources within the same cell, intra-cell co-channel interference becomes a serious issue. Co-channel interference defines the interference from a transmitting user on a receiving one using the same radio resource. In order to mitigate this interference, it is up to the scheduler to ensure that the users operating on the same radio resources interfere the least upon each other.

In our work, we consider a wireless network comprised of a full-duplex base station and half-duplex user equipment (UEs). We assume that such a separation of full-duplex

capabilities is necessary as to not burden the UEs with the power exhaustive task of self-interference cancellation. In this network scenario, the base station will allocate the available resources to *pairs* of uplink-downlink UEs. As such, on an allocated radio resource, one UE will be transmitting, one UE will be receiving and the base station–being the full-duplex node–will be concurrently transmitting and receiving. In such a network, self-interference is exhibited at the base station and it degrades the performance of uplink UEs. Intra-cell co-channel interference is experienced at downlink UEs, who are interfered upon by their paired uplink UEs.

Our work in this thesis is focused on devising scheduling and power allocation algorithms for full-duplex wireless networks. Starting with the scheduling task, we devise a global optimal formulation for scheduling in full-duplex and hybrid full-duplex/half-duplex wireless networks. We vary the objective of the global problem to obtain both greedy and fair scheduling algorithms. Furthermore, to avoid the added complexities of optimization, we propose heuristic algorithms with the same objectives. We show that these algorithms can achieve near optimal results, and that lucrative gains are possible with respect to current half-duplex wireless networks.

In order to properly assess the effects of intra-cell co-channel interference, full-duplex networks need information on the channel states in between all the UEs in a network. Inter-UE channel state information (CSI) is a new requirement for full-duplex wireless networks. No current wireless protocols count for the estimation or relaying of such information. As such, in our work we study the effects of incomplete CSI on the performance of full-duplex networks. We show that significant losses in performance could occur as a result. In order to circumvent the necessity of inter-UE CSI, we propose a reinforcement learning based scheduling algorithm for full-duplex wireless networks. This algorithm learns how to best allocate the resources, relying only on traditional feedback from the UEs to the base station. We show that our algorithm can match the performance of scheduling with complete CSI.

Moving on to the power allocation task, we present both centralized and distributed power allocation approaches. For the centralized approach, we propose a joint scheduling and power allocation algorithm aimed at improving UE radio conditions whilst maintaining fairness in the network. For the distributed approach, we propose a set of game theoretic based algorithms with varying objectives aimed at improving UE SINR values and curbing the network interferences. Via simulations, we comment on the importance, as well as limitations, of implementing power allocation algorithms alongside scheduling in full-duplex wireless networks.

Finally, in the context of multi-cellular networks, we study the impact on inter-cell interferences on the performances of full-duplex wireless networks, and discuss the importance

of cell cooperation on extracting gains from such networks. We consider both indoor and outdoor deployment scenarios and show via simulations that the gains from full-duplex wireless communications in multi-cellular networks are tied to the inter-cell interference mitigation provided by the deployment scenario.

Résumé

Avec plus de 5,7 milliards d'utilisateurs mobiles dans le monde et plus de 12 milliards de terminaux connectés d'ici 2022 [1], le besoin d'une connectivité sans-fil fiable et rapide est plus que jamais nécessaire. Aujourd'hui, pour répondre au besoin des communications sans-fil bidirectionnelles, les réseaux mettent en œuvre soit le duplexage par répartition en temps (TDD) ou le duplexage par répartition en fréquence (FDD). Dans le TDD, les signaux transmis et reçus par un terminal sans-fil sont envoyés sur la même fréquence mais à des instants différents. Dans le FDD, les signaux émis et reçus par un terminal sans-fil sont envoyés en même temps, mais sur des fréquences différentes. Cette séparation, que ce soit dans le domaine temporel ou fréquentiel, a toujours été jugée nécessaire. Si un terminal sans-fil devait émettre et recevoir, en même temps et sur la même ressource radio, c'est-à-dire fonctionner en full-duplex, le signal transmis, qui est généralement plusieurs fois plus fort sur le terminal, interférerait sur le signal reçu, ce qui rendrait sa réception et son décodage irréalisables. C'est ce qu'on appelle l'auto-interférence, et pendant des décennies de communications sans-fil, on a cru que c'était un obstacle permanent face aux communications sans-fil full-duplex.

Au tournant de la décennie, les technologies d'annulation d'auto-interférence (SIC) sont entrées en vigueur. SIC définit un ensemble de techniques d'annulation analogiques et numériques qui permettent d'atténuer l'auto-interférence au niveau d'un équipement full-duplex. L'existence et le développement continu de ces technologies ont rendu possible les communications sans-fil full-duplex. Avec la capacité d'émettre et de recevoir simultanément sur les mêmes ressources radio, un doublement théorique de l'efficacité spectrale peut être atteint. Cela pourrait impliquer un plus grand nombre d'utilisateurs connectés et à des débits de connexion plus élevés.

Néanmoins, l'auto-interférence n'est pas le seul problème d'interférence auquel font face les communications sans-fil full-duplex. Avec deux utilisateurs utilisant les mêmes ressources radio dans la même cellule, l'interférence co-canal intra-cellulaire devient un problème grave. L'interférence co-canal définit le brouillage causé par un utilisateur émetteur sur un utilisateur récepteur utilisant la même ressource radio. Il n'y a pas d'aspects technologiques

au traitement de l'interférence co-canal intra-cellulaire. C'est à l'ordonnanceur de s'assurer que les utilisateurs opérant sur les mêmes ressources radio s'interfèrent le moins possible entre eux.

Dans notre travail, nous considérons un réseau sans-fil composé d'une station de base full-duplex et de terminaux half-duplex. Nous partons du principe qu'une telle séparation des capacités full-duplex est nécessaire afin de ne pas imposer aux terminaux la tâche fastidieuse de l'annulation de l'auto-interférence. Dans ce scénario de réseau, la station de base allouera les ressources disponibles à des paires des terminaux mobiles (User Equipment en anglais, UE) de liaison montante et descendante. Ainsi, sur une ressource radio attribuée, un terminal émettra, un autre recevra et la station de base étant le nœud full-duplex, émettra et recevra simultanément. Dans un tel réseau, l'auto-interférence se manifeste à la station de base et dégrade la performance des terminaux de liaison montante dans le réseau. L'interférence co-canal intra-cellulaire est subie par les terminaux de liaison descendante, qui sont perturbés par les terminaux appariés de liaison montante.

Notre travail dans cette thèse s'est concentré sur la conception d'algorithmes d'ordonnancement et d'allocation de puissance pour les réseaux sans-fil full-duplex. En commençant par la tâche de d'ordonnancement, nous avons mis au point une formulation globale optimale pour la l'allocation des ressources dans les réseaux sans-fil full-duplex et hybrides half-duplex/full-duplex. Nous varions l'objectif de la formulation globale pour obtenir des algorithmes à la fois gloutons et équitables. De plus, pour éviter les complexités supplémentaires de l'optimisation, nous proposons des algorithmes heuristiques avec les mêmes objectifs. Nous montrons que ces algorithmes permettent d'obtenir des résultats quasi optimaux et que des gains substantiels peuvent être réalisés par rapport aux réseaux sans-fil half-duplex actuels.

Afin d'évaluer correctement les effets de l'interférence co-canal intra-cellulaire, les réseaux full-duplex ont besoin d'informations sur les gains des canaux entre tous les terminaux d'un réseau. L'information des gains des canaux inter-UE (Channel State Information CSI, en anglais) est une nouvelle exigence pour les réseaux sans-fil. Aucun protocole sans-fil actuel ne s'intéresse à l'estimation ou le relayage de ces informations. Ainsi, dans notre travail, nous étudions les effets de l'estimation imparfaite du canal sur la performance des réseaux full-duplex. Nous montrons qu'il pourrait en résulter une perte de performance importante. Afin de contourner la nécessité d'estimer le canal entre UE, nous avons proposé un algorithme d'ordonnancement basé sur l'apprentissage par renforcement pour les réseaux sans-fil full-duplex. Cet algorithme apprend comment allouer au mieux les ressources, en se basant uniquement sur les rapports de mesures classiques des terminaux à la station de base. Nous montrons que notre algorithme peut égaler la performance de l'ordonnancement avec une estimation parfaite du canal.

En ce qui concerne la tâche d'allocation de puissance, nous proposons des approches à la fois centralisées et distribuées d'allocation de puissance. Pour l'approche centralisée, nous avons proposé un algorithme conjoint d'ordonnancement et d'allocation de puissance visant à améliorer les conditions radio de l'UE tout en maintenant l'équité dans le réseau. Pour l'approche distribuée, nous avons proposé un ensemble d'algorithmes basés sur la théorie des jeux avec différents objectifs visant à améliorer les valeurs du SINR de l'UE et à réduire les interférences. Grâce à des simulations exhaustives, nous commentons l'importance, ainsi que les limites, de la mise en œuvre d'algorithmes d'allocation de puissance parallèlement à l'ordonnancement dans les réseaux sans-fil full-duplex.

Enfin, dans le contexte des réseaux multicellulaires, nous étudions l'impact des interférences intercellulaires sur les gains des réseaux sans-fil full-duplex et nous discutons de l'importance de la coordination cellulaire pour exploiter au mieux ces réseaux. Nous examinons des scénarios de déploiement à l'intérieur et à l'extérieur et montrons à l'aide de simulations que les avantages des scénarios multicellulaires full-duplex sont liés à l'atténuation de l'interférence intercellulaire fournie par le scénario de déploiement.

Contents

List of Figures

List of Tables

Nomenclature

Acronyms / Abbreviations

802.11ad Wireless Gigabit

AMPS Advanced Mobile Phone System

BS Base Station

CDMA Code-Division Multiple Access

CSI Channel State Information

DECT Digital Enhanced Cordless Telecommunications

DL Downlink

EDGE Enhanced Data Rate for GSM Evolution

EVDO Evolution-Data Optimized

FBMC Filter Bank Multi-Carrier

FDD Frequency Division Duplexing

FDMA Frequency Division Multiple Access

FD Full-Duplex

FPC Fractional Power Control

GPRS General Packet Radio Services

GSM Global System for Mobile Communications

HD Half-Duplex

HetNet Heterogeneous Networks

HSU/DPA High Speed Uplink/Downlink Packet Access

IEEE Institute of Electrical and Electronics Engineers

ILP Integer Linear Programming

IWF Iterative Water Filling

KKT Karush-Kuhn-Tucker

LNA Low Noise Amplifier

LTE – A Long Term Evolution Advanced

LTE Long-Term Evolution

Max SE Maximum Spectral Efficiency

Max SR Maximum Sum-Rate

Max TP Maximum Throughput

MCS Modulation and Coding Scheme

MIMO Massive Input Massive Output

MINLP Mixed Integer Non-Linear Programming

MOOP Multi-Objective Optimization

MS Max-SINR

NE Nash Equilibrium

NOMA Non-Orthogonal Multiple Access

NP Non-Polynomial

OFDMA Orthogonal Frequency Division Multiple Access

OFDM Orthogonal Frequency Division Multiplexing

PA Power Amplifier

PF Proportional Fair

RB Resource Block

RF Radio Frequency

RR Round Robin

RSI Residual Self-Interference

SE Spectral Efficiency

SIC Self-Interference Cancellation

SINR Signal-to-noise and Interference Ratio

SR Sum-Rate

TDD Time Division Duplexing

TDMA Time Division Multiple Access

TP Throughput

TTI Transmission Time Interval

UE User Equipment

UL Uplink

UMTS Universal Mobile Telecommunication Systems

WiMax Worldwide Interoperability for Microwave Access

Chapter 1

Introduction

1.1 The State of Wireless Communications

The proliferation of wireless devices is at an unprecedented level. Whether it is our mobile phones, laptops, or any other smart device, the need for better, faster, and reliable wireless connectivity is more pressing than ever before. With close to 13 billion mobile devices, along an estimated 77 exabytes of monthly mobile traffic by the year 2022 [1], the technology is barely able to keep up. For users, the failure of the infrastructure to keep abreast with the demand results in lost connectivity on a mobile device, or a weak signal in a crowded area. Symptoms of the problems that face wireless transmissions.

Wireless communications face two main challenges as they continue to evolve: signal attenuation and generated interferences. Due to the nature of the wireless medium, any transmitted signal will face rapid attenuation, making the distance between the transmitter and the receiver an important factor. Additionally, all wireless devices share the same medium and use a finite and limited set of radio resources. This means that wireless devices are always in contention for this medium, and the inevitable sharing of the available resources will lead to signal interference. The increasing need for capacity leads to frequency reuse and the densification of network deployment, adding thus to the inherit interference problems.

The troubles for wireless communications only increase once you consider the necessity for bidirectional communications. Any wireless device needs to transmit and receive in order to function properly. This is known as duplexing. Nonetheless, if two communicating wireless devices were to use the same radio resource at the same time to communicate, the generated interference would make it impossible for any signal to be properly received. As a result, two major mechanisms currently exist to allow duplexing [2]:

1. Time Division Duplexing or *TDD*, consists of separating the transmitted and received signals in the time domain. The latter is broken down into transmission time intervals (TTIs), and the two communicating devices take turns transmitting and receiving. With the devices not transmitting at the same time, naturally no interference would be generated. Technologies such as DECT [3] and IEEE 802.116 WiMax [4] implement TDD.

2. Frequency Division Duplexing or *FDD*, means that the nodes at either side of a communication link will use different frequencies to send and receive data. This will prevent the signals from interfering upon each other, even if the two devices are transmitting at the same time. Cellular systems such as GSM [5], CDMA2000 [6], and WiMax as well implement FDD.

In a TDD transmission, a wireless node is–at a certain instant in time–either transmitting or receiving. In an FDD transmission, twice the amount of radio resources is required in order to allow the nodes to transmit and receive within the same time frame. In either case, the wireless communication is said to be *half-duplex*, even if it attempts to emulate what is known as *full-duplex* communications.

A full-duplex node is one that can transmit and receive on the same radio resource, at the same time. Setting aside all the problems and limitations of both TDD and FDD, the aspect of full-duplex communications alone promises a doubling in the capacity of wireless networks. But no current wireless device is actually full-duplex. ***Why?*** Until quite recently the term "Full-Duplex Wireless" was considered to be an oxymoron.

1.2 The Problem With Wireless Full-Duplex

Queue the most quoted phrase in wireless networks literature, but Andrea Goldsmith's characterization of full-duplex wireless communications in her 2005 Cambridge Press book really captures the essence of the scientific consensus back then. Goldsmith wrote "It is generally not possible for radios to receive and transmit on the same frequency band because of the interference that results" [7]. Goldsmith then argued that separating uplink and downlink channels into orthogonal signaling dimensions, whether in the time domain like TDD, or in the frequency domain like FDD, was in fact the only way to support bidirectional communications.

Goldsmith was not technically wrong. Consider the network model we used in our work and illustrated in Fig. 1.1 below. In this scenario, the base station (BS) is considered to be the full-duplex node. The user equipment (UEs) are half-duplex *i.e.,* at a certain moment

they are either transmitting or receiving. During the same time frame, one uplink UE will use the same radio resource as one downlink UE. We say that these two UEs are paired on the resource. Being the full-duplex node, the BS concurrently transmits and receives on this same radio resource. This network will exhibit two major added interferences with respect to current half-duplex wireless networks:

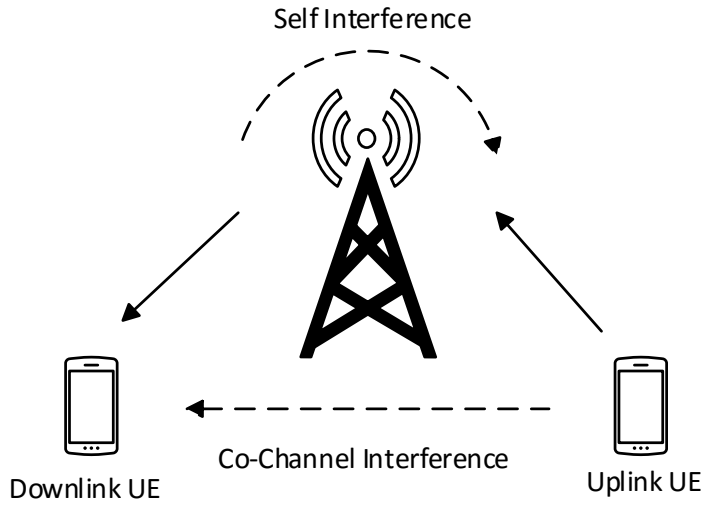

Figure 1.1 Full-duplex network model and interferences

1. Self-interference: It is the interference exhibited at a full-duplex node, where the transmitted signal on a certain radio resource is multiple times stronger than the signal being received on that same resource. The latter cannot be properly received as a result. In the aforementioned scenario, self-interference degrades the performance of UEs on the uplink.

2. Intra-cell co-channel interference: It is the interference resulting from two UEs using the same radio resources within the same cell. The signal from an uplink UE, typically several time stronger, interferes on the signal being received by a nearby downlink UE using the same radio resource. This causes a degradation in the performance of the latter.

These interferences are duplicated if the UEs are considered to be full-duplex as well. With half-duplex wireless networks already suffering from interference problems, it is evident why it was widely believed that these added interferences would simply make full-duplex communications impossible. Nonetheless, like always, technological advancement inevitably catches up with every thing once deemed impossible. For full-duplex wireless technologies, the introduction of self-interference cancellation (SIC) techniques for wireless devices at the beginning of this decade was a turning point.

1.3 Self-interference Cancellation

As the name itself suggests, SIC technologies allow a wireless node to cancel the self-interference generated due to full-duplex operations. Interference cancellation is not a new concept. It is rooted in the idea that if a node knows the signal it is transmitting, it can subtract it from the received signal and decode the remainder. However, the stronger the interference the harder this task gets. Strong self-interference would cause the analog to digital converter at the receiver to saturate. The latter would scale its quantization levels to match that of the self-interference. Since it has a finite resolution (up to 12 bits), the converter thus has a finite number of quantization levels. The weaker the information signal is with respect to the interference, the less of it remains retrievable after digitization. Digital components are not the only ones susceptible to saturation. Strong self-interference can also cause analog amplifiers to function improperly. As such, a set of analog and digital interference cancellation techniques are needed to properly receive and decode a signal at a full-duplex node [8, 9]:

1. Digital Cancellation: Provided that a full-duplex node has a good estimation of the transmitted signal (amplitude and phase), digital samples of this signal are passed through a self-interference channel model to create a digital signal of the interference. The latter is thereafter subtracted from the received digital signal. Digital cancellation can still be rendered useless in the case of very strong self-interference. As previously discussed, saturation of the analog to digital converter could make the useful signal unrecoverable.

2. Analog Cancellation: These cancellation techniques aim to cancel the interference from the radio frequency (RF) signal before it is digitized. They require knowledge of the transmitted RF signal to do so. Among popular analog cancellation techniques is phase offset. Phase offset uses the constructive and destructive interference patterns resulting from multi-path transmissions to reduce self-interference. The transmission from a signal node is split into two paths. One path is offset from the other by an odd multiple of half the carrier wavelength. This causes the two signals to add destructively at the receiver, reducing thus the self-interference. One way to implement cancellation using phase offset is to have multiple antennas with controlled placement and transmission powers. Other analog cancellation methods use vector modulation and signal inversion to minimize self-interference. These techniques are illustrated in Table 1.1.

As digital cancellation techniques are limited and vulnerable to the saturation of the analog to digital converter, a dual digital-analog cancellation process is necessary for full-duplex

functionality. The received signal goes first through an RF or analog cancellation process that aims to bring the interference down enough for the remaining digital architecture to take care of. This process is illustrated in Fig. 1.2. In order to prevent receiver saturation, the interfering signal must be sufficiently canceled in analog before it hits the low-noise amplifier (LNA).

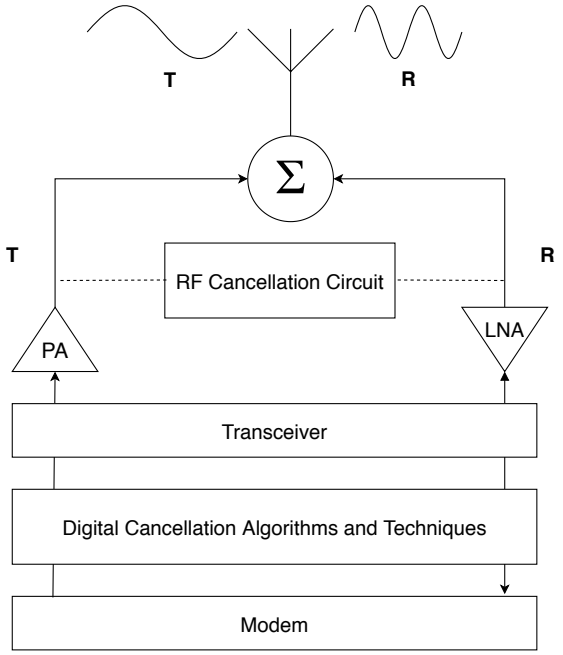

Figure 1.2 Self-interference cancellation: a set of analog and digital techniques

Table 1.1 Analog self-interference cancellation techniques

Technique	**Limitations**	**Summary**
Phase Offset	Cancels up to 60.7 dB, suitable for narrowband signals only (< 5 MHz).	Uses multiple antennas to create a multi-path effect aimed at canceling out the interference signal.
Vector Modulation	Cancels up to 36 dB, susceptible to saturation problems.	An interference signal sample is input to a vector modulator to adjust the phase and gain of the sample. This creates a cancellation signal that can remove the ambient interference from the input signal.
Signal Inversion	Bandwidth dependable, suitable for wideband signals.	Obtain an exact inverse of the transmitted signal and subtract it from the received signal.

In [10], the authors present a complete survey of SIC techniques from which we highlight the SIC requirements per mobile generation seen in Table 1.2 below.

Table 1.2 Full-duplex SIC requirements by generation

Generation	Technolgies	Frequency Range	Required SIC
1G	AMPS, FDMA	30 Khz	189 dB
2G	GSM, TDMA	200 kHz, 1.25 MHz	157-161 dB
2.5G	GPRS, EDGE	200 Khz	160 dB
3G	UMTS, CDMA	5 Mhz, 1.25 Mhz	150-156 dB
3.5G	HSU/DPA, EVDO	5 Mhz, 1.25 Mhz	50-156 dB
3.75G	Fixed WiMAX, LTE	10 Mhz, 20 Mhz	147-150 dB
4G	Mobile WiMAX, LTE-A	10 Mhz, 20 Mhz	147-150 dB
5G	802.11ad, FBMC	2 GHz, 60 Ghz	101-118 dB

The table mentions some of the technologies per each generation, the frequencies they operate on and consequently, the required SIC value. In the context of 5G technologies and beyond, 101-118 dB of interference cancellation is required. This is well accomplished with the available technology. Nonetheless, the efficacy of these technologies will always be tied to several factors from the transmit power at the full-duplex node, to the frequency in use, as well as the quality of the digital and analog cancellation circuits. As such, it is not realistic to assume that ideal cancellation exists. Residual self-interference post cancellation will still affect the performance of a full-duplex wireless network.

1.4 Scheduling and Power Allocation

The presence of SIC techniques, now well developed in the state-of-the-art, partially enables dealing with one ramification of full-duplex communications, self-interference. Nonetheless, this is not sufficient. Full-duplex networks must still deal with intra-cell co-channel interference as well as residual self-interference.

Radio resource management (RRM), encompassing both scheduling and power allocation, is necessary to extract gains from full-duplex wireless communications. Scheduling indicates how the network's available radio resources would be distributed to the UEs. In order to minimize intra-cell co-channel interference, UEs using the same radio resources should be sufficiently far apart from each other. Furthermore, power allocation can also help battle the network interferences. For instance, consider the network scenario illustrated in Fig. 1.1, lowering the transmit power from the BS to an adjacent downlink UE, while raising it from an uplink UE situated further away–and using the same radio resource–could significantly enhance user performance. Self-interference would be reduced with the decrease in the BS

transmit power, and co-channel interference would be decreased as a result of the distance between the two UEs.

Scheduling in wireless networks is a decades old problem. Countless algorithms exist in the state-of-the-art for scheduling in half-duplex wireless networks. These algorithms mostly revolve around traditional scheduling ideas. Max-SINR scheduling [11] seeks to allocate resources to UEs with the best radio conditions. This maximizes the system throughput and thus increases the operator's profits. However, this method of scheduling could cause bandwidth starvation for UEs at the boundaries of a cell. Their relatively poor radio conditions would see them deprived of any resources. Other scheduling techniques, such as Round Robin [12], would allocate radio resources to UEs in turn regardless of any other factor. Round Robin achieves total equity between the UEs at the cost of decreasing the system's throughput. The bandwidth is thus rendered inefficiently used. As a trade off between contradictory objectives, Proportional Fair [13] seeks to maximize UE throughput while at the same time ensuring a minimum level of service to UEs with poor radio conditions. It does so by allocating resources following a user priority function that factors in a UE's current and historic throughput capabilities.

Due to the added full-duplex interferences, both scheduling and power allocation play a vital role in enhancing the performance of a full-duplex wireless network. Current half-duplex radio resource and power allocation schemes benefit from orthogonal downlink and uplink channels which can be optimized independently. In contrast, in the context of full-duplex wireless communications, the optimization of scheduling and power allocation has to be done jointly for the uplink and the downlink because of the shared radio resources. Consequently, it is not possible to apply any traditional half-duplex scheduling or power allocation algorithms to full-duplex networks in a straightforward manner.

In our work, we build on the present SIC techniques to propose scheduling and power allocation algorithms for full-duplex and hybrid full-duplex/half-duplex wireless networks. The latter encompasses the allocation of radio resources to either a pair of UEs (full-duplex), or to a single UE (half-duplex) depending on which better improves the network's performance. Via a set of different proposals, which cover variant techniques and tools from optimization to machine learning and game theory, we aim to evaluate as well as maximize the possible gains of full-duplex wireless communications.

1.5 Our Contributions

With our work being focused around scheduling and power allocation specifically, we sought out the existent literature on full-duplex wireless networks. From there we set out our main

objectives with focus on filling the gaps in the state-of-the-art where necessary. In what follows we highlight the main contributions illustrated in this dissertation.

1. Global Optimal Scheduling Problems: First, we propose a global mathematical problem for scheduling in both full-duplex and hybrid wireless networks. The objectives of these global problems can be changed to yield different scheduling proposals with different goals. The traffic model used in our proposals is non-full buffer and accounts for dynamic arrivals. This makes our model rather unique with respect to the state-of-the-art.

2. Heuristic Scheduling Algorithms: Following the possible intractability of optimization problems when it comes to a high number of variables, we propose heuristic alternatives for the optimal scheduling problems. We show that our proposals decrease the complexity of the algorithms whilst incurring insignificant losses in UE throughput. Using these algorithms, we study the performance of full-duplex wireless networks under different SIC capabilities and in various scheduling scenarios ranging from UE clustering to heterogeneous traffic.

3. Incomplete Channel State Information: This dissertation includes a comprehensive study on the effect of incomplete channel state information (CSI) on the performance of a full-duplex wireless network. Scheduling in a full-duplex scenario introduces the notion of user-to-user radio channels. As illustrated in Fig. 1.1, and detailed later on, knowledge of this channel is essential in estimating the resulting co-channel interference between a pair of UEs. Nonetheless, no current wireless network protocol counts for estimating user-to-user channels or for how to relay such information back to the BS. In our work, we study the consequences of scheduling with partial to no knowledge of such inter-UE channels on UE and network performances.

4. Reinforcement Learning Scheduling: Based on our analysis of scheduling in full-duplex networks with incomplete CSI, we sought to propose a scheduling algorithm capable of functioning without this information. To this end, we employ a subclass of machine learning, known as reinforcement learning, to devise a scheduling algorithm capable of learning how to best allocate radio resources. We show that this algorithm is capable of mimicking the performance of scheduling with complete CSI, and that it incurs minimal loss in performance in comparison.

5. Optimal Power Allocation: Similar to our approach to scheduling, we propose a global optimal problem for power allocation in a full-duplex wireless network. This problem is aimed at enhancing user radio conditions whilst maintaining a sense of equity

between the UEs. We show that our proposal saves on power and that it improves UE performance in the case of low SIC capabilities. This approach is centralized $i.e.$, a central unit–in this case the BS–is responsible for taking the power allocation decision on both the uplink and the downlink.

6. Game Theory Based Power Allocation: With the aim of deviating from the centralized approach to power allocation, we use game theoretics to devise a distributed power allocation algorithm. We propose multiple non-cooperative games and afterwards compare how they fare against each other in different scheduling scenarios, illustrating the pros and cons of each one. In this distributed approach, no central authority or added signaling between the players is required to allocate power on the radio resources.

7. Scheduling in Multi-Cellular Full-duplex Networks: We study the performance of full-duplex wireless networks in a multi-cell scenario. We consider both indoor and outdoor deployments and illustrate how interference from neighboring cells affects the performance of the UEs. We highlight the importance of cell cooperation when it comes scheduling resources as it can aid in combating the full-duplex interferences. Finally, we propose a joint scheduling and power allocation algorithm for multi-cellular full-duplex wireless networks. We assume single cell scheduling and coordinated multi-cell power allocation. We subsequently show the gains and limitations of power allocation in a multi-cell setting.

1.6 Thesis Outline

The remainder of this thesis is organized as follows. Chapter 2 has the latest research in regards to scheduling and power allocation in full-duplex wireless networks. In it we present the relevant works and indicate how our approaches to radio resource management differ from those present in the state-of-the-art. Chapter 3 introduces our global mathematical problems for scheduling in full-duplex and hybrid full-duplex/half-duplex wireless networks. In that chapter, we introduce both greedy and fair approaches to scheduling with the assumption that complete CSI is available to the scheduler. In Chapter 4, the assumption of complete CSI is questioned. The performance of our scheduling algorithms in the absence of inter-UE channel information is studied as a result. Furthermore, a reinforcement learning approach to scheduling, one that does not need knowledge on inter-UE channel states, is introduced. We show that our proposal can match scheduling with complete CSI and that it provides good performances under different scheduling scenarios.

Chapter 5 and Chapter 6 have our proposals for power allocation in single-cell full-duplex wireless networks. In Chapter 5, we present a centralized approach to power allocation coupled with a fairness oriented scheduler. We show that our proposal can improve UE performance while saving on power expenditure. In Chapter 6, we present a distributed approach to power allocation. Our proposal is based in a game theoretic context. We put forward multiple super-modular games wherein the BS and the uplink UEs are considered to be competing selfish (non-cooperative) players. We study the efficiency of our approaches in different scheduling scenarios and show the pros and cons of each.

In Chapter 7, we study scheduling in a multi-cell environment. We introduce an algorithm for joint scheduling and power allocation in multi-cell full-duplex wireless networks. We highlight how the full-duplex interferences multiply and show that the gains from full-duplex wireless communications will be tied to the deployment scenario. In addition, we study the importance of cooperation between cells in regards to maximizing achievable performances.

Finally, we conclude this thesis and present some axes to be developed in future works in Chapter 8.

Chapter 2

The State-of-the-Art for Full-Duplex Wireless

2.1 Introduction

In this chapter, we give a general overview of where the state-of-the-art is at for full-duplex wireless communications. We classify the latter into three categories. The first deals with the development and progress of self-interference cancellation (SIC) techniques. It was essential for these technologies to be well established before researchers went any further with their work on full-duplex technologies. The second category encompasses early works in the domain which sought either to suggest different possible full-duplex scenarios, or merely to validate that gains could be extracted from full-duplex communications. The third category in the state-of-the-art, to which our work practically belongs, builds on the previous two to propose and simulate scheduling and power allocation algorithms for full-duplex wireless networks.

2.2 Self-Interference Cancellation Technologies

It was important for SIC technologies to be well developed and tested before any other work was done on full-duplex wireless. After all, the development of these technologies is what made full-duplex wireless communications feasible in the first place.

The authors in [14] were among the first to discuss the direct impacts of developed SIC techniques on full-duplex communications. They state that these technologies invalidate long-held assumptions regarding wireless network design, and they overview what would be required of interference cancellation techniques in order to propel full-duplex wireless

communications into reality. In one of the earliest works on in-band full-duplex for wireless networks, the authors in [15] survey a range of SIC techniques and touch on the main challenges facing full-duplex wireless networks. The articles in [16] and [17] aimed to evaluate the performance of self-interference in the context of full-duplex wireless communications. The authors in [16] conclude that the SIC performance increases as the signal bandwidth decreases, while those in [17] focus on the impact of amplitude and phase errors on the efficiency of interference cancellation technologies.

Furthermore, as we keep up with the state-of-the-art in terms of the progress of these technologies, the articles in [18–20] track the latest developments in the domain of interference cancellation. The authors in [18] propose a new analog SIC technique for single antenna in band full-duplex systems. They show that their model can cancel 40 dB of interference over a 35 MHz frequency bandwidth. They claim that it is enough to avoid the saturation of the analog to digital converter. The authors in [19] go into practical applications of interference cancellation and present a patch antenna model with a simple two-tap RF/analog domain-based SIC. Importantly, they attest that wideband SIC performance can be achieved. Finally, the authors in [20] design and implement a neural network aided SIC scheme for full-duplex radio. They verify via simulations that they can achieve good performance results with a computation complexity lower than that of existent technologies.

In the context of this dissertation, we are mostly concerned by the level of SIC provided by the current technology. In one of the most important papers in the domain of interference cancellation techniques, Bharadia *et all*. (2013) [21] demonstrate that 110 dB of self-interference can be canceled at a transmitter of 25 dBm power. We consider this to be a benchmark for our work, although it is safe to assume that the technology has evolved far beyond this mark.

2.3 Introduction to Full-Duplex Wireless Networks

After a consensus was reached on the viability of SIC techniques and on the role that these technologies could play in making full-duplex communications feasible, research in the domain pivoted towards exploring what full-duplex wireless networks would look like, and whether impediments other than self-interference would hinder extracting gains from full-duplex wireless communications.

The works in [22–25] revolve around assessing the possible gains of full-duplex wireless networks. Their authors study different implementations of full-duplex systems alongside the limitations and obstacles facing them.

Aiming towards full-duplex inclusion in upcoming 5G [1] protocols, the authors in [22] propose a full-duplex module with which they simulate two types of full-duplex networks: one where only the base station (BS) is full-duplex capable, and the other where both the user equipment (UEs) and the BS are full-duplex capable. Their aim was to assess the performance of full-duplex wireless communications in ultra-dense small cells. They conclude that more gains can be extracted when all the nodes in the network are full-duplex capable.

In [23], different scenarios and implementations of possible full-duplex wireless networks are discussed. Mainly, the authors present four representative scenarios: full-duplex MIMO networks, full-duplex cooperative networks, full-duplex OFDMA cellular networks, and full-duplex heterogeneous networks. The authors use resource management problems for the purpose of validating wireless full-duplex communications.

With a more practical approach, the papers in [24, 25] introduce more realistic models for full-duplex transmissions. In [24], the authors put forward a compact full-duplex receiver. With it at hand, they demonstrate via numerical evaluations the capacity gains of full-duplex communications, and they bring insights onto the impact of SIC techniques on the performance of full-duplex wireless networks. In [25], the authors present a single-channel full-duplex receiver with tunable self-interference canceling capability. They show that the performance of their receiver is enough for reliable reception.

In the context of this dissertation, we assume that the technology for implementing full-duplex transmission and reception is existent and well tested. The state-of-the-art is also well vested in different full-duplex network scenarios. Our work builds on this to propose scheduling and power allocation algorithms for full-duplex wireless networks.

2.4 Scheduling and Power Allocation

With SIC technologies now well established in the state-of-the-art, and with full-duplex technologies well motivated, it was only a matter of time before researchers in the wireless domain moved towards devising scheduling and power allocation algorithms for full-duplex wireless networks. Radio resource management has always been the pillar for any transmission technology. For full-duplex wireless networks specifically, there was more at stake. Scheduling and power allocation in this context is not only about better management of the radio resources, but also about mitigating full-duplex interferences. Without proper scheduling–capable of fighting off the effects on intra-cell co-channel interference–full-duplex communications would not be viable.

[1] As we later on discuss, full-duplex technologies were eventually overlooked in 5G. They are now spoken of in the context of 6G.

As a result, a plethora of papers in the state-of-the-art covered both scheduling and power allocation for full-duplex wireless networks. The authors of the article in [26] present a hybrid full-duplex OFDMA scheduler based on a greedy subcarrier allocation method and an iterative water filling power allocation algorithm. Their proposal seeks to maximize the sum-rate, choosing the pair of UEs which has the highest sum of instantaneous rates. The scheduling problem is formulated as a combinatorial problem of high complexity. An exhaustive search is needed to find the optimal solution. Thus, the authors introduce a heuristic algorithm with lower complexity. Furthermore, they make their algorithm hybrid by allocating certain time slots from each frame in full-duplex and others in half-duplex for either downlink or uplink UEs.

In [27], a joint user selection and rate allocation algorithm is proposed. It is formulated as a nonlinear non-convex problem with mixed discrete and continuous optimization. The authors note that finding a global optimum through an exhaustive search method is computationally difficult, thus a suboptimal method is considered. The article concludes that full-duplex networks have the potential to significantly increase the capacity of small cells under the presence of efficient SIC.

The authors in [28] propose an optimization problem with the purpose of allocating resources in what is described as a three-node system. The scenario implemented exhibits a full-duplex BS and half-duplex UEs which are paired on the radio resources. Constraints are added on the minimum SINR value for a UE to be allocated resources, and on the UE transmission powers as well. The problem thus belongs to the category of mixed integer nonlinear programming with high complexity and computational intractability. A sub-optimal heuristic is introduced as a result.

In [29], the authors formulate a problem for resource allocation in full-duplex OFDMA networks. The goal is to maximize the sum-rate, as well as address power allocation for the UEs. The problem they propose is non-convex with exponential complexity. As such, they develop an iterative solution that achieves local Pareto optimality in typical scenarios. Through simulations, they demonstrate that their proposal empirically achieves near optimal performance and that it outperforms other resource allocation schemes designed for half-duplex networks.

Many other articles we covered in the state-of-the-art had similar approaches. The authors in [30–32] all put forward joint power and resource allocation schemes. They propose optimization problems with greedy objectives focused on sum-rate maximization. The joint task of power allocation makes all these optimization problems of the category mixed integer nonlinear programming with high complexity and computational intractability. As such, the

authors work on heuristic solutions which can produce near optimal performances, but bear less complexity.

Tables 2.1, 2.2, 2.3, and 2.4 summarize the majority of the state-of-the-art concerned with scheduling and power allocation in full-duplex wireless networks. They highlight the full-duplex network scenarios used, and they state whether the referenced articles have power allocation algorithms alongside the scheduling proposals. The tables indicate whether these approaches to power allocation are distributed or centralized. Additional information on cell scenario and size, traffic type and the state of the SIC considered are included. Table cells marked "-" are for when the stated information is not given in the papers, or cannot be directly inferred from them.

The vast majority of the papers in the state-of-the-art introduce a full-duplex scenario similar to the one we used in our work. The BS is assumed to be the full-duplex node and the UEs remain half-duplex. This scenario is the one implemented in all the full-duplex OFDMA [30–32] models referenced as well. Other models in the related works focus on relay [33], MIMO [34], and even heterogeneous networks [35]. Though the latter three are not of direct connection to our work, we studied them due to the existence of a common problematic when it comes to dealing with full-duplex problems and interferences.

As for scheduling, almost all of the works in the state-of-the-art implement greedy approaches focusing on the maximization of the sum-rate (Max SR) [26] or the throughput (Max TP) [33]. Other greedy variations in the related works include maximizing the network's spectral efficiency (Max SE) [28], and maximizing the sum of the logarithmic rates [36] . Furthermore, a variance of power allocation algorithms are utilized with a good number of them being based on some form of optimization. Other approaches such as iterative water filling (IWF) [29], multi-objective optimization (MOOP) [34] , and fractional power control (FPC) [35] were used in some of the works.

Multi-cell scenarios are scarcely implemented in the state-of-the-art. This is mainly due to the exponential increase in complexity that both studying and simulating such scenarios would incur. Additionally, the existence of inter-cell interferences further complicate proving the feasibility and gains of full-duplex wireless communications. As we show later on in our work, not every multi-cell scenario produces gains with respect to half-duplex communications. Some papers in the state-of-the-art implement a simplistic model, as in [22], wherein unrealistic inter-cell interference assumptions are made. To the best of our knowledge, the paper in [36] has the most thorough multi-cell model in the related works. The authors consider both indoor and outdoor cell scenarios and pair their sum-rate maximization scheduling with an optimal power allocation problem. They consider single-cell scheduling and coordinated power allocation.

Self-interference cancellation technologies are a corner stone for full-duplex communications. Some articles in the state-of-the-art assume ideal conditions [32] *i.e.,* the technologies available are capable of canceling all of the self-interference. As we discussed before, this is not completely realistic. Other models assume near-ideal interference cancellation conditions, where a small residual self-interference (RSI) factor is added to the SINR calculation as noise. Another approach to modeling the effect of self-interference is via using an RSI model [24], wherein the RSI follows a probabilistic function such as a Gaussian law. Similar to our work, the majority of the papers reviewed use a set of interference cancellation factors to determine the RSI. Within the upper limits of 120 to 130 dB, these assumptions remain permissible.

Finally, a recapitulation of the buffer models used in the related works highlights the uniqueness of our approach to queue-awareness. Almost all the articles we reviewed in the state-of-the-art [26, 23, 28, 33, 34, 30–32, 37, 24, 29, 38–42, 35] used full buffer traffic models. Some authors [36] used a simple non-full buffer model, as for downloading a file, without incorporating queue-awareness into the traffic model.

Table 2.1 State-of-the-art for scheduling and power allocation (a)

	[22]	[26]	[23]	[28]	[33]
Network Type	BS/UEs FD	OFDMA	Multiple	BS FD	MIMO Relay
Scheduling	Max TP	Max SR	Max SR	Max SE	Max TP
Power Allocation	×	IWF	×	Optimal	×
Centralized	-	✓	-	×	-
Distributed	-	×	-	✓	-
Multi-Cell	Simple Scenario	×	×	×	×
Cell Size (R)	Small	40 m	-	100 m	-
Queue-Aware	✓	×	×	×	×
SIC State	Ideal	70-110 dB	-	110 dB	-

Table 2.2 State-of-the-art for scheduling and power allocation (b)

	[34]	[30]	[31]	[32]	[37]
Network Type	MU - MIMO	OFDMA	OFDMA	OFDMA	MC - NOMA
Scheduling	-	Max SR	Max SR	Max SR	Max SR
Power Allocation	MOOP	Optimal	Optimal	Optimal	Optimal
Centralized	✓	✓	✓	✓	✓
Distributed	×	×	×	×	×
Multi-Cell	×	×	×	×	×
Cell Size (R)	250 m	20/1000 m	-	Up to 1 km	600 m
Queue-Aware	×	×	×	×	×
SIC State	80 dB	130 dB	100 dB	Ideal	110 dB

Table 2.3 State-of-the-art for scheduling and power allocation (c)

	[36]	[24]	[29]	[38]	[39]
Network Type	BS FD	BS/UEs FD	OFDMA	OFDMA	BS FD
Scheduling	Max $\log$(R)	Max SR	Max SR	Max TP	Max SE
Power Allocation	Optimal	Optimal	IWF	$\times$	Optimal
Centralized	✓	-	✓	-	✓
Distributed	✓	-	$\times$	-	$\times$
Multi-Cell	✓	$\times$	$\times$	$\times$	
Cell Size (R)	Small	-	Up to 500 m	Up to 500 m	100 m
Queue-Aware	✓	$\times$	$\times$	$\times$	$\times$
SIC State	RSI Model	RSI Model	Near Ideal	Near Ideal	RSI Model

Table 2.4 State-of-the-art for scheduling and power allocation (d)

	[40]	[41]	[42]	[35]	[43]
Network Type	OFDMA	OFDMA	BS FD	Hybrid BS	OFDMA
Scheduling	Max SR	Max SR	Max SR	-	Max-Min
Power Allocation	IWF	Optimal	Optimal	FPC	Optimal
Centralized	✓	✓	✓	✓	✓
Distributed	$\times$	$\times$	$\times$	$\times$	$\times$
Multi-Cell	$\times$	$\times$	$\times$	Het-Net	$\times$
Cell Size (R)	Up to 200 m	100m	Up to 150 m	Small	100 m
Queue-Aware	$\times$	$\times$	$\times$	$\times$	-
SIC State	85 dB	Up to 120 dB	RSI Model	Ideal	110 dB

2.5 Our Work Compared to the State-of-the-Art

In what follows, we highlight the main novelties of our work in thesis with respect to what is already present in the state-of-the-art.

1. Queue-Aware Approach to Scheduling: Our traffic model is queue-aware. The number of bits in each UE's queue is finite and follows a dynamic arrival model. This is unique with respect to the state-of-the-art where the majority of the works consider full buffer traffic models. Our approach allows us to compute packet level metrics such as the waiting delay and is generally more representative of real life network scenarios. Non-full buffer traffic models real time arrivals and buffer statuses. Our scheduling proposals have to adapt to the fact that UEs might not always have data to transmit or receive. Assuming otherwise could allow the network to constantly exploit some advantageous schemes such as multi-user diversity. This will produce deceivingly positive results in otherwise disadvantageous scenarios. Finally, non-full buffer traffic

like streaming and video will make upwards of 78 % of the global mobile traffic by the year 2021 [1]. This further highlights the importance of accounting for dynamic arrivals.

2. Effect of Scheduling with Incomplete CSI on UE Performances: Very few articles in the state-of-the-art study the effects of imperfect CSI on the performances of full-duplex wireless networks. Namely, the articles in [39] and [44] discuss the lack of complete CSI and assume that an erroneous estimation of the channel is instead available. Our approach to studying the effects of imperfect CSI relies instead on the presence of different levels of channel information. As we detail in Chapter 4, partial availability scenarios of inter-UE information *i.e.,* pathloss information is present, are considered. We show via simulations that limited information regarding the inter-UE channel is sufficient to avoid the otherwise significant losses in UE performance that could occur as a result of scheduling with incomplete CSI.

3. A Reinforcement Learning Approach to Scheduling: As we highlighted the negative impact of scheduling with incomplete CSI, we introduce a method to circumvent the need for such information. We propose a machine learning algorithm capable of learning how to best allocate resources without the need for inter-UE CSI. This approach is unique with respect to state-of-the-art on scheduling in full-duplex wireless networks. Via simulations, we show that our proposal can emulate the performance of scheduling with complete CSI and that throughout different simulation scenarios, it remains more profitable than scheduling with incomplete CSI.

4. Distributed Approach to Power Allocation: In addition to our centralized approach to power allocation detailed in Chapter 5, we use game theory to propose a game theoretic framework for power allocation in full-duplex wireless networks. We use non-cooperative game theory, alongside a special class of games known as super-modular, to propose different games with varying objectives for power control. Probably the closest in the state-of-the-art to our objective in this area, are the papers in [40] and [45]. In [40], the authors use a game theoretic approach for resource allocation in full-duplex networks. While they implement a water filling algorithm for power control, their game theoretic approach focuses on greedy resource allocation with the purpose of sum-rate maximization. The authors in [45] suggest that a game theoretic approach could be used for power allocation in full-duplex wireless networks. Their article surveys possible applications in relation to scheduling and power allocation in different full-duplex network scenarios. While the authors of the latter practically present a survey with no specific algorithm proposals, the work in the former focuses mainly on

the scheduling task. Our games are designed for power allocation specifically and as we illustrate in Chapter 7, they cover different objectives from improving UE SINR to enhancing energy efficiency.

5. Scheduling in a Multi-Cell Environment: In our work, we study the performance of full-duplex networks in a multi-cell environment. The authors in [36] are–to the best of our knowledge–the only ones who proposed a comprehensive study of multi-cell full-duplex wireless scenarios. They assume single cell scheduling and a coordinated multi-cell approach to power control. In this thesis, we sought to present a complete analysis of the profitability of full-duplex communications in a multi-cell setting. Additionally, we highlight the importance of cooperation between cells in order to improve the gains which can be extracted from full-duplex wireless communications.

Chapter 3

Scheduling with Complete Channel State Information

3.1 Introduction

In this chapter, we introduce a mathematical optimal algorithm for scheduling in full-duplex and hybrid full-duplex/half-duplex wireless networks. Our generic optimization problem is queue-aware and addresses the new challenges that arise from working with full-duplex wireless networks: self-interference and intra-cell co-channel interference. We apply this optimization with different scheduling objectives, tackling issues such as SINR maximization and user fairness. Accordingly, we first propose an optimal full-duplex Max-SINR scheduling algorithm and an optimal full-duplex Proportional Fair scheduling algorithm. Additionally, and since full-duplex communications may not always be profitable, we introduce an optimal hybrid Max-SINR scheduling algorithm and an optimal hybrid Proportional Fair scheduling algorithm. These algorithms switch between full-duplex and half-duplex transmissions, so as to enhance network performance. Moreover, to avoid possible intractability with the optimization problems, we propose heuristic versions of our algorithms. We assess the performance of our heuristic proposals in multiple challenging scheduling scenarios and show that they achieve near-optimal results.

3.2 Network Model

The network model introduced in this chapter is the same one used for the remainder of this dissertation up until the multi-cell scenarios discussed in Chapter 7. It is comprised of a full-duplex base station (BS), and half-duplex user equipment (UEs). The main intent is to

keep the costs and complexities of implementing self-interference cancellation (SIC) away from the UEs. The size, battery, and cost limitations of UEs make them imperfect recipients of SIC technologies. Analog antenna cancellation, for example, requires multiple transmit antennas as well as enough separation between them, something inherently difficult and costly to achieve with UE size limitations. While it is quite realistic to assume that future technology will adapt effective SIC to the UEs, it is also safe to assume that using half-duplex terminals is currently the most feasible recourse.

3.2.1 Radio Model

We consider a single-cell full-duplex wireless network. This network is comprised of a full-duplex BS, and half-duplex UEs. The UEs are virtually divided into two sets: an uplink set, denoted by $\mathcal{I}$ and a downlink set, denoted by $\mathcal{D}$. This virtual division instigates that a certain moment in time, a UE either wants to transmit or receive. The scheduling algorithms would pair between uplink and downlink UEs on the resource blocks (RBs) k of the set $\mathcal{K}$, whereon one UE will transmit and the other will receive. This network is illustrated in Fig. 3.1.

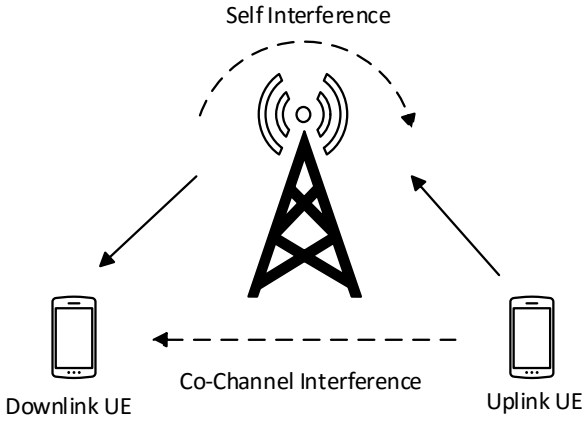

Figure 3.1 Network model and interferences

In our work, we assume that the physical layer is operated using an OFDMA structure. The latter is used in both 4G and 5G technologies [46]. The radio resources are divided into time-frequency RBs. In the time domain, an RB contains an integer number of OFDM symbols. In the frequency domain, an RB contains adjacent narrow-band subcarriers and experiences flat fading. Scheduling decisions for downlink and uplink transmissions are made in every transmission time interval (TTI). At the beginning of each TTI, K RBs are to be allocated. The TTI duration is chosen to be smaller than the channel coherence time. With these assumptions, UE radio conditions will vary from one RB to another, but remain

constant over a TTI. The modulation and coding scheme (MCS), that can be assigned to a UE on an RB, depends on its radio conditions. For performance evaluation, we consider LTE like specifications, with an RB being composed of 12 subcarriers and 7 OFDM symbols [11].

An adapted formula is used to calculate the SINR that takes into consideration the co-channel interference between a pair of UEs, and the self-interference cancellation performed by the BS. Let P_{ik} denote the transmit power of the *i*th uplink UE, on the *k*th RB. P_{0k} is the transmit power of the BS on the kth RB. We denote by h^u_{ik} the channel gain from the *i*th uplink UE to the BS on RB *k*, and by h^d_{jk} the channel gain from the BS to the *j*th downlink UE, on that same RB. Furthermore, $h_{ij,k}$ denotes the channel gain between the *i*th uplink UE and the *j*th downlink UE, on the *k*th RB. $P_{ik}|h_{ij,k}|^2$ is thus the co-channel interference on downlink UE j caused by uplink UE i, using the same RB k. The self-interference cancellation level at the BS is denoted SIC. In particular, $\frac{P_{0k}}{SIC}$ represents the residual self-interference power at the BS, on the *k*th RB. Finally, N_{0k} and N_{jk} denote the noise powers at the BS and at the *j*th downlink UE, on the *k*th RB, respectively. Equations (3.1) and (3.2) denote the formulas for SINR calculation for a pair of uplink-downlink UEs. For the uplink UE i at the BS,

$$S^u_j(i,k) = \frac{P_{ik}|h^u_{ik}|^2}{N_{0k} + \frac{P_{0k}}{SIC}},\ i \in \mathcal{I},\ j \in \mathcal{D}. \tag{3.1}$$

And at its paired downlink UE j,

$$S^d_i(j,k) = \frac{P_{0k}|h^d_{jk}|^2}{N_{jk} + P_{ik}|h_{ij,k}|^2},\ i \in \mathcal{I},\ j \in \mathcal{D}, \tag{3.2}$$

where $S^u_j(i,k)$ is the SINR of uplink UE i on RB k while using the same radio resources as downlink UE j. Similarly, $S^d_i(j,k)$ is the SINR of downlink UE j on RB k while using the same radio resources as uplink UE i.

3.2.2 Channel State Information

Legacy half-duplex networks are concerned mainly with the channel in between the BS and the UEs ($i.e.$, h^u_{ik} and h^d_{jk}). They would rely on feedback from the latter to determine the current channel state on the downlink. The channel state information (CSI) would be estimated at the receiver, quantized, and then fed back to the transmitter. A popular approach in estimating the CSI is by using a training (pilot) sequence, where a known signal is transmitted, and the channel matrix $\mathbf{H}$ is afterwards estimated using the combined knowledge of the transmitted and received signals [47]. Different techniques are used to determine how

often, and on which RBs, would this feedback on the CSI be required. The more periodic the feedback, the more accurate the channel estimation is.

Full-duplex communications add to the complexity of determining the CSI. In full-duplex networks, additional information on the channel in between the UEs of a certain pair ($i.e.$, $h_{ij,k}$) is required. Not only do current wireless systems not count for such information, there is also no implemented method for which a UE can estimate such UE-to-UE channels. Additionally, it is perceivable that measuring and continuously updating such information by a UE would cause excessive overhead and loads that it cannot handle. Consequently, precisely estimating inter-UE channels might not be feasible. In our work, we statistically model the inter-UE channel as follows:

$$h_{ij,k} = G_t G_r L_p A_s A_f \tag{3.3}$$

G_t and G_r are the antenna gains at the transmitter and the receiver, respectively. L_p represents the path loss, or equivalently the median attenuation the signal undergoes in this channel. A_s and A_f are two random variables that respectively represent the shadowing effect, and the fast fading effect. In this chapter, we assume that the scheduler has complete knowledge of all the network's wireless links. In Chapter 4, we discuss the effects of incomplete CSI on scheduling in full-duplex wireless networks.

3.2.3 Traffic Model

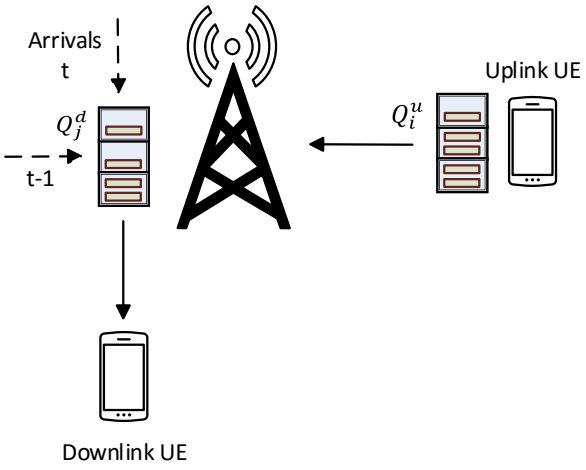

Figure 3.2 Traffic model: UE pair i-j with uplink and downlink queues

Our scheduling is queue-aware (Fig. 3.2). Each UE has a predefined throughput demand which determines the rate at which the UE will transmit or receive. A downlink UE has a

queue at the BS, denoted Q_j^d, that it wants to receive. An uplink UE has a queue of bits it wants to transmit to the BS, denoted Q_i^u. UE queues are updated each TTI. They are filled according to a Poisson process with an average arrival rate λ equal to the throughput demand. Once the scheduling is done for a certain TTI, the number of bits each UE can transmit or receive is calculated, and the UE queues are deducted accordingly. The traffic is packeted into small units known as transport blocks. The modulation and coding scheme (MCS) that can be assigned to a UE is based on its SINR. Following the MCS used and the number of RBs allocated for a UE, its transport block size is determined for the TTI. Any bits remaining in a UE queue at the end of a TTI are carried on to the next one.

3.2.4 Performance Model

The mapping between a UE's SINR and the number of bits it can transmit/receive is done following an MCS. Using LTE-like configurations, we set 15 channel quality indicator (CQI) values. The CQI values are used to identify the coding rates selected between 1/8 and 4/5, and the modulations chosen among 4-QAM, 16-QAM and 64-QAM. Figure 3.3 shows the mapping between the UE SINR values and the assigned CQI value.

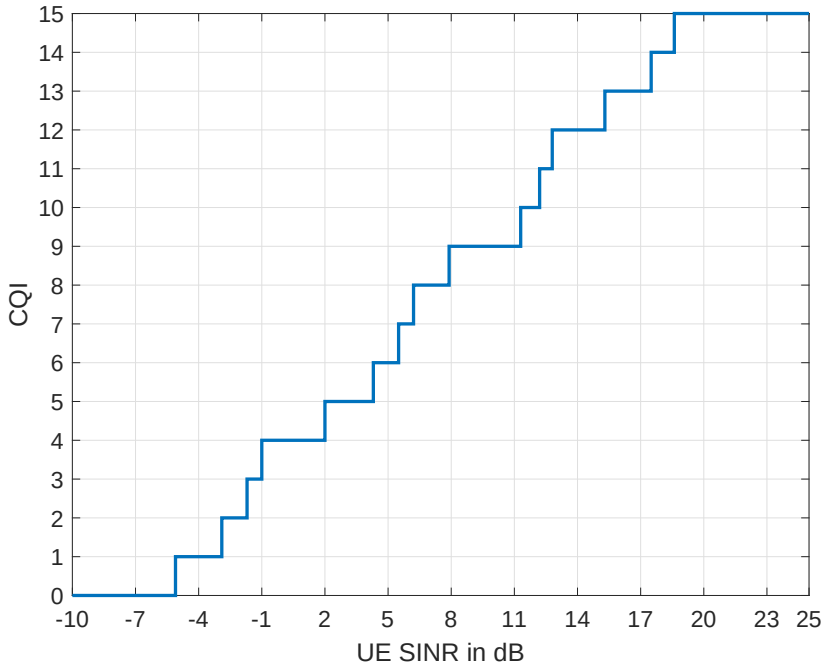

Figure 3.3 CQI as a function of UE SINR

Furthermore, Table 3.1 shows the relationship between the CQI level and the MCS schemes used. Based on the MCS used, the number of bits each UE can transmit or receive on the resources allocated to it is recorded. At the end of the simulation, the UE throughput is

calculated as the number of bits the UE has transmitted divided by the simulation duration. Finally, the average UE waiting delay is calculated using Little's formula as the average queue length divided by the packet arrival rate.

Table 3.1 Modulation and coding scheme

CQI	Modulation	CodingRate	N°Bits/RB
0	-	-	0
1	QPSK	1/8	21
2	QPSK	1/5	33.6
3	QPSK	1/4	42
4	QPSK	1/3	55.44
5	QPSK	1/2	84
6	QPSK	2/3	111.72
7	QPSK	3/4	126
8	QPSK	4/5	134.4
9	16-QAM	1/2	168
10	16-QAM	2/3	223.44
11	16-QAM	3/4	252
12	16-QAM	4/5	268.8
13	64-QAM	2/3	336
14	64-QAM	3/4	378
15	64-QAM	4/5	307.2

3.3 Generic Scheduling Algorithm

3.3.1 Queue-Aware Full-Duplex Scheduling Algorithm

We propose an optimal scheduling algorithm for full-duplex networks. The optimal problem is run every TTI to determine how the resources will be allocated to the UEs. We define the UE pair-RB assignment variable $z_{ijk}, \forall\, k \in \mathcal{K}, \forall\, i \in \mathcal{I}, \forall\, j \in \mathcal{D}$. z_{ijk} is equal to one if uplink UE i is paired with downlink UE j on RB k. It is equal to zero otherwise. Let $F_j^u(i,k)$ is the utility function of uplink UE i on RB k, while it is paired with downlink UE j. Likewise, $F_i^d(j,k)$ is the utility function of downlink UE j on RB k, while it is paired with uplink UE i. T_{ijk}^u is the number of bits UE i can transmit on RB k while paired with UE j. Similarly, T_{ijk}^d is the number of bits UE j can receive on RB k while paired with UE i. T_{ijk}^u and T_{ijk}^d depend mainly on the radio conditions of the UEs. In addition, D_i^u is the demand of uplink UE i $i.e.$, the number of bits in its queue. Likewise, D_j^d is the demand of downlink UE j. We formulate the optimization problem as follows.

Global Full-Duplex Scheduling Problem (G_t^1) =

$$\underset{z_{ijk}}{\text{Maximize}} \quad \sum_{k\in\mathcal{K}}\sum_{i\in\mathcal{I}}\sum_{j\in\mathcal{D}} z_{ijk}(F_j^u(i,k)+F_i^d(j,k)), \tag{3.4a}$$

$$\text{Subject to} \quad \sum_{i\in\mathcal{I}}\sum_{j\in\mathcal{D}} z_{ijk} \leq 1,\ \forall k \in \mathcal{K}, \tag{3.4b}$$

$$\alpha_p \sum_{k\in\mathcal{K}}\sum_{j\in\mathcal{D}} z_{ijk}T_{ijk}^u \leq D_i^u,\ \forall i \in \mathcal{I}, \tag{3.4c}$$

$$\alpha_p \sum_{k\in\mathcal{K}}\sum_{i\in\mathcal{I}} z_{ijk}T_{ijk}^d \leq D_j^d,\ \forall j \in \mathcal{D}, \tag{3.4d}$$

$$z_{ijk} \in \{0,1\},\ \forall i \in \mathcal{I}, \forall j \in \mathcal{D}, \forall k \in \mathcal{K}. \tag{3.4e}$$

Equation (3.4a) expresses the objective of our problem: to maximize the total sum of the utilities of the UE pairs that are allocated RBs. According to (3.4b), each RB should be allocated to a maximum of one UE pair.

We define $\alpha_p \in$ [0,1] as the resource utilization factor. This factor is needed to verify that the RBs are being efficiently scheduled and not allocated to UEs which do not need or make good use of them. Consider the constraints (3.4c) and (3.4d). They insure that a UE will transmit or receive at least α_p of the bits it can on the resources allocated to it. If $\alpha_p = 1$, then a UE is allocated an additional resource if the number of bits in its queue is greater than or equal to the number of bits it can transmit or receive on the resources allocated to it. If $\alpha_p = 0.8$, then a UE is allocated an RB if the number of bits in its queue is at least 80% of the number of bits it can transmit or receive on the resources allocated to it. The latter might create a scenario where a UE is allocated an RB on which it transmits few or no bits. The former might create a scenario in which a UE still has bits in its queue but is denied more RBs because it does not have enough to fully utilize the additional RB. As we devise a queue-aware model, the number of bits that each UE would receive or transmit in a certain TTI varies, and the optimal value of α_p is as such dependent on each UE and its current radio conditions. Via simulations, we show that the best recourse is to set α_p to one, as it would produce the best UE throughput results in the vast majority of the cases. The optimization problem is run every TTI to determine how the radio resources will be allocated to the UEs.

3.3.2 Queue-Aware Hybrid Scheduling Algorithm

The feasibility of full-duplex communications is related to the cell radio conditions, as well as the resulting interference problems. This hybrid algorithm allows the scheduler to choose between allocating the RBs in full-duplex to two UEs, or in half-duplex to one, depending on which yields a higher sum of UE utility functions.

Let $y^u_{ik}, \forall\, k \in \mathcal{K}, \forall\, i \in \mathcal{I}$ be the uplink UE-RB half-duplex assignment variable. It is equal to one if uplink UE i is allocated RB k in half-duplex. It is equal to zero otherwise. Similarly, y^d_{jk} is the downlink UE-RB half-duplex assignment variable. The hybrid scheduling problem is formulated as follows.
Global Hybrid Scheduling Problem (G^2_t) =

$$\underset{z_{ijk}, y^d_{jk}, y^u_{ik}}{\text{Maximize}} \quad \sum_{k\in\mathcal{K}} \sum_{i\in\mathcal{I}} \sum_{j\in\mathcal{D}} z_{ijk}(F^u_j(i,k) + F^d_i(j,k)) + \sum_{k\in\mathcal{K}} \sum_{i\in\mathcal{I}} y^u_{ik} F^u(i,k) + \sum_{k\in\mathcal{K}} \sum_{j\in\mathcal{D}} y^d_{jk} F^d(j,k), \tag{3.5a}$$

Subject to

$$\sum_{i\in\mathcal{I}} \sum_{j\in\mathcal{D}} z_{ijk} + \sum_{i\in\mathcal{I}} y^u_{ik} + \sum_{j\in\mathcal{D}} y^d_{jk} \leq 1,\ \forall k \in \mathcal{K}, \tag{3.5b}$$

$$\alpha_p\Big(\sum_{k\in\mathcal{K}} \sum_{j\in\mathcal{D}} z_{ijk} T^u_{ijk} + \sum_{k\in K} y^u_{ik} T^u_{ik}\Big) \leq D^u_i,\ \forall i \in \mathcal{I}, \tag{3.5c}$$

$$\alpha_p\Big(\sum_{k\in\mathcal{K}} \sum_{i\in\mathcal{I}} z_{ijk} T^d_{ijk} + \sum_{k\in K} y^d_{jk} T^d_{jk}\Big) \leq D^d_j,\ \forall j \in \mathcal{D}, \tag{3.5d}$$

$$z_{ijk}, y^u_{ik}, y^d_{jk} \in \{0,1\},\ \forall i \in \mathcal{I}, \forall j \in \mathcal{D}, \forall k \in \mathcal{K}. \tag{3.5e}$$

$F^u(i,k)$ and $F^d(j,k)$ are the utility functions for half-duplex uplink UE i and half-duplex downlink UE j, respectively. T^u_{ik} is the number of bits uplink UE i can send on RB k if it gets it in half-duplex. Similarly, T^d_{jk} is the number of bits downlink UE j can send on RB k if it gets it in half-duplex. The objective of this problem stated in (3.5a) is to maximize the networks' sum of UE utility functions. The constraints in (3.5b) impose that an RB is allocated only once, either in full-duplex to two UEs, or in half-duplex to one. The constraints in (3.5c) and (3.5d) serve the same purpose as (3.4c) and (3.4d), with the possibility of a half-duplex allocation considered. These constraints ensure the resources are allocated efficiently in an environment with dynamic traffic arrivals. In what follows, we propose different expressions for the utility function thus generating algorithms that are either greedy or fairness oriented.

3.4 Optimal Resource Allocation

In this section, we present our optimal algorithms for scheduling in full-duplex wireless networks. By changing the expressions of the utility functions in both the full-duplex and hybrid models, we are able to propose four algorithms with different scheduling objectives. We change the objective function in (3.4a) such that the utility function F is equal to the UE

SINR:

$$\sum_{k\in\mathcal{K}}\sum_{i\in\mathcal{I}}\sum_{j\in\mathcal{D}} z_{ijk}(S_j^u(i,k)+S_i^d(j,k)), \tag{3.6}$$

This algorithm, full-duplex Max-SINR, calculates the SINR, on every RB, for each possible pair between an uplink UE and a downlink UE. It then proceeds to allocate each RB to the corresponding UE pair in a way that maximizes the objective function. This approach favors the best performing UEs, leading to an increase in the system's overall throughput. Nonetheless, UEs with bad radio conditions could experience bandwidth starvation.

Full-duplex Max-SINR is as such greedy and opportunistic. While such an approach could lead to the most efficient utilization of resources, it is generally unfair. We are interested in taking a different, and more fair advance on the scheduling task. Therefore, we propose an optimal full-duplex Proportional Fair algorithm. We set the utility function in (3.4a) to be equal to the UE priority. This yields the objective function presented by our second proposal full-duplex Proportional Fair.

$$\sum_{k\in\mathcal{K}}\sum_{i\in\mathcal{I}}\sum_{j\in\mathcal{D}} z_{ijk}(\rho_j^u(i,k)+\rho_i^d(j,k)), \tag{3.7}$$

where $\rho_j^u(i,k)$ is the priority of uplink UE i, and $\rho_i^d(j,k)$ is the priority of downlink UE j, when paired with each other. The priority of a UE is defined as a function of its current radio conditions, represented by the number of bits a UE can transmit on the selected RB, and its historic radio conditions, represented by the number of bits it has already transmitted. The priority for an uplink UE i while paired with downlink UE j on RB k, for example, is defined as:

$$\rho_j^u(i,k)=\frac{T_{ijk}^u}{T_i}, \tag{3.8}$$

where T_i is the number of transmitted bits within a certain time window. The priority of a UE thus decreases as it transmits more. This gives higher priority to UEs which have not transmitted in a while, while still factoring in their current radio conditions.

Making the algorithms hybrid guarantees that the system is always working in the transmission mode that enhances its performance. As we demonstrate later on via simulations, depending on the radio conditions, and the quality of the SIC techniques available, full-duplex communications might not always even be viable. For low values of the SIC factor, uplink UEs could be totally denied access to the system resources. We thus seek to allow the scheduler to astutely choose between allocating an RB to a single UE (half-duplex) or to a pair of UEs (full-duplex).

We set the utility function F in equation (3.5a) to be equal to the UE SINR to yield a

hybrid Max-SINR algorithm:

$$\sum_{k\in\mathcal{K}}\sum_{i\in\mathcal{I}}\sum_{j\in\mathcal{D}} z_{ijk}(S_j^u(i,k)+S_i^d(j,k))+\sum_{k\in\mathcal{K}}\sum_{i\in\mathcal{I}} y_{ik}^u r^u(i,k)+\sum_{k\in\mathcal{K}}\sum_{j\in\mathcal{D}} y_{jk}^d r^d(j,k), \tag{3.9}$$

where $r^u(i,k)$ and $r^d(j,k)$ are the SINR of UEs i and j in half-duplex. Similarly, replacing F with the UE priority yields a hybrid Proportional Fair algorithm:

$$\sum_{k\in\mathcal{K}}\sum_{i\in\mathcal{I}}\sum_{j\in\mathcal{D}} z_{ijk}(\rho_j^u(i,k)+\rho_i^d(j,k))+\sum_{k\in\mathcal{K}}\sum_{i\in\mathcal{I}} y_{ik}^u \rho^u(i,k)+\sum_{k\in\mathcal{K}}\sum_{j\in\mathcal{D}} y_{jk}^d \rho^d(j,k), \tag{3.10}$$

where $\rho^u(i,k)$ and $\rho^d(j,k)$ are the half-duplex priorities of UE i and j $i.e$, their priorities if they were to be allocated resources solely. In both algorithms, the scheduling decision is done following the allocation mode that would maximize the objective function (3.5a). In hybrid Max-SINR for example, if the maximum half-duplex UE SINR value on a certain RB is higher than the corresponding full-duplex highest sum of SINR values, the RB is allocated in half-duplex. Otherwise, it is allocated in full-duplex. Note that in case of half-duplex scheduling the SINR for an uplink UE i on an RB k is calculated as:

$$r^u(i,k)=\frac{P_{ik}|h_{ik}^u|^2}{N_{0k}},\ i\in\mathcal{I},\ k\in\mathcal{K}. \tag{3.11}$$

And for a downlink UE j,

$$r^d(j,k)=\frac{P_{0k}|h_{jk}^d|^2}{N_{jk}},\ j\in\mathcal{D},\ k\in\mathcal{K}, \tag{3.12}$$

As for the priorities of the half-duplex UEs, they are calculated as a function of the number of bits a UE can transmit or receive on an RB. For example, for an uplink UE i transmitting solely on an RB k, the half-duplex UE priority can be written as:

$$\rho^u(i,k)=\frac{T_{ik}^u}{T_i}, \tag{3.13}$$

In presence of sufficient SIC at the BS and reduced co-channel interference as an effect of scheduling, our full-duplex algorithms will perform identically to our hybrid algorithms, albeit with less complexity. The hybrid algorithms would always be allocating resources in full-duplex, because the system conditions will always make it the more lucrative choice. However, if that was not the case, the hybrid algorithms would be trading more complexity for better resource allocation. A practical evaluation of the complexity is presented in the following section.

3.5 Complexity of the Optimal Problem

3.5.1 Full-duplex Scheduling Model

The variables in this optimization problem are all integers. The objective function and the constraints, which depend on the binary value of z_{ijk}, are linear. The problem is thus of type integer linear (ILP) [48]. The number of constraints and variables are important factors when estimating if this problem is tractable. These problems can, in principle, be solved by complete enumeration of candidate solutions. This method is known as branch and bound [49], where the set of candidate solutions is thought of as forming a rooted tree with the full set at the root. The branch and bound algorithm explores the branches of this tree, which represent subsets of the solution set. Before enumerating the candidate solutions of a branch, the branch is checked against upper and lower estimated bounds on the optimal solution, and is discarded if it cannot produce a better solution than the best one found so far by the algorithm. Such a problem could become mathematically intractable as the number of variables increase.

3.5.2 Hybrid Scheduling Model

This model is similar in form to the full-duplex model. All the variables are binary, and the constraints are linear, and dependent of the binary variables. The problem is thus also of type ILP and therefore NP-Complete [48]. Containing more variables and more constraints, this problem would take slightly more time to solve than the previous one.

The complexity of the optimization problem, which can become prohibitive for an increased number of resources and UEs, motivates a heuristic approach. In the following section, we provide heuristic algorithms with the same objectives as the optimization problems, albeit bearing less complexity.

3.6 Heuristic Algorithms

Seeking scheduling solutions with less complexity, we present heuristic algorithms corresponding to our optimal propositions. First, we introduce a heuristic full-duplex Max-SINR algorithm. This algorithm seeks to couple between two half-duplex UEs, one on the uplink and one on the downlink, on the same RBs. The traffic is non-full-buffer. As such, a UE that has depleted its queue is excluded from the resource allocation within the same TTI. For each RB k of the set $\mathcal{K}$, the algorithm calculates the SINR for each possible pair between an uplink UE and a downlink UE. We compute the SINR as indicated in equations (3.1) and

(3.2), and allocate the currently selected RB to the pair of UEs which has the highest value of the sum: $S_j^u(i,k) + S_i^d(j,k)$, where i belongs to the set of uplink UEs and j to the set of downlink UEs. This algorithm is iterative. In contrast with the globality of the optimization problem, which makes the allocation decision for all the RBs at the same time, the decision here is made for each RB in turn. Moreover, in case it is impossible to pair between UEs due to one of the uplink or downlink sets being empty (either all uplink or all downlink UEs have emptied their queues), the scheduler allocates the RB to a single UE in half-duplex.

If all the UEs empty their queues before the resources are depleted, the remaining RBs are marked as free. The function Update(x), in Algorithm 1, is responsible for updating the queue status and the UE sets after resource allocation. The number of transmitted bits is calculated for each UE allocated an RB depending on the MCS used and decremented from its corresponding queue. The pseudo-code for full-duplex Max-SINR is shown in Algorithm 2, when the utility function is equal to the UE SINR.

Algorithm 1 Queue Update Function

Update (x)
if $x \in \mathcal{I}$
    $Q_x^u \leftarrow Q_x^u - T_{xjk}^u$
    if Q_x^u == 0
        $\mathcal{I} \leftarrow \mathcal{I} - \{x\}$
    end if
end if
if $x \in \mathcal{D}$
    $Q_x^d \leftarrow Q_x^d - T_{ixk}^d$
    if Q_x^d == 0
        $\mathcal{D} \leftarrow \mathcal{D} - \{x\}$
    end if
end if

Similarly, we propose a heuristic version of our full-duplex Proportional Fair algorithm. For every RB, the UE pair with the highest sum of priorities is chosen. The corresponding pseudo-code is shown in Algorithm 2, when the objective function is equal to the priority of the UEs.

We further propose a heuristic implementation of our hybrid Max-SINR algorithm. The scheduling decision for this algorithm is done based on the following criteria. For every RB, pair allocation is used if the following condition is met:

$$S_j^u(i^*,k) + S_i^d(j^*,k) > r(e^*,k), \tag{3.14}$$

where $r(e^*, k)$ is the highest SINR value for a half-duplex UE. Under this condition, we assume that we have sufficient SIC and/or acceptable radio conditions to support full-duplex communications. Otherwise, the scheduler allocates the RB in half-duplex to the UE with the highest SINR (uplink or downlink). The pseudo-code for the algorithm is illustrated in Algorithm 3 when the objective function is equal to the UE SINR.

Algorithm 2 Full-Duplex Heuristic Scheduling

for $k = 1, \ldots, K$
  if $\mathcal{I} \neq \phi \; and \; \mathcal{D} \neq \phi$
    (i^*, j^*) = $\underset{i \in \mathcal{I}, j \in \mathcal{D}}{\operatorname{argmax}}(F_j^u(i,k) + F_i^d(j,k))$
    Allocate RB k to couple (i^*, j^*)
    Update(i^*), Update(j^*)
  else
    e^*=$\underset{e \in \mathcal{I} \cup \mathcal{D}}{\operatorname{argmax}}(F(e,k))$
    Allocate RB k to user e^*
    Update(e^*)
  end if
end for

Algorithm 3 Hybrid Heuristic Scheduling

for $k = 1, \ldots, K$
  (i^*, j^*) = $\underset{i \in \mathcal{I}, j \in \mathcal{D}}{\operatorname{argmax}}(F_j^u(i,k) + F_i^d(j,k))$
  e^*=$\underset{e \in \mathcal{I} \cup \mathcal{D}}{\operatorname{argmax}}(F(e,k))$
  if $F_{j^*}^u(i^*,k) + F_{i^*}^d(j^*,k) > F(e^*,k)$
    Allocate RB k to couple (i^*, j^*)
    Update(i^*), Update(j^*)
  else
    Allocate RB k to user e^*
    Update(e^*)
  end if
end for

Similarly, we propose a heuristic hybrid Proportional Fair algorithm. The scheduling decision for this algorithm is done based on the following criteria. For every RB, pair allocation is used if the sum of full-duplex priorities of any UE pair is greater than the highest priority value of a single half-duplex UE:

$$\rho_j^u(i^*,k) + \rho_i^d(j^*,k) > \rho(e^*,k), \tag{3.15}$$

where $\rho(e^*, k)$ is the highest priority value for a half-duplex UE. We assume that we have sufficient SIC and/or acceptable radio conditions to support full-duplex communications. Otherwise, the scheduler allocates the RB in half-duplex to the UE with the highest priority (uplink or downlink). The pseudo-code for the algorithm is illustrated in Algorithm 3, when the utility function is set to be equal to the priority of the UEs.

Finally, we introduce the last of our proposed algorithms, full-duplex Round Robin. The general idea is to make a list of random UE pairs, and then proceed to allocate the RBs to the pairs on this list in turn, regardless of any other factor. This might cause some UEs to be at a great disadvantage if the UEs of a pair are close to each other, or far away from the BS. As a bad luck protection mechanism, we randomly re-pair the UEs at the beginning of every TTI. Algorithm 4 explains the process.

Algorithm 4 Full-Duplex Round Robin

```
Form a set of random UE pairs P of size n
P_s=1 Selected Pair Index
for k = 1, ..., K
    Allocate k to couple (i,j) of the pair P_s
    Update(i), Update(j)
    if P_s < n + 1
        P_s=P_s+1;
    else
        P_s=1;
    end if
end for
```

Note that if only one UE of a certain pair has emptied its queue (and accordingly removed from its corresponding dowlink or uplink UE set), its paired UE keeps getting the RBs during the pair's turn till the end of the TTI, albeit this time in half-duplex.

3.7 Complexity of the Heuristic Algorithms

Our heuristic algorithms have complexities of the same order. The wireless system has I uplink UEs, and $\mathcal{D}$ downlink UEs. This amounts to a total of $n = I \times \mathcal{D}$ possible UE pairs. In our algorithms, we seek to sort these pairs based on SINR or priority. The complexity of these heuristic algorithms is thus of the order $\mathcal{O}$(n) [50].

We compare the simulation duration for each of the optimal and heuristic Max-SINR algorithms. Under identical conditions and using the simulation parameters in Table 3.3. The SIC value is set to 10^{11}. 10 UEs are simulated along with 20 RBs. We note the time taken

by the simulator to allocate the resources during one TTI. A statistical interpretation of the results is given in Table 3.2. The criteria are measured in seconds. The machine used for the simulations has an INTEL(R) core i3-4170 CPU at 3.70 GHz processor. It runs on 8 GB of RAM.

Table 3.2 Heuristic vs. optimal: simulation time

Criteria	**Optimal (s)**	**Heuristic (s)**
Mean	1.3125	0.1710
1^{st} Quartile	0.1563	0.1646
Median	0.1563	0.1692
3^{rd} Quartile	0.1836	0.1748

For a limited number of RBs and UEs, the optimal algorithm can solve the resource allocation problem faster than the heuristic one. However, there are few exceptions as indicated by the higher mean value for the optimal algorithm. This would no longer be the case as we increase the number of UEs and RBs, where the simulation time for the optimal algorithm could significantly increase.

3.8 Simulation and Results

We have four main objectives to tackle through this set of simulations. First, we want to affirm the gains that full-duplex wireless networks bring, compared to half-duplex networks, and in varying simulation scenarios. Second, we want to assess the effects of having different scheduling objectives, both greedy and fair, on UE throughputs and performances. third, we seek to justify the necessity for a hybrid algorithm, illustrating the cases where full-duplex alone would not be viable. Finally, we want to validate our heuristic algorithms, and show that they achieve near optimal performances.

The channel gain takes into account the path loss, the shadowing and the fast fading effects. The path loss is calculated using the extended Hata path loss model [51]. The shadowing is modeled by a log-normal random variable $A_s = 10^{(\frac{\xi}{10})}$, where ξ is a normal distributed random variable with zero mean and standard deviation equal to 10. The fast fading is modeled by an exponential random variable A_f with unit parameter. This model is used for urban zones, and it takes into account the effects of diffraction, reflection and scattering caused by city structures. In this simulation set, the transmit power per RB is fixed and set to a value lower than the maximum possible.

Table 3.3 Simulation parameters for scheduling with complete CSI

Parameter	Value
Cell Specifications	Single-Cell, 120 m Radius
Number of RBs	50
BS Transmit Power	24 dBm
Maximum UE Transmit Power	24 dBm
α_p	1
SIC Value	10^{11}-10^{8}
Number of UEs	10 DL, 10 UL
UE Distribution	Uniform
Demand Throughput	2-4 Mbps
Fast Fading	Exponential variable
Shadowing	Log-normal variable
Path Loss Model	Extended Hata Path Loss Model

3.8.1 General Performance of the Full-Duplex Algorithms

The global optimal problem is NP-complete, and as we demonstrate later on, our heuristic algorithms produce near-optimal results. As such, we are going to consider multiple scheduling scenarios in order to better study the performances of the heuristic algorithms, and full-duplex wireless networks in general. Following the parameters indicated in Table 3.3, we simulate our full-duplex Max-SINR, Round Robin, and Proportional Fair algorithms. As a half-duplex reference, we simulate a traditional half-duplex Max-SINR algorithm.

Figure 3.4 is a cumulative distribution function (CDF) plot of the throughput values attained by the UEs across the simulations. The trends which are set by the scheduling techniques are clear. Max-SINR, whether in half-duplex implementation, or in our full-duplex algorithm, seeks to serve the UEs with the best radio conditions. Nonetheless, around 70 % of the full-duplex Max-SINR UEs attained a throughput equal to the demand, significantly more than that of its half-duplex counterpart at 45 %.

On the other hand, Proportional Fair scheduling seeks equity between the UEs. The percentage of full-duplex Proportional Fair UEs which have attained a throughput equal to the demand sits at around 45 %, less than that of full-duplex Max-SINR. However, the least attained UE throughput for full-duplex Proportional Fair is about 0.8 Mbps, compared to 0 Mbps (by 50 % of the UEs simulated) for half-duplex Max-SINR and around 0.1 Mbps, the lowest for a full-duplex Max-SINR UE. Full-duplex Proportional Fair will degrade the performance of UEs with excellent radio conditions, in order to provide resources to UEs with poor conditions.

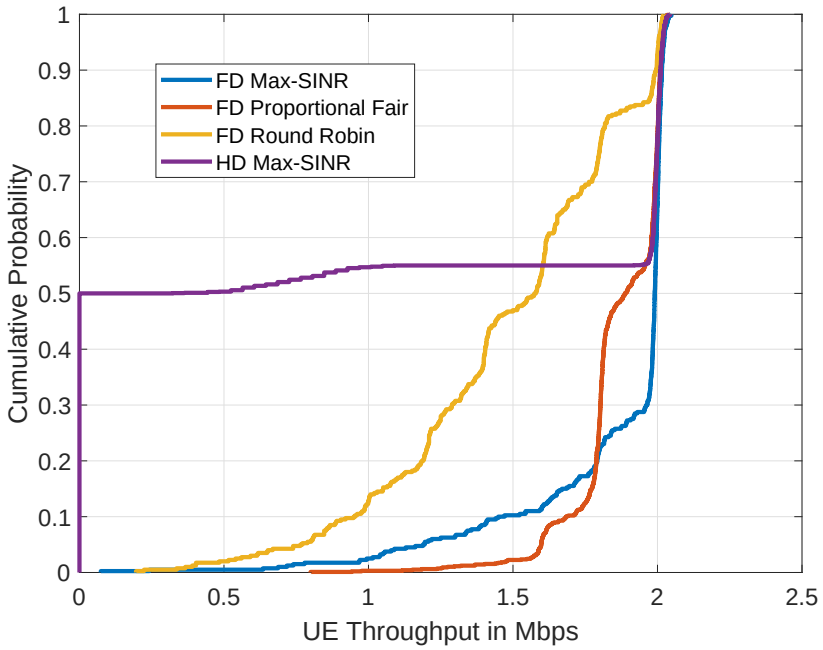

Figure 3.4 Full-duplex algorithms performance in terms of UE throughput

Finally, our full-duplex Round Robin algorithm shows that even with random allocation, full-duplex transmissions can provide significant improvement with respect to half-duplex communications. Whilst half-duplex Max-SINR produces more UEs with throughput equal to the demand, our full-duplex Round Robin gave better throughput values for about 55 % of the UEs. The median UE throughput value for full-duplex Round Robin is about 1.6 Mbps.

We compute the fairness index, for each of the four algorithms, for the current simulation scenario. We use Jain's fairness index [52] to determine whether the resources are getting allocated fairly under our proposed scheduling algorithms. This index is computed according to the Raj-Jain equation as follows:

$$\mathcal{J}(x_1, x_2, \ldots, x_n) = \frac{(\sum_{i=1}^{n} x_i)^2}{n. \sum_{i=1}^{n} x_i^2}. \tag{3.16}$$

$\mathcal{J}$ represents the fairness of a scheduling algorithm, for n UEs, of x_i throughput each. The results for an algorithm is between $\frac{1}{n}$ and 1. It is maximum when all the UEs receive the same allocation. Full-duplex Proportional Fair allocates resources more fairly than the others, with a Jain index value equal to 0.97. Full-duplex Max-SINR sits near 0.80, and half-duplex Max-SINR with the lowest value at 0.58. Max-SINR is opportunistic and greedy, it would not allocate resource fairly. This is shown clearly in the case of half-duplex Max-SINR, but rather concealed with full-duplex Max-SINR. With full-duplex scheduling UEs have practically double the RBs at their disposal remedying the unfair nature of Max-SINR scheduling.

Furthermore, we compare between these algorithms in terms of the average waiting delay for the UEs. The average waiting delay is calculated using Little's formula as the average queue length divided by the packet arrival rate. Figure 3.5 has box plots of the average waiting delay for the UEs, per simulation run, across the four algorithms we simulated in this section.

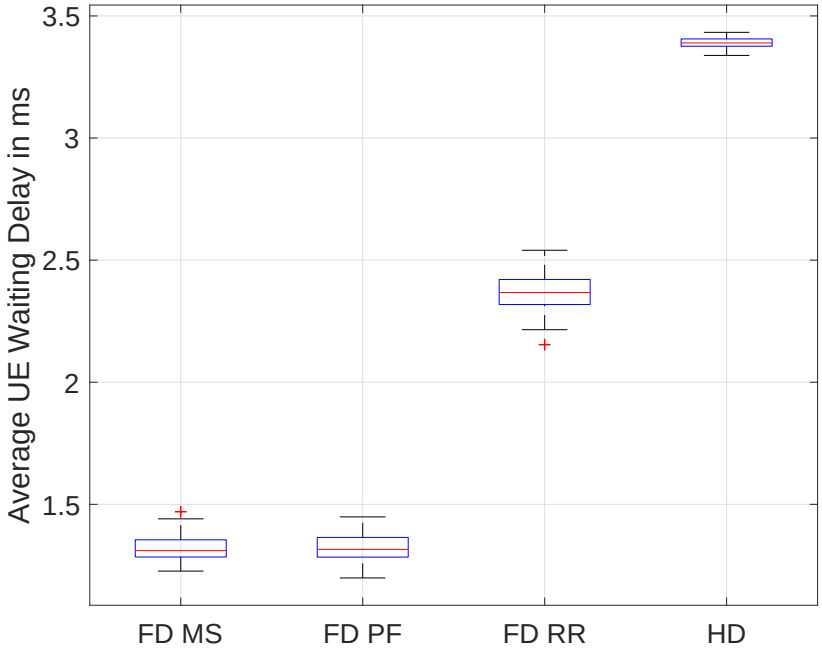

Figure 3.5 Full-duplex algorithms performance in terms of UE waiting delay

The box plot, also known as the box and whisker diagram [53], is a standardized way of displaying the distribution of data based on a five number strategy: minimum, first quartile, median, third quartile, and maximum. In the simplest box plot the central rectangle spans the first quartile to the third quartile (the interquartile range). A red segment inside the rectangle shows the median, and the segments in black or "whiskers" above and below the box show the minimum and maximum. In some cases, a red cross will indicate a certain data value that stood out from the rest, and could not be grouped with the majority of the data.

Our full-duplex Proportional Fair and Max-SINR algorithms heavily outperform the rest in terms of maximum delay, with full-duplex Max-SINR edging out full-duplex Proportional Fair when it comes to UEs with bad radio conditions. Moreover, it is noticeable that all the full-duplex algorithms outperform half-duplex ones in terms of waiting delay. Naturally, with good SIC, full-duplex UEs will on average be getting double the resources, and thus experiencing half the delay. Full-duplex RR UEs experience on average 1 ms less delay than half-duplex UEs, while full-duplex Proportional Fair and Max-SINR UEs experience on average more than 2 ms less waiting delay.

3.8.2 Effect of Heterogeneous Traffic on UE Performance

We repeat the same simulations, but with heterogeneous traffic for the UEs. With equal probability, the throughput demand for the UEs is set to either 2 or 4 Mbps. All other parameters remain unchanged from the previous section. Figure 3.6 shows the throughput attained by the UEs, while scheduling using each of our proposed full-duplex heuristic algorithms.

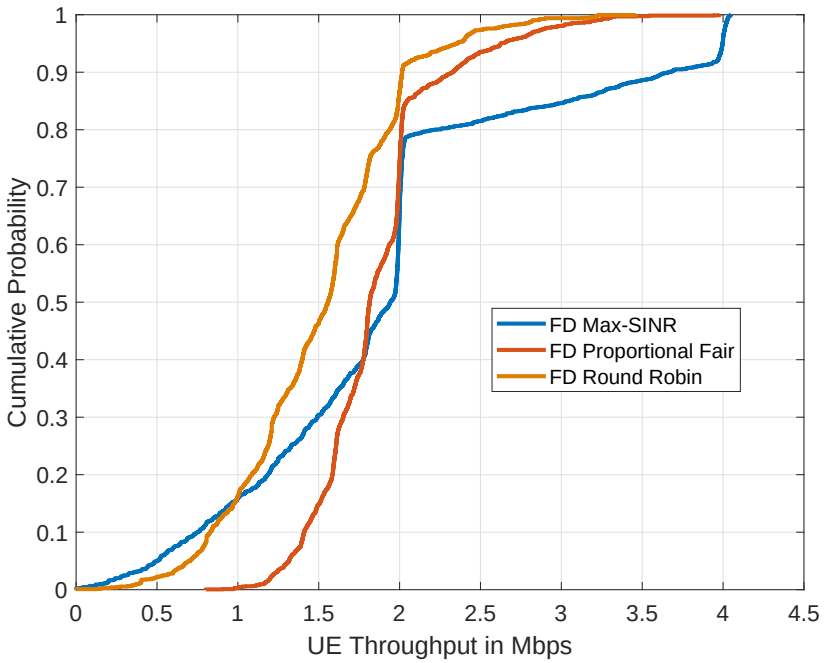

Figure 3.6 Full-duplex algorithms performance in the case of heterogeneous traffic

The trends by the algorithms we observed in the previous section remain pertinent. Full-duplex Max-SINR allocates resources to the UEs with the best radio conditions. The Max-SINR algorithm thus has the highest percentage of UEs attaining a throughput equal to their demand, be it 2 or 4 Mbps. The tendency for full-duplex Proportional Fair to allocate resource more fairly is also visible. No full-duplex Proportional Fair UE attained a throughput less than 0.75 Mbps. All other algorithms have UEs which have been totally denied resources. The Jain fairness index reflects this, with full-duplex Proportional Fair having an index value of 0.95, compared to 0.73 for full-duplex Max-SINR.

3.8.3 Effect of Clustering on UE Performance

In this subsection, we study the effects of UE clustering on the performance of our algorithms. The cell has 20 UEs, 10 uplink (UL), and 10 downlink (DL), with 50 RBs to be allocated.

The throughput demand is 2 Mbps. The SIC value is set to 10^{11}. All other parameters remain as in Table 3.3. We form a cluster containing all 20 UEs. The circular cluster's center is 50 m away from the BS, and has a radius of 10 m. The clustering of UEs means bringing them closer to each other. As such, the intra-cell co-channel interference would spike. This affects the SINR of downlink UEs in a full-duplex system as illustrated in equation (3.2). Therefore, we plot the uplink and downlink UE throughput values separately. Figure 3.7 has box

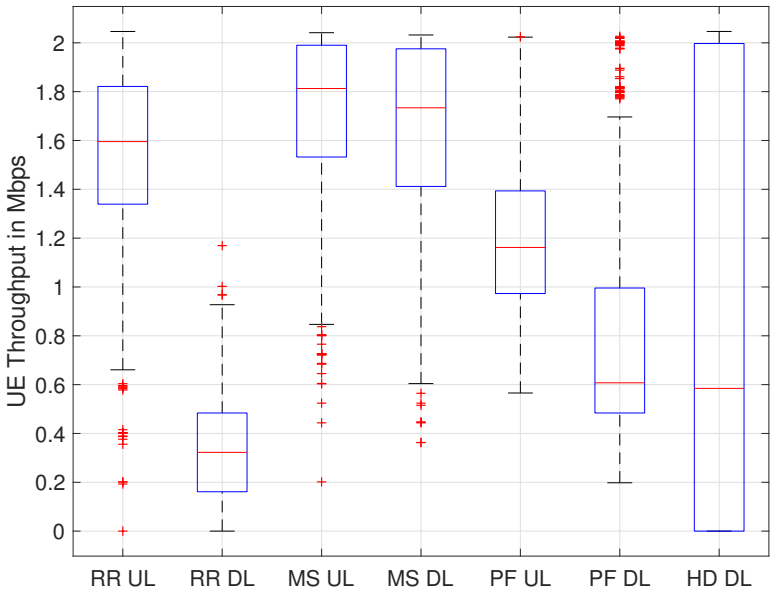

Figure 3.7 Effect of UE clustering on UE throughput

plots of the UE throughput values for this simulation scenario. For all of our full-duplex algorithms, a degradation in performance of downlink UEs, with respect to their uplink counterparts, is expected. The full-duplex Round Robin algorithm UEs suffer the most. Since no method is implemented in this case to avoid scheduling pairs with bad radio conditions, the chance of selecting downlink UEs with bad radio conditions increases. Downlink UEs scheduled with the full-duplex Proportional Fair algorithm also have their throughput values decreased, although to a lesser extent. Nonetheless, because of the small cell size, and the greedy nature of the algorithm, full-duplex Max-SINR downlink UEs are effected the least by the clustering. Following these results, we can argue the need for a hybrid algorithm that could switch scheduling to half-duplex when a certain threshold, below which full-duplex communications are no longer profitable, is reached.

3.8.4 Necessity of Hybrid Algorithms

The effect of UE clustering on the performance of downlink UEs, shown in the previous section, is just a part of the argument for hybridity. We examine the performance of our heuristic full-duplex Max-SINR algorithm, in comparison to that of our hybrid Max-SINR algorithm in the presence of insufficient interference cancellation. The SIC factor is set at the relatively low value of 10^8. The box plots in Fig. 3.8 show the UE throughput per simulation for both downlink and uplink UEs.

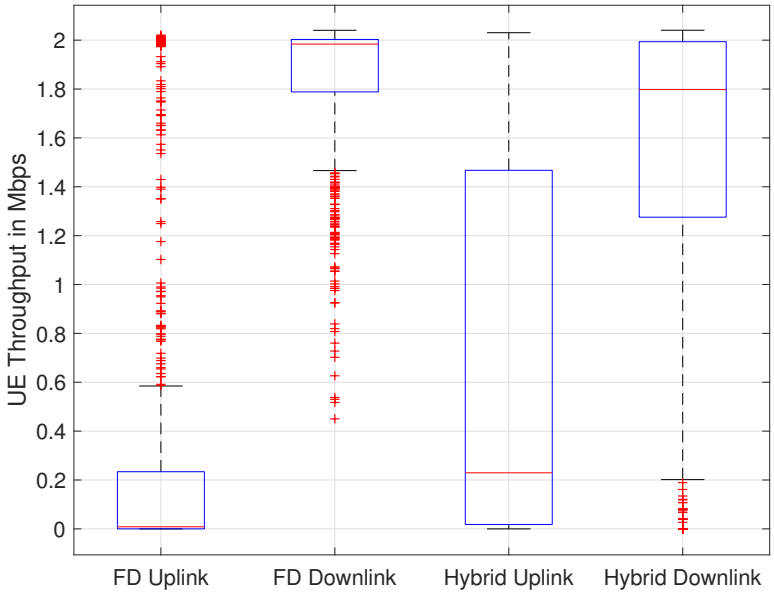

Figure 3.8 Effect of low SIC on UE throughput

Figure 3.8 shows a median on the verge of 0 Mbps average throughput for full-duplex Max-SINR UEs in the uplink. These UEs are completely denied any resources. Self-interference degrades the performance of uplink UEs, as shown in equation 3.1, where the decrease in the SIC factor decreases the uplink UEs' SINR. Downlink UEs do not suffer under low SIC values, however, their good performance in this case is not of importance, as we would not operate a wireless network in which there can be little to no transmission on the uplink. On the other hand, the hybrid Max-SINR algorithm does far better. Almost none of the hybrid algorithm UEs got denied throughput, and the median on the uplink is greater than 200 kbps. Therefore, the availability of a hybrid algorithm improves the performance of the system, especially when UE radio conditions go below that certain threshold where full-duplex communications are no longer profitable.

Finally, we compare our hybrid algorithm to traditional half-duplex Max-SINR schedul-

ing. In the worst case scenario, the hybrid algorithm would choose to allocate all the resource in half-duplex, and would thus match half-duplex Max-SINR's performance. We verify this by showing, in Fig. 3.9, the box plots for the network throughput of 500 simulations runs, for both half-duplex Max-SINR and our hybrid Max-SINR algorithm. The parameters remain unchanged as above for this simulation, with the SIC value still at the relatively low value of 10^8. Figure 3.9 shows that for all the simulations, the hybrid algorithm would attain a higher network throughput than its half-duplex counterpart. Moreover, the median hybrid network throughput is close to 22.5 Mbps, significantly higher than that of half-duplex Max-SINR at about 19 Mbps. In conclusion, not only do we show that is it necessary to have a hybrid option, we also prove that we can still outperform half-duplex operation with only a partial implementation of full-duplex communications.

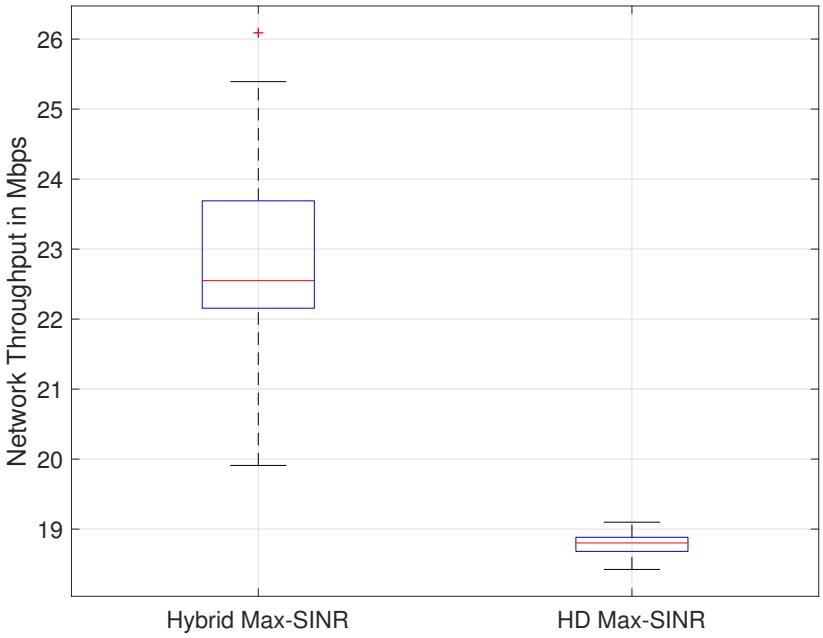

Figure 3.9 HD Max-SINR vs. hybrid Max-SINR. SIC = 10^8

3.8.5 Validity of the Heuristic Algorithms

We seek to verify that our heuristic algorithms produce near optimal performances. To this end, we first simulate our optimal full-duplex Max-SINR and Proportional Fair algorithms vs. their heuristic counterparts. In this simulation, the cell has 10 UEs, and the SIC value is set to 10^{11}. The number of RBs available is 20, and the throughput demand is 2 Mbps. The remainder of the parameters are as in Table 3.3. Figure 3.10 has the box plots for the UE throughputs achieved by each of these four algorithms.

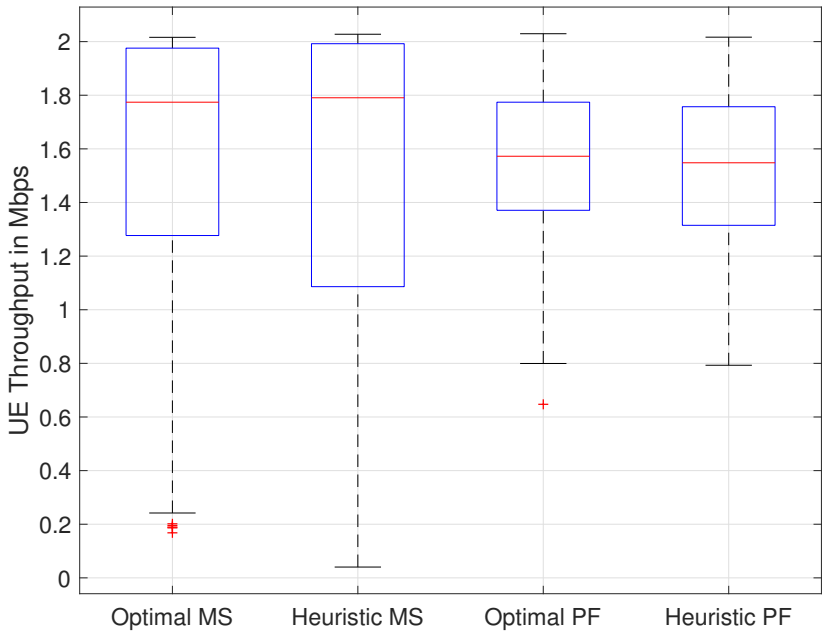

Figure 3.10 Optimal vs. heuristic implementations of the full-duplex algorithms

For both full-duplex Max-SINR and Proportional Fair, the optimal and heuristic box plots are very similar. For full-duplex Max-SINR, both the optimal and heuristic algorithms show a maximum of 2 Mbps and a minimum close to 0 Mbps. The median is around 1.8 Mbps. Nonetheless, the box plot for the optimal Max-SINR algorithm is slightly shifted upwards, indicating that the optimal algorithm does in fact still produce better throughput values for some UEs. The same goes for full-duplex Proportional Fair. The slightly upward shifted box plot for the optimal algorithm shows that some optimal UEs are doing better than their heuristic counterparts, but the vast majority are still performing almost identically. The box plots also highlight the greedy nature of the full-duplex Max-SINR algorithms and the fairness orientation of the Proportional Fair algorithms. The rectangular boxes for the Proportional Fair algorithms are small, indicating that the UE throughput values are close to each other. It is the opposite for Max-SINR, where the long boxes show a big span of UE throughput values, albeit with a gain in throughput for the UEs with good radio conditions. The respective box plots show that more than quarter of the Max-SINR UEs have attained a throughput equal to the demand.

We repeat the same simulation but for hybrid Max-SINR. Figure 3.11 shows a box plot for the ratio between the objective value (sum of SINR) of the heuristic algorithm to that of the optimal algorithm. Except for a few outliers, the heuristic algorithm matches the optimal one with a minimum of 85% of the value, outside of some outliers. In the vast majority of the cases, it matches it with an efficiency higher than 90%.

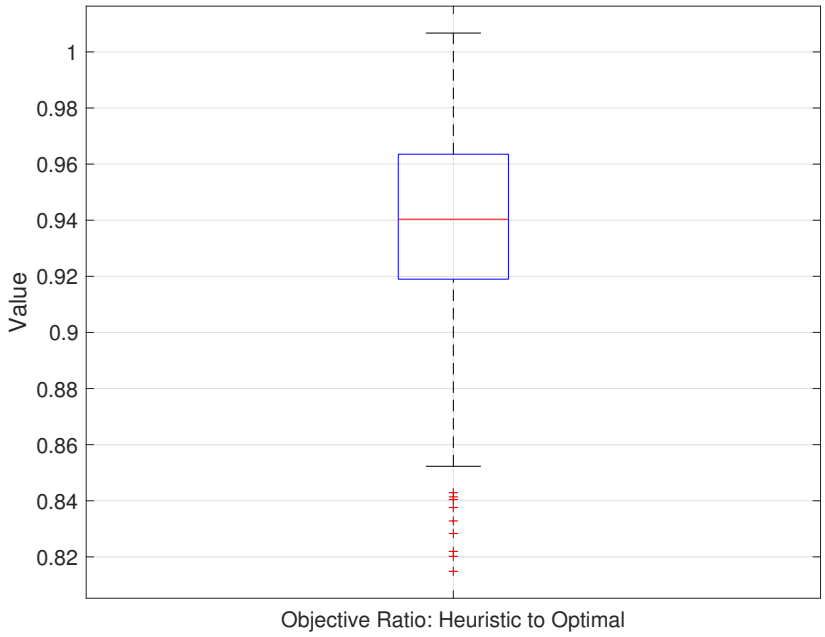

Figure 3.11 Optimal vs. heuristic implementations of hybrid Max-SINR

3.8.6 Effect of the Resource Utilization Factor α_p

For the same simulation parameters used in the previous subsection, we study the effect of varying the resource utilization factor α_p on both the objective of our global optimal problem and the resulting UE throughput values. For this simulation, Max-SINR scheduling is assumed. Figure 3.12 has a CDF plot of the objective values of the optimal problem *i.e.,* the network's sum-SINR. The variation of the objective is tracked for α_p = 0, 0.2, 0.4, 0.6, 0.8, and 1. The lower the value of α_p the higher the objective value is. For α_p = 0 the results vary between 1100 and 2350 dB. As the value of α_p increases, the plots recede. α_p = 0.8 and α_p = 1 produce the lowest objectives values.

Furthermore, we plot the UE throughput values corresponding to the previous simulation. Figure 3.13 has a CDF plot with the results. Opposite to the objective value, the higher the value of α_p the better the algorithm seems to perform. For α_p = 0 about 29% of the UEs are totally denied throughput. Only about 18% of the UEs attain a throughput equal to the demand. For α_p = 0.6, the median throughput value increase to about 1.4 Mbps. For α_p= 0.8, it is around 1.65 Mbps.

Even though the relation between the objective function and the attainable throughput values is inversely proportional with respect to the value of α_p, it is not contradictory. A lower value of α_p would allow the scheduler to regularly select the UEs with the highest SINR values. Nonetheless, those UEs might not always have any bits to transmit/receive. In the case we simulated above, α_p = 1 produces the best results in terms of UE throughput values.

The optimal value for α_p will always lie in the vicinity of 1 but it would vary depending on the simulation scenario. As a result, in our simulations in this chapter, and in all subsequent uses of the optimal formulation, we consider $\alpha_p = 1$ as it guarantees that no resources are wasted, even if it is not the optimal value.

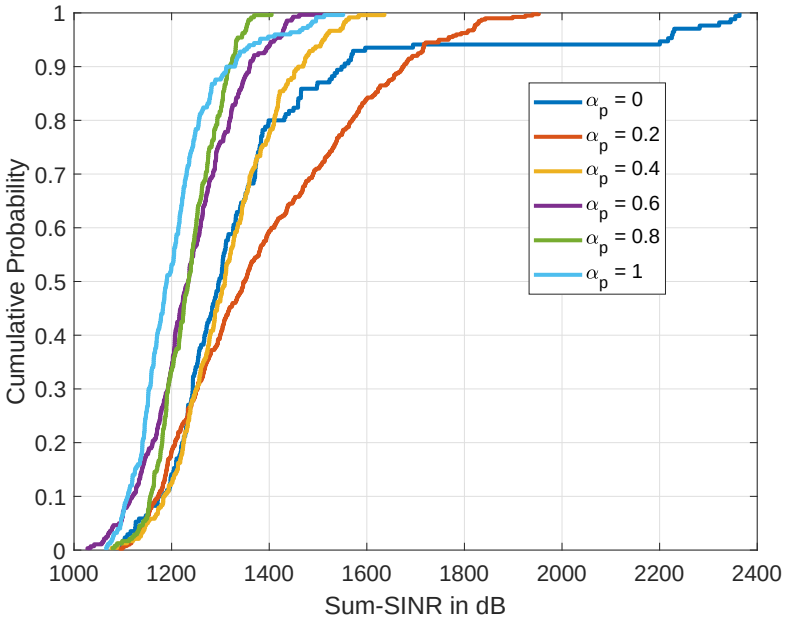

Figure 3.12 The objective of the optimal formulation as a function of α_p

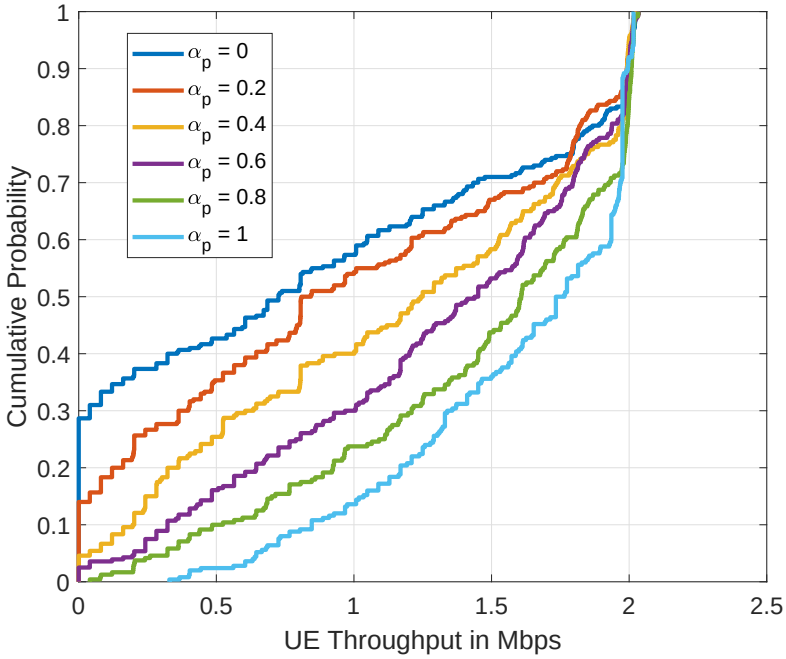

Figure 3.13 The objective of the optimal formulation as a function of α_p

3.9 Conclusion

In this chapter, we presented a generic optimal scheduling algorithm for full-duplex and hybrid full-duplex/half-duplex wireless networks. We implemented this algorithm with different scheduling objectives. With focus on UE SINR, we proposed an optimal full-duplex Max-SINR algorithm that allocates resources to UE pairs with the highest sum-SINR. We additionally proposed an optimal hybrid Max-SINR algorithm that chooses between allocating resources in half-duplex or full-duplex depending on the UE SINR values. With focus on fairness, we proposed an optimal full-duplex Proportional Fair algorithm that allocates resources to UE pairs that have the highest priority. Similarly, we proposed an optimal hybrid Proportional Fair algorithm that can choose to allocate the resources in half-duplex or full-duplex depending on the UE priorities. We then proposed heuristic versions of these four algorithms, and proved that their performance is near optimal. Under different simulation scenarios, we illustrated the gains full-duplex wireless networks provide in comparison with current half-duplex networks, and we verified that the hybrid algorithms provide a good alternative to full-duplex scheduling in the case of low SIC. We showed that with sufficient SIC, full-duplex communications can almost double the throughput for the UEs while cutting the waiting delay in half.

Chapter 4

Scheduling with Incomplete Channel State Information

4.1 Introduction

In the previous chapter, we presented our approach to scheduling in full-duplex wireless networks in the presence of complete channel state information (CSI). Nonetheless, there is still no evident manner in which full-duplex networks can achieve this state of completeness. After all, no existing wireless network protocols count for estimating inter-user channels or for how such channel information could be relayed back to the base station (BS). In order to properly schedule and distribute resources among pairs of uplink-downlink user equipment (UEs), the network needs exact information on the channels between all the UEs, in addition to all the traditional half-duplex UE-to-BS channels. In a single small cell network of five uplink and five downlink UEs, the BS would have to be continuously updated with information on up to 35 radio channels. Ten of which are of type UE-to-BS and 25 of type UE-to-UE. A number that would dramatically increase in large cell scenarios. Considering that scheduling is done on a small time scale (ms), scheduling with complete CSI is rendered even more complex with a signaling overhead further burdening the UEs. In this chapter, we address the consequences of scheduling in full-duplex wireless networks with incomplete CSI, and afterwards put forward a reinforcement learning scheduling algorithm that can allocate radio resources without the need for such information.

4.2 The Effect of Incomplete Channel State Information

The state of a wireless channel is determined by the combined effect of several factors, the most pertinent of which, are the path loss, the shadowing, and the fast fading. Knowledge of the channel on a certain wireless link permits adapting the transmission to the communication channel. This is essential in achieving reliable communications, and for making efficient resource allocation decisions.

Legacy half-duplex wireless networks would rely on feedback from the UEs to determine the current channel state. These networks are concerned mainly with the channel in between the BS and the UEs, and different techniques are used to determine how often, and on which resource blocks (RBs), would this feedback information be required. Because channel conditions are constantly varying, the CSI needs to be estimated on a short-term basis. It also needs to be relayed back to the BS within the channel coherence time, else this information would be nugatory.

Full duplex communications add to the complexity of determining the CSI. In full-duplex networks, additional information on the channel in between the UEs of a certain pair is required. Not only do current wireless systems not count for such information, there is also no implemented method for which a UE can estimate such UE-UE channels. Additionally, it is perceivable that continuously updating such information by the UEs would cause excessive overhead and loads that UEs cannot handle. Consequently, precisely estimating inter-UE channels might not be feasible. As we previously indicated, we statistically model the inter-UE channel as follows:

$$h_{ij,k} = G_t G_r L_p A_s A_f, \tag{4.1}$$

where G_t and G_r are the antenna gains at the transmitter and the receiver, respectively. L_p represents the path loss, or equivalently the mean attenuation the signal undergoes in this channel. A_s and A_f are two random variables that respectively represent the shadowing effect, and the fast fading effect.

In this chapter, we aim to assess the vitality of inter-UE CSI to the functioning of a full-duplex network. To this end, we examine the components of the statistical CSI of the inter-UE channels, jointly and independently. We simulate our proposed algorithms for multiple scenarios of CSI availability. First, we assume that the inter-UE channel information is completely unavailable. Second, we consider that the path loss component of the CSI is available to the scheduler at the BS. Since the path loss is related to the distance between the UEs, we assume that the presence of a geographical positioning system helps estimate it. Finally, we assume that the shadowing information is also available. This would form an additional level of complexity that we consider is possible to model, if knowledge of

the terrain is present. Additionally, the path loss and the shadowing vary less often than other factors, such as the fast fading. It would need less periodical updates to convey such information to the BS. Our aim is to study the impact of the lack–as well as the partial availability–of inter-UE channel information on the performance of a full-duplex wireless network. These three scenarios of CSI availability are simulated and compared to the optimal case, where the CSI is completely known at the BS.

4.2.1 Simulation Parameters

The parameters used to run the simulations in this section are presented in Table 4.1 below.

Table 4.1 Simulation parameters for scheduling with incomplete CSI

Parameter	**Value**
Cell Specifications	Single-Cell, 120 Radius
Number of RBs	50
BS Transmit Power	24 dBm
Maximum UE Transmit Power	24 dBm
SIC Value	10^{11}
Number of UEs	10DL, 10UL
Demand Throughput	2 Mbps

4.2.2 Effect Of Incomplete CSI on Greedy Allocation

In this section, we study the effect of incomplete CSI on UE throughput in the case of greedy resource allocation. Note that under our simulation parameters of 50 resource blocks and 20 UEs, the system is considered to be under heavy load conditions. The channel in between a pair of UEs is the focus of our work.

We simulate multiple scenarios of CSI availability for our full-duplex Max-SINR algorithm presented in the previous chapter. Figure 4.1 is a CDF plot of the throughput attained by the UEs across the different simulation scenarios. For reference, a traditional half-duplex Max-SINR algorithm is simulated under complete CSI. The throughput attained by full-duplex Max-SINR UEs when the channel state information is complete is the highest among those simulated. Around 70% of those UEs attained a throughput equal to the demand, with the lowest UE throughput recorded being around 300 kbps. The performance of UEs degrades depending on the channel estimation error. The lack of any information on the inter-UE channels incurs the most degradation in performance. In this case, about 12% of the UEs attain zero throughput, with the rest of the UEs transmitting with a rate lower than the

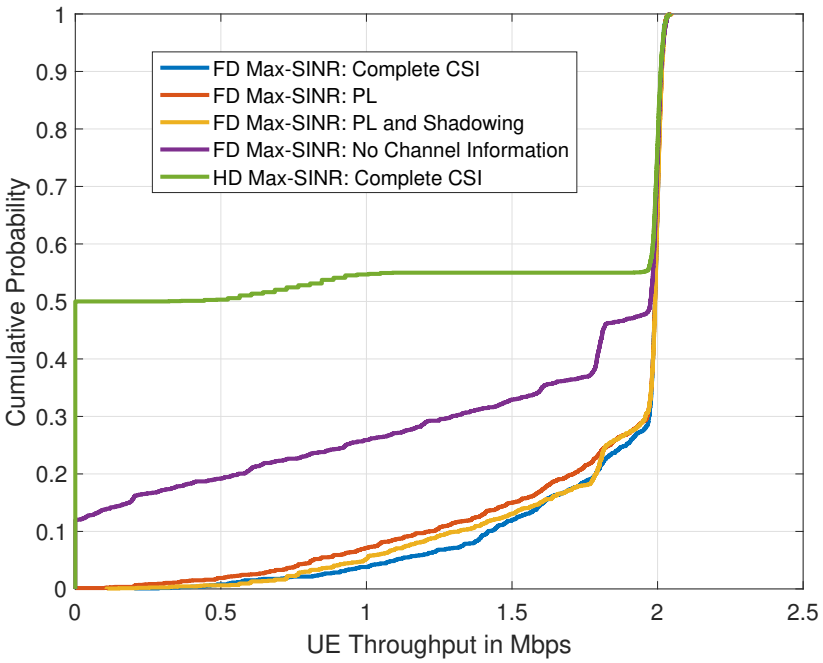

Figure 4.1 Effect of incomplete CSI on full-duplex Max-SINR

optimal case. The performance of the algorithm improves when parts of the channel become known at the BS. When the path loss information is available, full-duplex Max-SINR UEs show substantial improvement in performance, where almost half of the UEs got an average increase in throughput close to 1 Mbps. When the shadowing information is also available, the number of UEs which were denied throughput drops to zero, with 150 kbps being the lowest attained UE throughput. In both these cases however, the performance of the UEs is still degraded when compared with the case for complete CSI. Nonetheless, full-duplex Max-SINR outperforms half-duplex Max-SINR regardless of the channel estimation errors. Under these simulation parameters, almost 50% of the half-duplex UEs were denied throughput, compared to 12% the worst case scenario for full-duplex. In addition, for any UE simulated, the throughput attained by a full-duplex UE is higher than that attained by a half-duplex UE. To conclude, it is evident that scheduling without complete information on the channel between the UEs degrades the performance of full-duplex networks, but this performance remains much better than that of traditional half-duplex Max-SINR scheduling.

4.2.3 Effect Of Incomplete CSI on Fair Allocation

In this section, we study the effect of incomplete CSI on fair scheduling techniques. Figure 4.2 has box plots of the resulting UE throughputs for our full-duplex Proportional Fair algorithm under different scenarios of CSI availability. A half-duplex Proportional Fair algorithm is

also simulated under complete CSI.

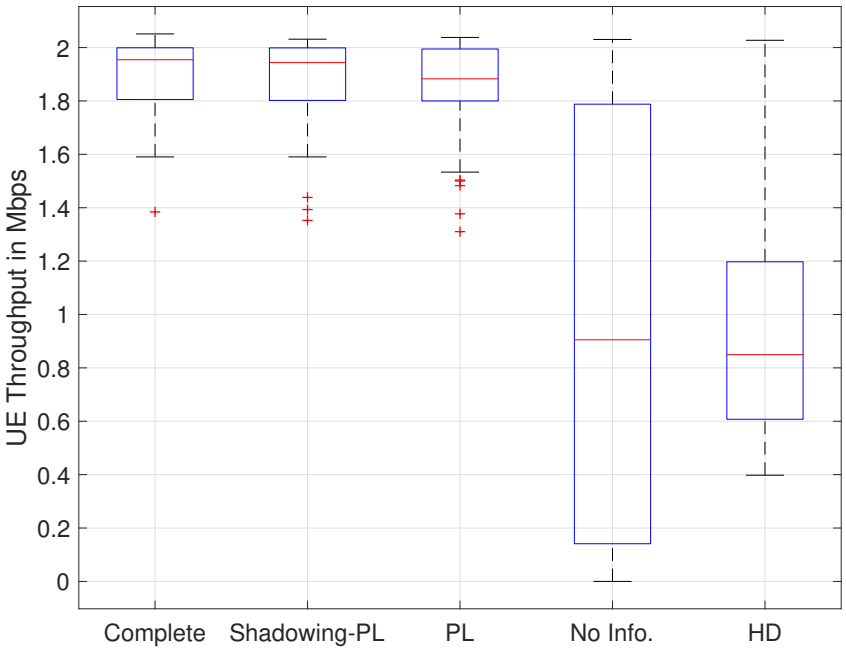

Figure 4.2 Effect of incomplete CSI on full-duplex Proportional Fair

Similar to the case of full-duplex Max-SINR, the lack of CSI deteriorates the performance of the algorithm, and the presence of partial CSI is sufficient for near-optimal performance. Nonetheless, in the case where no information on the inter-UE channel is available, the median value for UE throughput dropped more than 1 Mbps, and the gains with respect to half-duplex Proportional Fair become questionable. Although the full-duplex algorithm maintains higher UE throughput values for the majority of the UEs, the fairness of the algorithm is severely struck. This can be inferred from the size of the box corresponding to no CSI information, where it spans nearly all the possible values. This effect is due to the nature of the algorithm, where the scheduling decision at a certain instant is tied to the previous one in terms of transmitted bits. This incurs that a previously erroneous decision will be carried on and even magnified.

4.2.4 On Scheduling with Incomplete CSI

In the first part of this chapter, we studied the effects of incomplete CSI on scheduling in full-duplex wireless networks. We showed that significant losses in performance were to be expected when inter-UE CSI is not present at the scheduler. Furthermore, the losses incurred are likely to massively increase in the cases of low SIC or when UEs are situated farther away from the BS. In our work, we sought an alternative for knowing the exact states of the inter-

UE channels. As such, we introduce a reinforcement learning based scheduling algorithm for full-duplex wireless networks. Inter-UE channel information is not a prerequisite for this scheduling approach which rather learns how to best allocate the network's radio resources.

Multiple articles in the state-of-the-art have previously addressed utilizing machine learning to tackle intricate scheduling tasks. The authors in [54] propose a learning based approach to address multiple cellular network challenges such as limited data availability and convoluted sample data. The papers in [55] and [56] propose using deep learning to schedule resources in half-duplex wireless networks. The authors in [57] present a machine learning based antenna selection algorithm for wireless networks. These and countless others applications of machine learning in wireless networks exist in the related works [58]. Nonetheless, our approach in using reinforcement learning to schedule resources in full-duplex wireless network was a first.

In what follows, we detail our approach to reinforcement learning scheduling. We show that our proposal can match scheduling with complete CSI in terms of user equipment throughput, and that it performs well under multiple testing scheduling scenarios: increased UE numbers, randomized UE demand, and UE clustering, among others.

4.3 The Reinforcement Learning Problem

In this section, we briefly explain the general reinforcement learning problem. Reinforcement learning is the idea of learning from interaction to achieve a goal [59]. The learner *i.e,* the decision maker in such a problem, is known as the agent. Everything else interacting with this agent is known as the environment. The environment and the agent interact at a sequence of discrete time steps, t = 0,1,2,3,.... At a moment in time t, the environment is in a state $\mathcal{S}_t$. The agent takes an action A_t from the set of actions available in the current state $\mathcal{A}(\mathcal{S}_t)$. As a consequence of the selected action, the agent will receive a reward $\mathcal{R}_{t+1}$, and subsequently, it will find itself in a new state $\mathcal{S}_{t+1}$. This agent-environment interaction model is shown in Fig. 4.3.

Furthermore, the agent, in a state s, selects an action a with a probability p. This mapping is called the agent's policy, and is denoted π_t. $\pi_t(a|s)$ is thus the probability that $\mathcal{A}_t = a$ if $\mathcal{S}_t = s$. As time progresses, a reinforcement learning algorithm should change its policy following the experience it has gained. The agent's goal when implementing new policies is to maximize the received rewards. Reinforcement learning casts a wide net. Its framework is flexible and can be applied to different problems and via several ways. In what follows, we implement the abstract of reinforcement learning on the problem of scheduling in full-duplex wireless networks.

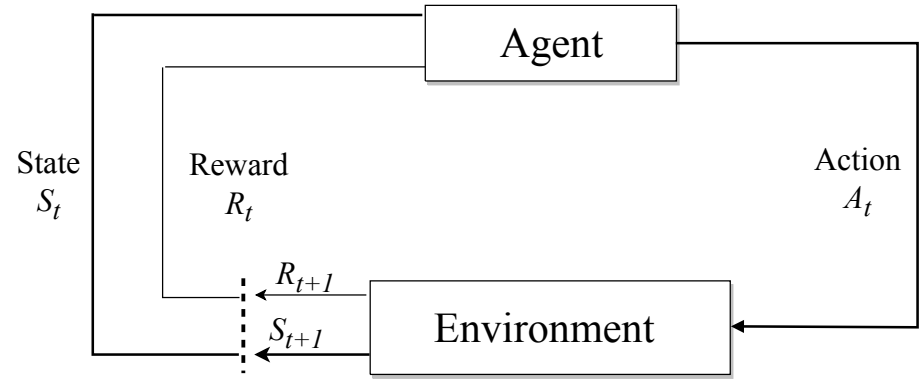

Figure 4.3 Reinforcement learning model

4.4 Reinforcement Learning Scheduling Algorithm

Let $p_{ijk}(t)$ be the probability that uplink UE i gets paired with downlink UE j on RB k, during TTI t. The sum of all pairing probabilities is equal to 1 for each RB k $i.e$, $\sum_{i\in\mathcal{U}}\sum_{j\in\mathcal{D}} p_{ijk}(t)$ = 1 $\forall\ k \in \mathcal{K}$, $\forall\ t$. Let θ_{ij} be a binary value that is equal to one if pair (i,j) is allocated RB k, and 0 otherwise. At $t = 0$, and at the beginning of the scheduling process, all possible UE pairings have equal probabilities of getting any resource. After any RB is allocated, the probabilities are updated as follows.

$$p_{ijk}(t+1) = \begin{cases} p_{ijk}(t) + \beta\mathcal{R}(1 - p_{ijk}(t)), & \text{if } \theta_{ij} = 1, \\ p_{ijk}(t) - \beta\mathcal{R}p_{ijk}(t), & \text{otherwise,} \end{cases} \tag{4.2}$$

where β is the learning rate, chosen between 0 and 1, and $\mathcal{R}$ is the reward. The reward is evaluated as the number of bits the UE pair has transmitted/received (T_{ij}) on the allocated RB, divided by the maximum number of bits (T_{max}) the UE pair could ideally send/receive over the channel on the RB $i.e$, if it was alone in the cell and using the highest modulation order and coding rate. T_{max} is constant for all pairs. The reward is as such chosen in direct relation to a pair's radio conditions. The algorithm will reward UE pairs which best utilize the RBs, thus using the network bandwidth with utmost efficiency, without the need for inter-UE channel information. The more frequently a pair makes good use of the RB, the more likely it is to get it within subsequent time slots. In case an RB is not allocated as a result of all UE queues being empty, the probabilities remain intact. $\mathbf{P}$ is a 3-D matrix containing all the variables p_{ijk}.

The learning rate β controls both the speed with which the algorithm converges towards a preferred scheduling choice, as well as its efficiency. A high value of β would incur that the algorithm arrives at a preferred choice quicker, but it would be a less efficient one. Ideally,

we want to chose the highest value of β that would always lead to a good scheduling decision with respect to maximizing UE throughput values.

In our problem, the agent is the scheduler at the BS. The environment is the UEs, as well as the resulting UE radio conditions after the pairing decisions. The reward is expressed in terms of bits transmitted by a UE pair on an allocated resource. Finally, the action is the process of selecting a UE pair to allocate an RB to.

4.5 Challenges

Scheduling via a reinforcement learning algorithm poses several problems and challenges. In this section, we highlight these challenges and go over our approaches in tackling them.

Non-Full Buffer Traffic

In our work, we focus on non-full buffer traffic scenarios. As such, any UEs which have emptied their queue within an allocation round, should be excluded from the scheduling process in the following one. UEs will be leaving and rejoining the network. Subsequently, all pairs which have an excluded UE should have their selection probability set to 0. Furthermore, when an excluded UE has new arrivals, it is re-factored into the scheduling task. With it are all the possible pairs within which this UE is contained. This raises another problem, what probabilities should these pairs take then ?

We address this problem by introducing a temporary probability matrix $\mathbf{V}$ with pair-resource probability values v_{ijk}. At the beginning of each TTI, $\mathbf{V}$ will hold a copy of $\mathbf{P}$. Resources are allocated within the current TTI according to the temporary matrix. After an RB is allocated, $\mathbf{P}$ is updated following equation (4). When a UE empties its queue within a TTI, all pairs containing this UE have their probabilities in $\mathbf{V}$ set to 0. This insures that this UE will not get allocated anymore resources within the same TTI. The values of the remaining probabilities are normalized, $i.e.$, each probability, for a certain RB, is divided by the sum of the remaining probabilities. This keeps the sum of probabilities equal to one, unless of course all UE queues are empty. New arrivals are expected at the beginning of the new TTI (at least a limited number of bits). All UEs are now back in the scheduling process and the temporary matrix $\mathbf{V}$, used for allocation, gets its values from the up-to-date $\mathbf{P}$. The pseudo-code for the reinforcement learning algorithm is presented in Algorithm 5. Note that the total number of possible UE pairings $\mathcal{N}$ is defined as the number of uplink UEs multiplied by the number of downlink UEs.

Algorithm 5 RL Scheduling Algorithm

Requires: Set of states $\mathcal{S}$, actions $\mathcal{A}$, and rewards $\mathcal{R}$
Input: Learning rate $\beta \in [0,1]$
Initialize: $p_{ijk}(1) \leftarrow \frac{1}{\mathcal{N}}$, $\forall\ (i,j,k) \in (\mathcal{U} \times \mathcal{D} \times \mathcal{K})$
for TTI t=1,...,T
  $\mathbf{V} \leftarrow \mathbf{P}$
  for k=1,...,K
    Draw a pair according to the probabilities in $\mathbf{V}$
    Allocate k to the drawn UE pair $(i'j')$
    Compute $\mathcal{R} = T_{i'j'}/T_{max}$
    for $(i,j,k) \in (\mathcal{U} \times \mathcal{D} \times \mathcal{K})$
      if $\theta_{ij} == 1$
        $p_{ijk}(t+1) \leftarrow p_{ijk}(t) + \beta\mathcal{R}(1 - p_{ijk}(t))$
      else
        $p_{ijk}(t+1) \leftarrow p_{ijk}(t) - \beta\mathcal{R}p_{ijk}(t)$
      end if
    end for
    if i' emptied its queue
      $v_{i'jk}(t) = 0$, $\forall\ (j,k) \in (\mathcal{D} \times \mathcal{K})$
      Normalize $\mathbf{V}$
    end if
    if j' emptied its queue
      $v_{ij'k}(t) = 0$, $\forall\ (i,k) \in (\mathcal{U} \times \mathcal{K})$
      Normalize $\mathbf{V}$
    end if
  end for
end for

Exploration and Exploitation

Our proposal makes it feasible to account for dynamic traffic. With UEs constantly leaving and joining back, the algorithm would not always select the same UE pair for any RB. Every allocation the algorithm deems most suitable to maximize throughput values is only temporary, and bound to change once the pair(s) exits the allocation process or the radio conditions change. This makes our reinforcement learning algorithm similar to that of an ϵ-greedy one, where the algorithm will go into exploration with a probability ϵ [59]. However, in our case, the value of ϵ is determined by the demand of the UEs. For a low UE demand, ϵ is relatively high, and the algorithm could fall back into exploration several times within the same TTI. In the case of full buffer traffic, ϵ is equal to zero, and the algorithm would

never go into exploration. Since we implement a non full-buffer traffic model, it is counter intuitive to manually assign a value for ϵ.

Online Learning and Dynamic Radio Conditions

As a result of shadowing and the time variant fast fading, any suitable pair selected by the learning algorithm to maximize UE and network throughput values, will not remain the best choice over the following TTIs. The radio conditions of each UE pair are bound to change from one TTI to another. In the case of non-full buffer traffic, this does not pose a major problem. After all, the algorithm is bound to regularly go into exploration mode. In all cases, our learning algorithm cannot be expected to find the relatively best allocation within one TTI. As such, it is correct to assume that the algorithm is learning the average radio conditions of the UE pairs across the TTIs, rather than the instantaneous ones. This is bound to be somewhat costly with respect to a greedy allocation method with full CSI.

Because of our non full-buffer traffic model, dynamic arrivals, as well as the varying radio conditions, our algorithm is constantly learning. The dynamics of the network imply that the UE pair that would maximize UE and network throughput on a certain RB is constantly changing. We show, via our simulations, that our algorithm is capable of adapting to this change, as the allocation probabilities per RB are updated each TTI.

Positive Reinforcement

In our proposal, we always use a positive payoff. Unless a selected UE pair transmits zero bits, its probability of selection would always increase, no matter how slightly, for the next TTI. In the context of our simulation scenarios, we cannot determine if the number of bits a certain UE pair sent/received is good enough or not. A UE pair situated away from the BS might return a small reward, but it could still be among the best performing pairs in the current network. Using a negative payoff, *i.e.,* reducing the probability of selection for this pair, could in fact set the algorithm farther away from reaching its goal of maximizing UE and network throughput values.

4.6 Simulation and Results

We seek via our different simulation scenarios to address the validity and practicality of our machine learning scheduling proposal. First, and as the research into full-duplex communications shifts from micro to macro cells, we assess the performance of our algorithm in a larger cell scenario. Second, we test the limits of our proposal, and show that with adequate

parameters, it can match the performance of scheduling with complete CSI. Additionally, we test our algorithm under different circumstances: variable UE traffic, increased UE numbers, low SIC values, and UE clustering among others.

Table 4.2 Simulation parameters for reinforcement learning based scheduling

Parameter	**Value**
Cell Specifications	Single-Cell, 120,500,1000 m Radius
Number of RBs	50
SIC Value	10^{11} or 10^{9}
Number of UEs	5DL, 5UL or 10DL, 10UL
Demand Throughput	4 Mbps
TTI Duration	1 ms

The simulation parameters we used are presented in Table 4.2. In assessing the performance of our algorithm, we do not take into account the first few TTIs (up to 10% of the total) where the allocation process can be arbitrary. In section 4.6.1 of the simulations the value of β is varied between 0.015 and 0.9 in order to study the significance of the learning rate. In the remainder of the simulations, the value of β is fixed at 0.015. This value of β guarantees the learning algorithm explores enough to find the pairs that maximize UE and network throughput every time.

4.6.1 Effect of the Learning Rate β

Case of small cell

We seek to study the effect of varying the learning rate on the performance of the algorithm. We consider a small cell of radius 120 m, the cell has 10 UEs: 5 uplink and 5 downlink. The throughput demand is 4 Mbps. The UE throughput values attained for β = 0.1, 0.3, 0.5, 0.7, and 0.9 are plotted in the CDF plot of Fig. 4.4.

For reference, a greedy full-duplex Max Sum-Rate algorithm we enhanced is also plotted. This algorithm allocates resources to UE pairs that can get the highest throughput values. This makes it an ideal reference to the performance we expect from a full-duplex system which has complete channel knowledge. Additionally, we plot a random resource allocation scheme in our full-duplex Round Robin algorithm, and a fair allocation scheme in our full-duplex Proportional Fair algorithm. These three algorithms are simulated with complete CSI. For β = 0.1, around 70% of the learning algorithm UEs attained a throughput equal to their demand of 4 Mbps. This is almost identical to the full-duplex Max Sum-Rate algorithm. As the value of β increases, the number of UEs attaining the nominal throughput value decreases. For β =

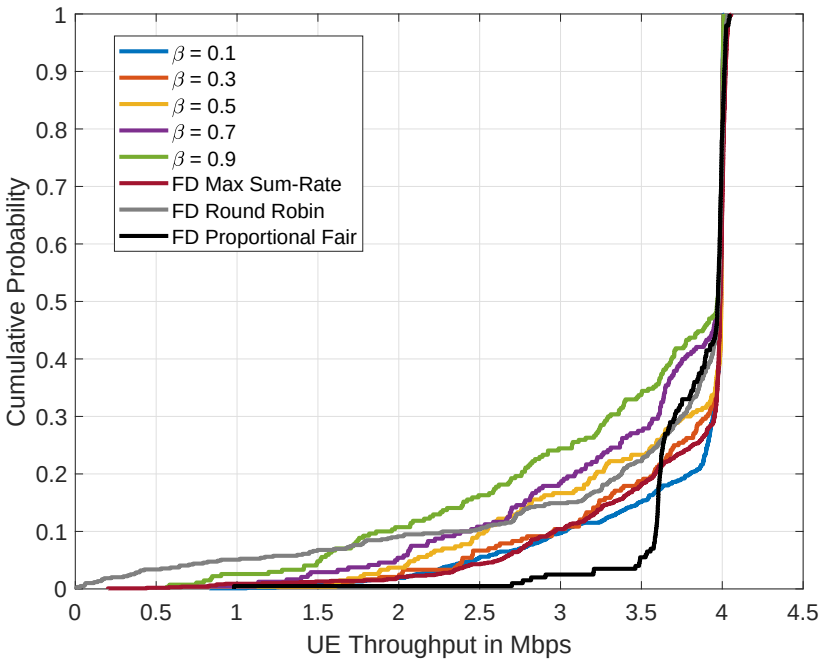

Figure 4.4 Throughput as a function of the learning rate β in a small cell

0.9, only about 50% of the simulated UEs attain a throughput equal to their demand. The resource allocation process becomes near random for this value of β, hence the similarity to the full-duplex Round Robin algorithm. Moreover, the plot for full-duplex Proportional Fair contrasts the difference in objectives with respect to our greedy algorithm. Only about 55% of the full-duplex Proportional Fair algorithm UEs got a throughput equal to the demand of 4 Mbps, significantly lower than the 70% for our learning algorithm. However, for all except one of the Proportional Fair UEs, the lowest recorded throughput value is 2.7 Mbps, significantly larger than 0.6 Mbps, the lowest recorded value for our learning algorithm (for $\beta = 0.1$). Our learning based algorithm is greedy and seeks to extract the utmost gain from the bandwidth, while full-duplex Proportional Fair seeks to balance between bandwidth efficiency and achieving fairness between the UEs.

Finally, as we illustrate later on, the lower the value of β, the more likely it is that the learning algorithm identifies the best pair to allocate each RB to. Nonetheless, it would take longer for the algorithm to find this pair. That is to say that the higher the value of β is the quicker the algorithm can react to a change in the network, albeit at the cost of making more incorrect scheduling decisions with respect to maximizing UE throughput values.

Case of large cell

Whilst full-duplex communications are most suitable for small cells, the current state-of-the-art cancellation technologies allow mitigating self-interference by values up to 110 dB. This means that medium to large cell scenarios are pretty feasible. We repeat our simulation from the previous section, albeit with a cell radius of 500 m. This change in cell size, with the transmission powers being fixed, is bound to put more UEs in disadvantageous radio conditions. Cell edge UEs are more likely to have low SINR values. A bad scheduling decision is now more heavily punished. The results are shown in Fig. 4.5.

For $\beta = 0.1$, about 30% of the UEs attained a throughput equal to the demand. The full-duplex Max Sum-Rate proposal attained a value close to 47%. Similar to before, the higher the value of β, the lower the performance of the algorithm. For $\beta = 0.5$, only about 25% of the UEs attained a throughput equal to the demand. Nonetheless, the gains with respect to HD wireless communications remain evident. HD Max Sum-Rate UEs has more UEs attaining a throughput equal to the demand in comparison to our reinforcement learning proposal ($\beta = 0.5$). Nonetheless, it also has about 30% of the UEs with zero throughput. Almost none of the service based learning UEs, regardless of the value of β, are denied throughput.

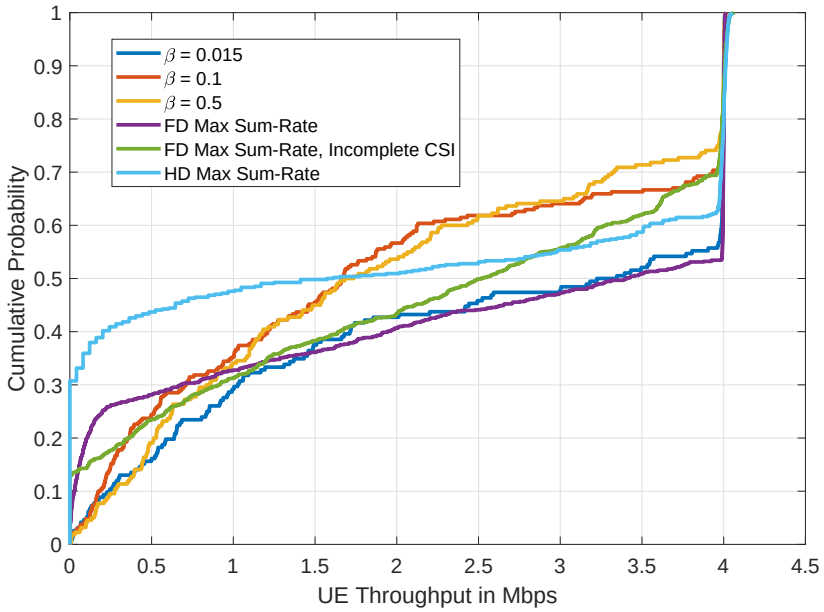

Figure 4.5 UE throughput as a function of β. 500 m cell radius

Additionally, we compare our machine learning solution to a full-duplex Max Sum-Rate algorithm simulation done without any information on the UE-UE channels. In such a case, almost 13% of the UEs were denied service, and 30% of the UEs attained a throughput

equal to the demand. The performance of our algorithm for $\beta = 0.1$ thus barely outperforms scheduling with incomplete CSI. As such, we lower the value of the learning rate and simulate our learning algorithm for $\beta = 0.015$. In this case, our proposal can better match the performance of scheduling with complete CSI with about 44% of the UE attaining a throughput equal to the demand and less than 1% of them being denied throughput.

Selection of the value of the learning rate

In our aim to deduct the best value for β, we simulate our algorithm for different values of the learning rate β and record how the algorithm would fare in terms of total network throughout with respect to scheduling with complete CSI, in each time slot. Figure 4.6 has a logarithmic scale plot with the results for $\beta = 0.015$, 0.1, and 0.5 for one simulation run across 6000 TTIs. In this simulation, and for the purpose of better distinguishing between the results, the radius of the cell is increased to 1 km. A wrong scheduling decision could now be more costly for the network.

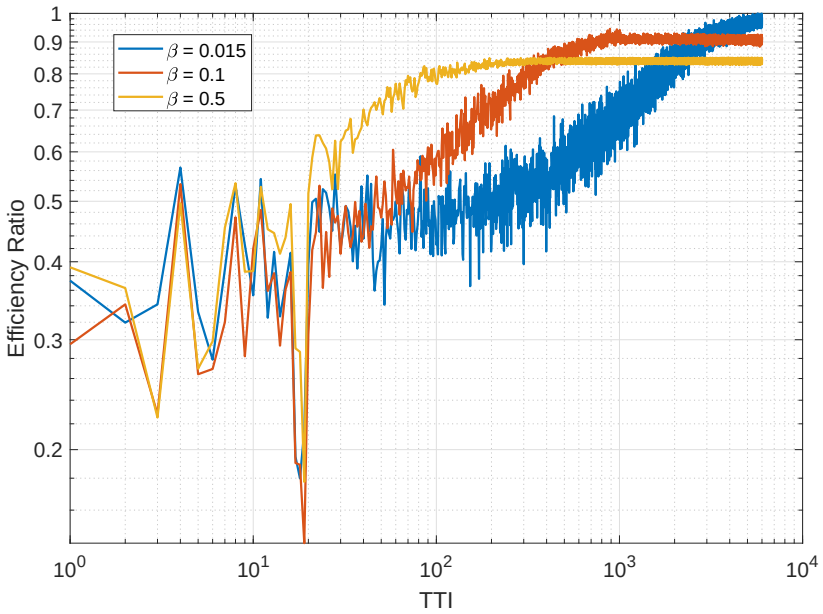

Figure 4.6 Efficiency of the algorithm as a function of time and β

For $\beta = 0.5$, the algorithm will reach an efficiency of about 85% in 200 TTIs. It no longer improves. For $\beta = 0.1$, the algorithm will take about 1000 TTIs to reach an efficiency of 90% where it no longer improves on average. For $\beta = 0.015$, the algorithm is shown to be constantly improving. For this simulation, it would eventually reach upwards of 99% efficiency. A lower value of β would eventually lead to better efficiency, but at the cost of requiring more time to do so.

Since the value of $\beta = 0.1$ can barely outperform scheduling with incomplete CSI as illustrated in Fig. 4.5, a lower value of β is required for our macro-cell simulations. As such, for the remainder of the simulations, the value of β is set to 0.015.

4.6.2 Performance evaluation as a function of time

At the beginning of the simulation, the allocation process by our learning algorithm can be said to be arbitrary. Nonetheless, each TTI the algorithm learns how to better allocate resources in a manner that maximizes UE and network throughput. For a 500 m cell radius, and a value of $\beta = 0.015$, we track the progress of our algorithm as a function of time.

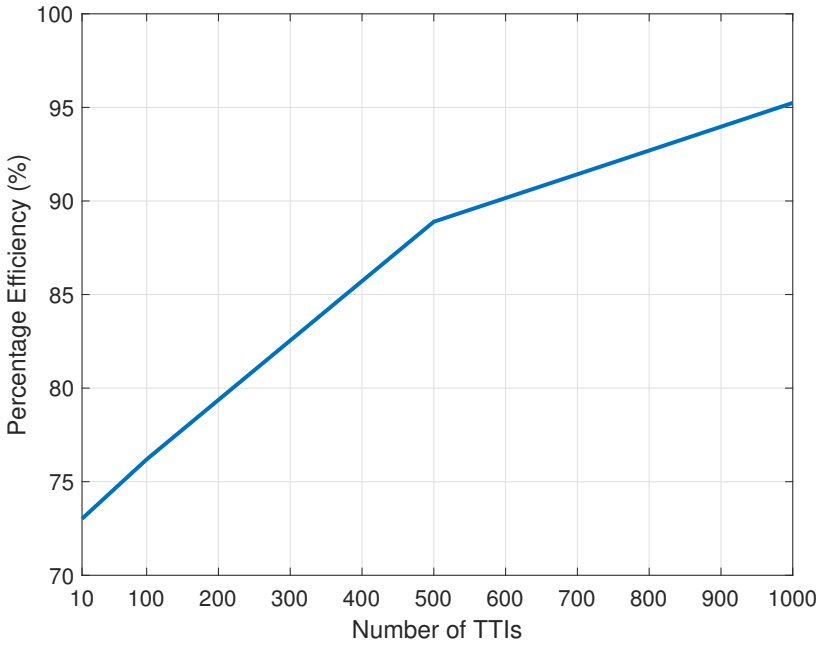

Figure 4.7 Efficiency of the learning algorithm as a function of time

We define the efficiency of the algorithm as the total network throughput attained by the learning algorithm divided by that attained by the full-duplex Max Sum-Rate algorithm (with complete CSI). As explained before, we consider the latter to be a reference due to the similarity in objectives. Figure 4.7 has a plot with the results. 10 TTIs, equivalently 10 ms, are enough for the algorithm to reach a 73% efficiency. At 1000 TTIs, or 1 s, the learning algorithm achieves about 95% of the throughput attained by full-duplex Max Sum-Rate. From these results we can conclude that the learning algorithm can respond quickly to changes in the network, whether caused by dynamic radio conditions (Rayleigh fading channel), UEs leaving or rejoining the network, or even UE mobility.

4.6.3 Proximity to Greedy Scheduling with Complete CSI

Whilst our learning algorithm can still provide good results in cases where wrong decisions are heavily punished (4.6.1), it still clearly trails scheduling with complete CSI. Figure 4.5 shows that our algorithm provided less UEs with the required demand, in comparison with full-duplex Max Sum-Rate. We aim to determine how closely our algorithm can mimic the performance of scheduling with complete CSI. The value of β is set to 0.015. This allows the algorithm to make thorougher explorations. The rest of the parameters remain as in the previous subsection with 10 UEs present in a 500 m radius cell. For the same UE distributions and radio conditions, we record the number of bits transmitted or received by each UE when scheduled by both our reinforcement learning proposal and by full-duplex Max Sum-Rate scheduling with complete CSI. Let δ be the difference in throughput assigned to the same UEs by the two algorithms. Figure 4.8 shows a CDF plot of the results.

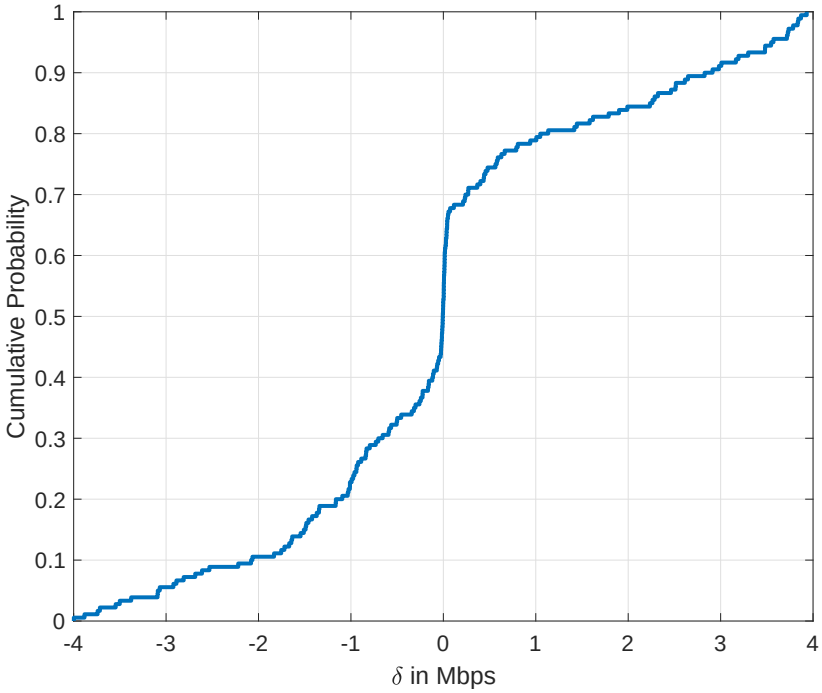

Figure 4.8 Proximity to scheduling with complete CSI

More than 25% of the time, the UEs will get the exact same throughput values. Moreover, the curve is almost perfectly symmetrical with respect to $\delta = 0$. This indicates that even when our learning algorithm decided to give resources differently than full-duplex Max Sum-Rate scheduling with complete CSI, it allocated them to pairs which were doing just as good. In fact, the reinforcement learning approach would lose at most 2% in total network throughput, even though it takes scheduling decisions without any information on the inter-UE channels.

4.6.4 Effect of Varying User Characteristics

In this section, we vary different UE characteristics from randomizing traffic to clustering UEs and increasing UE numbers, and study the effects they have on UE performance. We show that regardless of the scenario at hand, our learning algorithm can mimic the performance of scheduling with complete CSI with high efficiency, and that it remains more profitable than scheduling without information on the inter-UE channels.

Effect of Randomized User Demand

In this subsection, we aim to study the effect of different UE throughput demands on the performance of our reinforcement learning algorithm. To this end, we simulate the learning algorithm vs. full-duplex Max Sum-Rate in a 500 m radius cell scenario with 10 UEs present. The throughput demand for each UE is set to random value uniformly chosen between 0 and 4 Mbps.

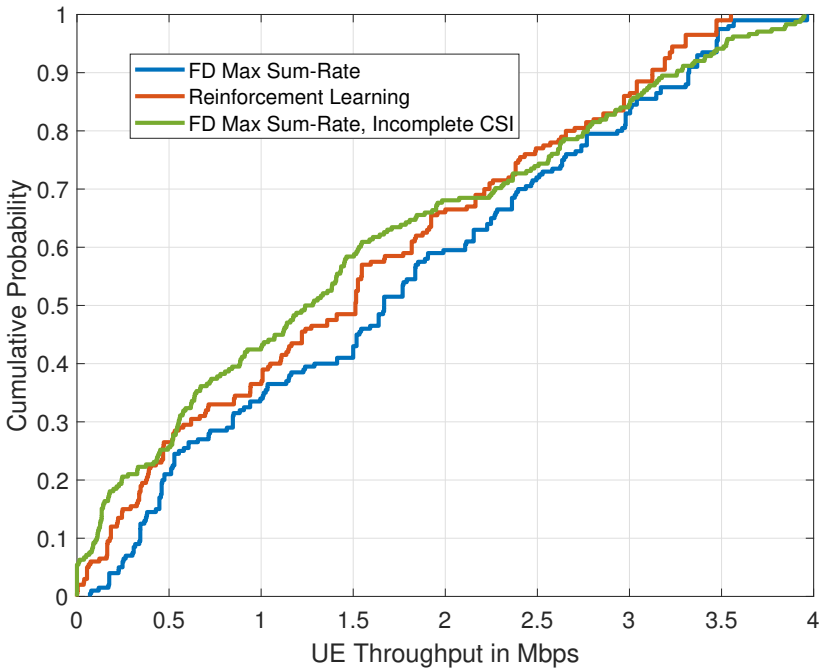

Figure 4.9 Effect of randomized UE traffic

The performance of our reinforcement algorithm mimics that of greedy allocation with complete CSI, as illustrated in Fig. 4.9. Nonetheless, it is also evident that it lags in performance. The reinforcement learning algorithm denies throughput to about 1% of the UEs and has a median throughput value of 1.5 Mbps. On the other hand, scheduling without inter-UE channel information denies throughput to about 5% of the simulated UEs and has a

median throughput value of 1.25 Mbps. This scenario is not very punishing to scheduling with incomplete CSI as many UEs have low throughput demands.

Performance Assessment in the Case of UE Clustering

Additionally, we seek to study the effect of UE clustering on the performance of our algorithm. For a cell of 500 m radius, the UEs are all placed within 200 m distance from the BS. The SIC value is returned to the relatively good value of 10^{11}, and the remainder of the simulation parameters are left unchanged. Following the SINR calculation for downlink UEs in equation, the proximity of uplink and downlink UEs (as a result of UE clustering) degrades the radio conditions of downlink UEs. A wrong scheduling decision is bound to now have a more grievous effect on the performance in general, and on downlink UEs throughputs specifically.

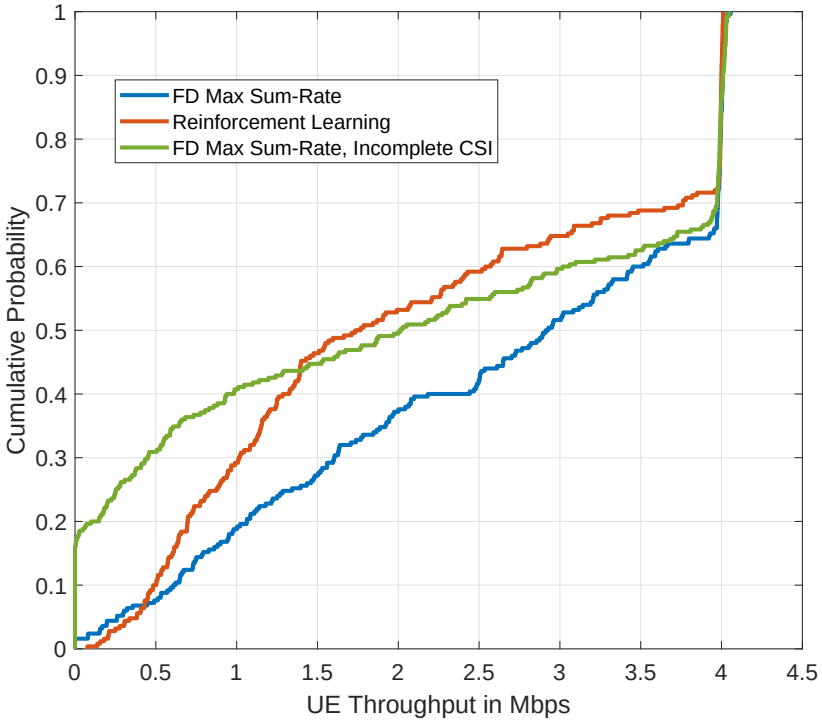

Figure 4.10 Effect of clustering on downlink UE performance

Figure 4.10 shows the CDF plots of the downlink UE throughput values for full-duplex Max Sum-Rate scheduling with both complete and incomplete CSI, and that of our learning proposal as well. The complete CSI full-duplex Max Sum-Rate scheduling algorithm edges out the learning algorithm in terms of UEs attaining a throughput equal to the demand (35% to 28%). The losses for the network are mainly found in downlink UEs which on average deliver around 86% of the throughput attained by the UEs scheduled with complete CSI.

This form of UE clustering incurs a small performance penalty on our reinforcement learning scheduling proposal. Nonetheless, Max Sum-Rate scheduling with incomplete CSI incurs a higher loss. In this case, 18% of the simulated downlink UEs are denied any resources with about 30% of the simulated UEs attaining a throughput equal to the demand.

Effect of UE Mobility on Performance

In this section, we study the effect of mobile UEs on the performance of our algorithm. We consider a random walk model [60] in determining the movement of the UEs. Each TTI, the UEs will move from a current location to a new one by choosing a speed and a direction randomly from the uniform intervals [*speedmin*,*speedmax*] and [0,2π], respectively. The minimum and maximum speeds are chosen as the average velocity of a walking person (0.5 m/s) and the average velocity of a moving car (20 m/s), respectively. As the positions of the UEs change, their individual radio conditions will vary. This variation is related to their proximity to the BS, as well as to the resulting changes in the shadowing and the fast fading effects. We simulate our learning algorithm alongside full-duplex Max Sum-Rate in both complete and incomplete CSI scenarios. The simulation is done with 10 UEs present in a 500 m radius cell. Figure 4.11 has a CDF plot of the resulting UE throughputs.

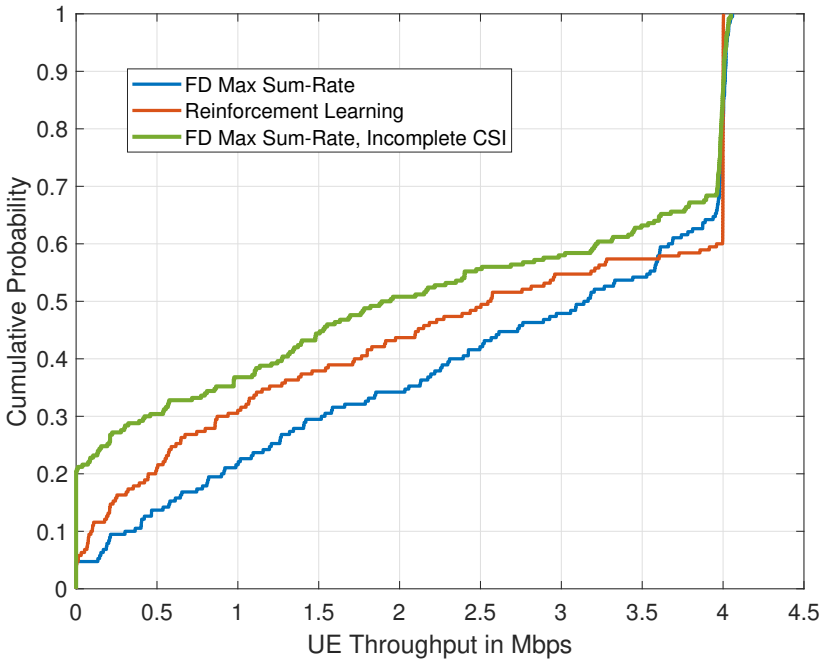

Figure 4.11 Effect of UE mobility on performance

Our algorithm shows more UEs attaining the throughput demand (40% to about 35%). Nonetheless, on average full-duplex Max Sum-Rate UEs, scheduled with complete CSI,

will get higher throughput values. It has a median UE throughput value equal to about 3.2 Mbps compared to a 2.6 Mbps median value for our learning algorithm. UE mobility will force erroneous decisions (with respect to maximizing UE throughput) and incite changes in performance for both algorithms. However, there is no noticeable added degradation in performance for our proposal in comparison to scheduling with complete CSI, and with respect to previous scheduling scenarios. Our learning algorithm can adapt over time to changes in UE radio conditions, limiting thus its losses. In comparison, scheduling without information on the inter-UE channels incurs higher losses in throughput. Around 20% of the UEs in that case attain a throughput of 0 Mbps with only about 31% attaining a throughput equal to the demand.

Effect of an Increase in the Number of UEs

We seek to study the effect of increased UE numbers in the cell on the performance of our proposal. The number of UEs is increased to 20: 10 uplink and 10 downlink. The number of RBs is also doubled. Our aim is to study how the learning algorithm copes with increased scheduling options and not to increase the network load. The cell radius is 500 m and the SIC value remains at the relatively good value of 10^{11}. The throughput demand is 4 Mbps and the learning factor β is set to 0.015. Accordingly, there are 100 different possible pairing scenarios. We simulate the learning algorithm vs. the full-duplex Max Sum-Rate proposal for both scenarios of complete and incomplete CSI.

Figure 4.12 has the CDF plot of the corresponding UE throughputs. Around 45% of the full-duplex Max Sum-Rate UEs–simulated with complete CSI–attained a throughput equal to the demand compared to 38% for the learning algorithm. Around 14% of the former UEs were completely denied throughput compared to none in the case of the learning algorithm. Our proposal makes good enough scheduling decisions to mimic the full-duplex Max Sum-Rate algorithm with complete CSI. The learning algorithm will lose a small part of the efficiency in terms of total network throughput. Arguably, this is a trade-off between efficiency and a more fair resource allocation. Furthermore, we simulate how the full-duplex Max Sum-Rate algorithm would fare if the inter-UE channel information was not available. In such a case, almost 30% of the UEs are completely denied throughput. Additionally, every simulated UE attains a throughput value lower than that achieved by our learning proposal.

Scalability of the Problem

Furthermore, we look at how an increase in the number of UEs in the network affects the time needed for the algorithm to become efficient. Figure 4.13 has a plot detailing the number of

TTIs needed for our learning algorithm to reach 90% efficiency (with respect to full-duplex Max Sum-Rate scheduling with complete CSI).

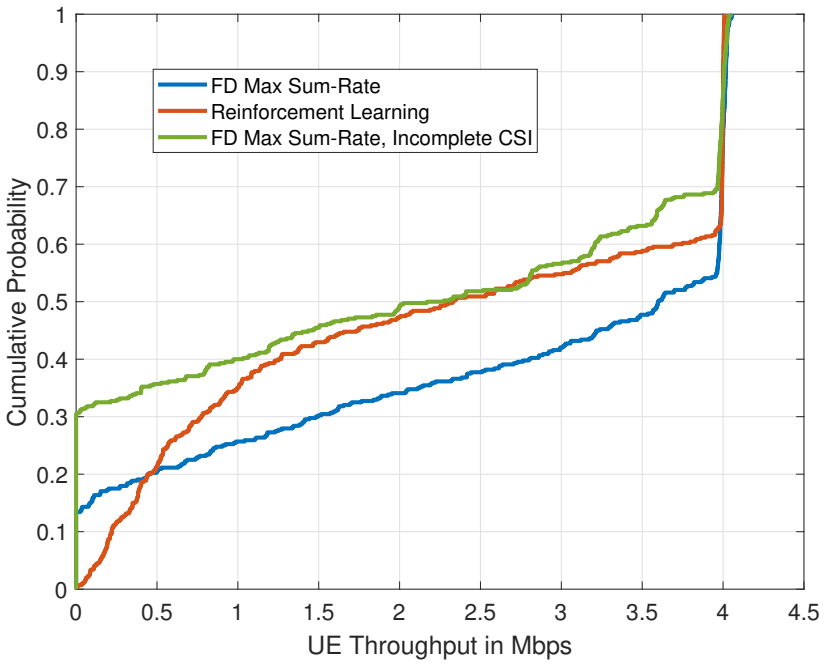

Figure 4.12 UE throughput as a function of UE numbers

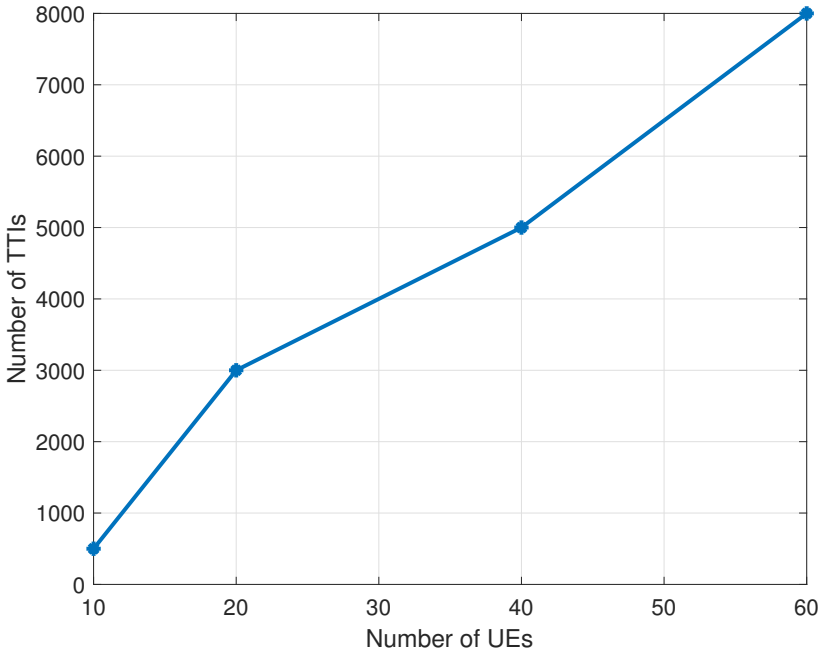

Figure 4.13 TTIs needed to attain 90% efficiency as a function of the number of UEs

As the number of UEs in the network increases, more time is required to reach the 90% efficiency mark. At 20 UEs, 3000 TTI are needed. At 60 UEs, about 8000 TTIs are needed. Nonetheless, with 1 TTI equaling 1 ms, the problem remains scalable even as the number of UEs in the network increases.

Finally, we compare how both our proposal and scheduling with incomplete CSI fare with respect to scheduling with complete CSI in terms of total network throughput, in each of the aforementioned scenarios. Table 4.3 has the average percentage efficiency of both proposals in each of the mentioned cases.

Table 4.3 Efficiency with respect to scheduling with complete CSI

	Randomized Demand	Clustering	Mobility	Increased UE numbers
RL Algorithm	91%	90%	90%	93%
Incomplete CSI	89%	78%	79%	78%

In the case of randomized UE traffic, scheduling with incomplete CSI and our RL algorithm fare similarly. After all, the fact that many UEs have a limited amount traffic mitigates the losses of the scheduling without inter-UE channel information. In each of the remaining scenarios, our proposal significantly outperforms scheduling with incomplete CSI.

4.6.5 UE Performance Under Low SIC

We lower the value of the SIC factor to 10^9. With 10 UEs present in a 500 m radius cell, the remainder of the simulation parameters remain unchanged as above. This is bound to negatively impact the performance of uplink UEs in the network as their SINR values degrade. Multiple uplink UEs, especially those on the cell borders, would now suffer from bad radio conditions. An incorrect scheduling decision, with respect to maximizing UE and network throughput, made by the learning algorithm would be more severely punished than before.

Figure 4.14 has box plots [61] of the resulting UE throughput values for our reinforcement learning algorithm and full-duplex Max Sum-Rate, both with and without complete CSI. Both our algorithm and Max Sum-Rate scheduling with complete CSI show again a similar distribution of UE throughputs with maximums equal to the demand, and minimums equal to zero. Nonetheless, the full-duplex Max Sum-Rate algorithm with complete CSI has more UEs achieving a throughput equal to the demand, and fewer ones attaining zero throughput. The increased cost on scheduling errors incurred by lowering the SIC factor are visible on the network performance as a whole, where the learning algorithm would lose up to 19% in total network throughput with respect to scheduling with complete CSI. This is not a significant drop in performance. Nonetheless, uplink UEs are the most affected by this degradation.

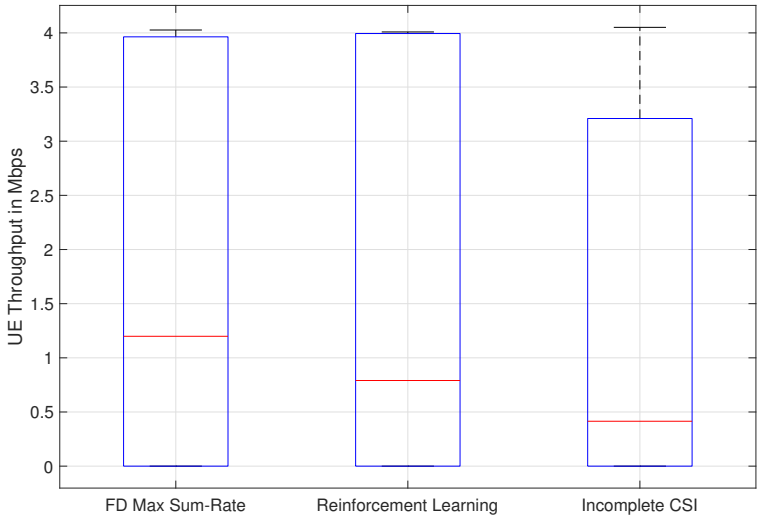

Figure 4.14 Effect of low SIC on UE performance

Downlink UEs scheduled by our learning algorithm attain throughputs, on average, equal to 97% of those achieved by their complete CSI full-duplex Max Sum-Rate counterparts, but uplink UEs only manage around 60%. In comparison to scheduling with incomplete CSI, the median UE throughput value for our algorithm sits at about 0.75 Mbps. For the former, it is about 0.4 Mbps. In addition, uplink UEs scheduled without information on the inter-UE channels manage only about 40% efficiency in comparison to scheduling with complete CSI.

4.7 Conclusion

In this chapter, we went over the consequences of scheduling with incomplete CSI on the performance of full-duplex wireless networks. We simulated both our fair and greedy scheduling proposals in multiple levels of incomplete CSI, and showed that significant losses in performances are incurred as a result. As an alternative. we presented a reinforcement learning based approach to scheduling in full-duplex wireless networks. The main objective was to avoid the added intricacies of scheduling in such networks. Specifically, we let go the unrealistic assumption of perfect CSI, as well as the regularly expected knowledge of all UE-to-UE channel states. We detailed the main challenges facing a machine learning scheduling proposal, focusing on the effects of non-full buffer traffic and dynamic radio conditions on the performance of the algorithm. We tested our proposal in multiple scheduling scenarios from randomized UE traffic, to UE clustering and in the presence of low SIC. While UE clustering degrades the performance of downlink UEs, and low SIC that of uplink UEs,

we illustrated that our learning proposal still performs well in terms of UE and network throughput. Accordingly, we verified the validity of our algorithm regardless of any obstacles facing the scheduling task.

Chapter 5

Centralized Approach to Power Allocation

5.1 Introduction

In this chapter, we propose a centralized optimal approach to scheduling and power allocation in full-duplex wireless networks. We aim to use power allocation alongside scheduling to overcome the interference problems generated by full-duplex wireless communications. Since both co-channel interference and self-interference are tied to the powers on the uplink and the downlink, respectively, power allocation has the potential to play an important role in mitigating these interferences. In this centralized approach, a central unit, $i.e.$, the base station (BS) is assumed to have all the information necessary to both schedule and allocate power on the resources. We formulate a queue-aware fair scheduling and power allocation problem for full-duplex wireless networks. Due to its intractability, we decompose this problem into two: a scheduling problem and a power allocation problem. We compare our proposal to the state-of-the-art, and show that it improves fairness among the user equipment (UEs) at no cost in the system's performance.

5.2 Problem Formulation

We propose a queue-aware scheduling and power allocation optimal problem for full-duplex wireless networks. Our aim is to maximize the UEs' SINR values, while at the same time enforcing fairness amongst them. Solving such a problem requires information on the UE radio conditions, their queue statuses, as well as an innate definition of fairness. As such, we define a UE pair priority and formulate the problem with the objective of maximizing the

sum of these priorities.

The priority of a UE pair is defined as a function of its current radio conditions, represented by the sum of the log of the pair's UE SINR values, and its historic radio conditions, represented by the number of bits these UEs have already transmitted. The priority for an uplink-downlink UE pair i-j, on resource block (RB) k, is defined as:

$$\rho_{ijk} = \frac{\log(S_j^u(i,k)) + \log(S_i^d(j,k))}{T_i^u + T_j^d}, \tag{5.1}$$

where T_i^u is the number of bits UE i has transmitted in a certain time window. Consequently, the fairness is relative to the UE SINR. The priority of a certain pair, and with it the priority of the UEs which have transmitted for a prolonged period of time will drop. The sum of logarithmic functions of the SINR enforces fairness as illustrated in [62]. It dictates that no UE will attain an SINR equal to zero. Furthermore, the UE queue is finite, and the UE priorities are dependent on the transmitted bits, as such, they are periodically reset. This guarantees that no UE priority will be zero, as long as it can, and has, bits to transmit. The UE pair-resource scheduling variable z_{ijk}, is defined $\forall\ k \in \mathcal{K}$, $\forall\ i \in \mathcal{I}$, $\forall\ j \in \mathcal{D}$, and is equal to one if uplink UE i is paired with downlink UE j on RB k. It is equal to zero otherwise. In this optimization problem, the variables are the UE pair-RB scheduling variables, and the uplink and downlink powers. We formulate the problem for TTI t as follows:
Scheduling and Power Allocation Problem ($\mathcal{P}^t$) :

$$\underset{z_{ijk},P_{0k},P_{ik}}{\text{Maximize}} \quad \sum_{k\in\mathcal{K}}\sum_{i\in\mathcal{I}}\sum_{j\in\mathcal{D}} z_{ijk}\cdot\rho_{ijk}. \tag{5.2a}$$

$$\text{Subject to} \quad \sum_{i\in\mathcal{I}}\sum_{j\in\mathcal{D}} z_{ijk} \leq 1,\ \forall k \in \mathcal{K}, \tag{5.2b}$$

$$\sum_{k\in\mathcal{K}}\sum_{j\in\mathcal{D}} z_{ijk}T_{ijk}^u \leq D_i^u,\ \forall i \in \mathcal{I}, \tag{5.2c}$$

$$\sum_{k\in\mathcal{K}}\sum_{i\in\mathcal{I}} z_{ijk}T_{ijk}^d \leq D_j^d,\ \forall j \in \mathcal{D}, \tag{5.2d}$$

$$\sum_{k\in\mathcal{K}} P_{0k} \leq p_0^{max}, \tag{5.2e}$$

$$\sum_{k\in\mathcal{K}} P_{ik} \leq p_i^{max},\ \forall i \in \mathcal{I}, \tag{5.2f}$$

$$P_{ik} \geq p_i^{min},\ \forall i \in \mathcal{I}, \forall k \in \mathcal{K}^i \tag{5.2g}$$

$$P_{0k} \geq p_0^{min},\ \forall k \in \mathcal{K}, \tag{5.2h}$$

$$z_{ijk} \in \{0,1\},\ \forall i \in \mathcal{I}, \forall j \in \mathcal{D}, \forall k \in \mathcal{K}. \tag{5.2i}$$

$\mathcal{K}^i$ is the set of RBs allocated to UE i. The resource utiliziation factor introduced in Chapter 3 is assumed to be equal to one in the context of this chapter. Equation (5.2a) is the objective of our problem, to select the pairs which have the highest priorities. According to (5.2b), each RB should be allocated to either one or no pair. Equations (5.2c) and (5.2d) help incorporate queue-awareness. By estimating the number of bits a UE can transmit (T^u_{ijk}) or receive (T^d_{ijk}) on an RB, these constraints ensure that a UE will get a certain number of resources, if and only if, it is going to use them in their entirety. Equation (5.2e) indicates the power budget at the BS. The Equations in (5.2f) limit the transmit power of a UE to a maximum value. Due to the necessity of giving minimum power values on the RBs as to avoid mathematical intractability ($i.e., \log(0)$), we add the constraints (5.2g) and (5.2h). p^{min}_i and p^{min}_0 are constants and equal to 0.001 W and 0.005 W, respectively. Note that the UEs on the uplink and the BS on the downlink will only transmit on allocated RBs.

The scheduling problem presented is combinatorial in nature. Addressing it together with power allocation in an optimal manner is challenging, especially as the combined problem is of type mixed integer non-linear programming (MINLP). It will become intractable as the number of UEs and RBs increase. As such, we solve this problem according to the framework presented in the following section.

5.3 Problem Solving Framework

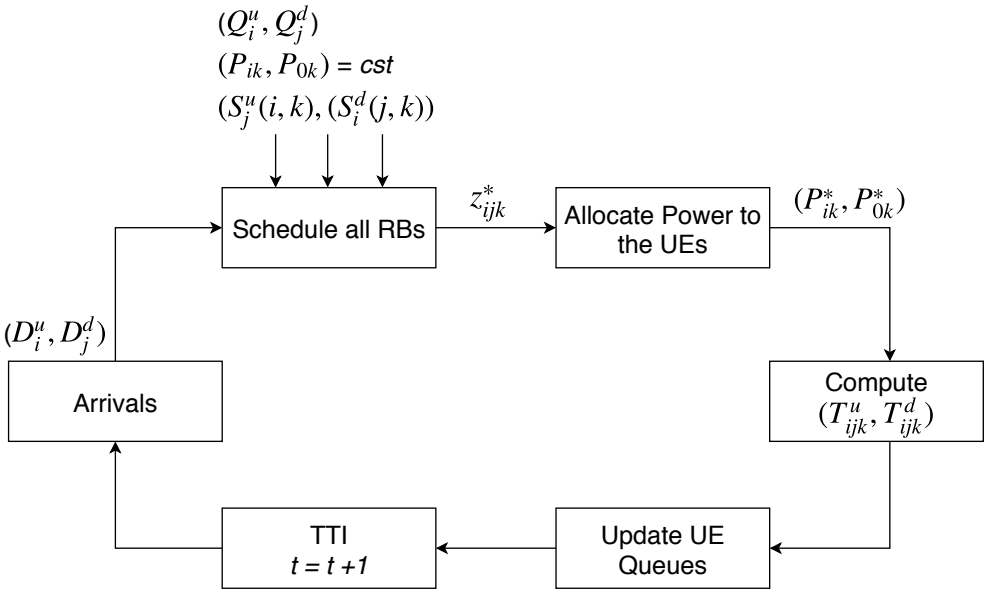

Figure 5.1 Scheduling and power allocation framework

The optimal problem is decomposed and solved according to the framework illustrated in Fig. 5.1 below. Knowing the UE radio conditions and their queue statuses, we obtain an optimal resource allocation matrix z^*_{ijk} with fixed uplink and downlink power values within the feasible limits $i.e.$, satisfying the power constraints. Afterwards, the power allocation problem takes this matrix as input, and computes the powers on the uplink and the downlink. The UE SINR values are recomputed using the optimal power values, and the number of bits each UE can transmit, or receive, is calculated. The UE queues Q^u_i and Q^d_j are then appropriately deducted depending on the resources each UE was allocated. At the beginning of the next TTI, new arrivals are added to the UE queues, and the UE demands D^u_i and D^d_j are updated.

5.3.1 Scheduling Problem

According to the proposed framework, and with fixed powers on the RBs, the optimization variables are now the values of z_{ijk}. The scheduling problem is written as follows:
$(\mathcal{P}^t_S)$:

$$\begin{aligned} &\underset{z_{ijk}}{\text{Maximize}} && \sum_{k\in\mathcal{K}}\sum_{i\in\mathcal{I}}\sum_{j\in\mathcal{D}} z_{ijk}\cdot\rho_{ijk}. \\ &\text{Subject to} && \text{(5.2b) to (5.2d)} \end{aligned} \tag{5.3}$$

The values of z_{ijk} are binary. The constraints are linear. This problem is as such of type integer linear programming (ILP). The number of constraints and variables are important factors when estimating if this problem is tractable. Generally, ILP problems are solved using a linear-programming based branch-and-bound approach. The idea of this approach is to look for an integer solution by branching and bounding on the decision variables provided by the LP relaxations. Thus, the number of integer variables determines the size of the search tree and influences the running time of the algorithm.

5.3.2 Power Allocation Problem and Convex Transformation

Power allocation is performed after the resources are scheduled. The optimization variables are now the power levels on the RBs P_{0k} and P_{ik}. The problem is written as follows:
$(\mathcal{P}^t_{PA})$:

$$\begin{aligned} &\underset{P_{0k},P_{ik}}{\text{Maximize}} && \sum_{k\in\mathcal{K}}\sum_{i\in\mathcal{I}}\sum_{j\in\mathcal{D}} \frac{z^*_{ijk}}{T_i+T_j}.(\log(\frac{P_{ik}|h^u_{ik}|^2}{N_{0k}+\frac{P_{0k}}{C_{SI}}})+\log(\frac{P_{0k}|h^d_{jk}|^2}{N_{jk}+P_{ik}|h_{ij,k}|^2})), \\ &\text{Subject to} && \text{(5.2e) to (5.2h).} \end{aligned} \tag{5.4}$$

The expression of the SINR has the following form:

$$\log(\frac{ax}{b+cy}), \tag{5.5}$$

where a, b, and c are constants. x and y are the optimization variables that represent the powers. Maximizing a concave function, subject to linear and convex constraints, leads to a convex problem. We perform a logarithmic change to the variables and the constants, *i.e.,* $\hat{x} = \log x$. This changes equation (5.5) into

$$\log(e^{\hat{x}+\hat{a}}) - \log(e^{\hat{b}} + e^{\hat{y}+\hat{c}}) = \hat{x} + \hat{a} - \log(e^{\hat{b}} + e^{\hat{y}+\hat{c}}), \tag{5.6}$$

$\hat{x} + \hat{a}$ is a linear function, therefore it is a concave function [50]. The function $\log \sum e^x$ is convex, therefore $-\log \sum e^x$ is concave. Thus, the expression in (5.6) is concave. As the objective function is concave, we still need to proof that the constraints are convex. These constraints can be written in the form of:

$$\sum x \leq d. \tag{5.7}$$

With the change of variables we did, it becomes:

$$\sum e^{\hat{x}} - d \leq 0. \tag{5.8}$$

$\sum e^x$ is a convex function and d is a constant, this means that (5.8) is convex. In conclusion, the power allocation problem can be transformed into a non-linear convex problem, and can be solved efficiently by standard convex program solvers such as CVX [63]

5.4 Simulation and Results

5.4.1 Simulation Parameters

The simulation parameters we used are presented in Table 5.1. In the case where power allocation is not used, maximum transmit power per RB is assumed.

5.4.2 Gain In Throughput and Fairness

We seek to compare our proposed algorithm to the state-of-the-art. As such, we plot the throughputs attained by the UEs for our full-duplex Priority Based algorithm, and for the sum-rate maximization algorithm proposed in [26].

Table 5.1 Simulation parameters for centralized power allocation

Parameter	**Value**
Cell Specifications	Single-Cell, 120 m Radius
Number of RBs	50
SIC Value	10^{11} or 10^{8}
Number of UEs	10 UL,10 DL
Demand Throughput	2 Mbps

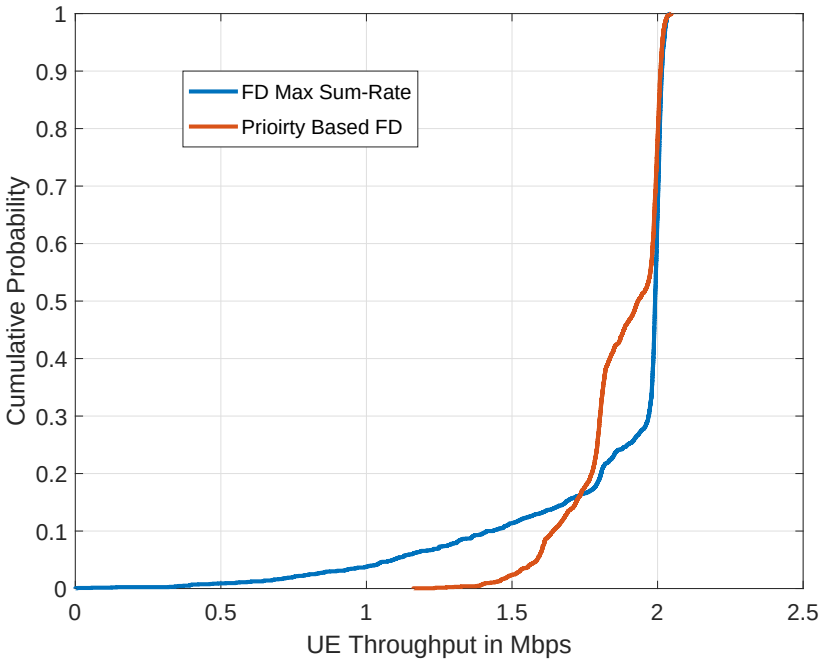

Figure 5.2 UE Throughput: Priority Based full-duplex and Max Sum-Rate

The graph in Fig. 5.2 has a CDF plot with the results. In comparison to the sum-rate maximization algorithm we simulated, our full-duplex algorithm has less UEs attaining the maximum throughput value of 2 Mbps. However, it has no UEs attaining values lower than 1.2 Mbps, whilst the lowest throughput for the sum-rate algorithm is 0 Mbps. Our algorithm focuses more on the aspect of UE fairness, giving more resources to UEs which have transmitted less often than others.

Furthermore, we seek to study the effect this added fairness has on the overall network performance. Figure 5.3 has box plots for network throughputs attained by our algorithm, and by the sum-rate maximization algorithm throughout the simulations. The highest network throughput attained by the sum-rate algorithm, between 500 simulation runs, is around 38 Mbps, compared to 38.4 Mbps for our algorithm. The latter has 36.3 Mbps as the lowest attained network throughput, compared to around 35.6 Mbps for the sum-rate algorithm.

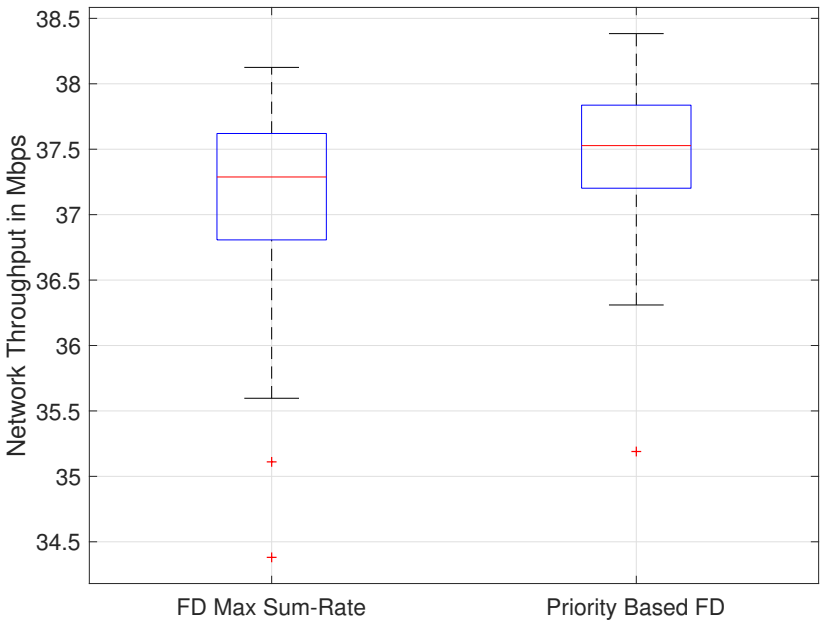

Figure 5.3 Network throughput: Max-Sum Rate and Priority Based full-duplex

In general, our algorithm slightly improves the overall network throughput, and the added fairness comes at no cost in the overall system performance. This is mainly due to the effects of multi-user diversity and dynamic traffic. With UEs having finite queues and limited bits to transmit, UEs with high SINR values will not hog the resources and transmit indefinitely. If the UEs were to have full buffer traffic, the sum-rate algorithm would always produce higher network throughput. Nonetheless, this is not the case neither in our model, nor in real life wireless networks.

5.4.3 Power Expenditure and Effect on UE Throughput

In this subsection, we seek to compare the difference in power expenditure by our algorithm, in the presence and absence of power allocation. For the case where the powers are not optimally allocated, the transmit power of a UE on an RB is equal to the maximum transmit power, divided by the number of RBs it was allocated during that TTI. On the downlink, it is the BS maximum transmit power divided by the number of allocated RBs. In order to compare the total power expended we plot the total power spent by UEs on the uplink and by the BS on the downlink, when our power allocation algorithm is used. The results can be seen in the CDF plot of Fig. 5.4.

The maximum transmit power for the UEs and the BS–used when simulating the scheduling algorithm without power allocation–is also shown. From the plot for the uplink UEs transmit power, we can notice that in our simulations power allocation massively saved

on power. Almost half of the the UEs on the uplink did not transmit at maximum power. However, no such savings can be seen on the downlink, where in the few cases where the BS did not transmit at maximum power, it actually transmitted at a value pretty close to just that. In the end, because of how the SINR values on the uplink and the downlink are interconnected, it will always be a trade-off on where the algorithm can save or expend power. A relation can also be drawn to the SIC factors. If the network struggles on the uplink (due to high self-interference for example), the power allocation could decrease the power on the downlink and increase it on the uplink.

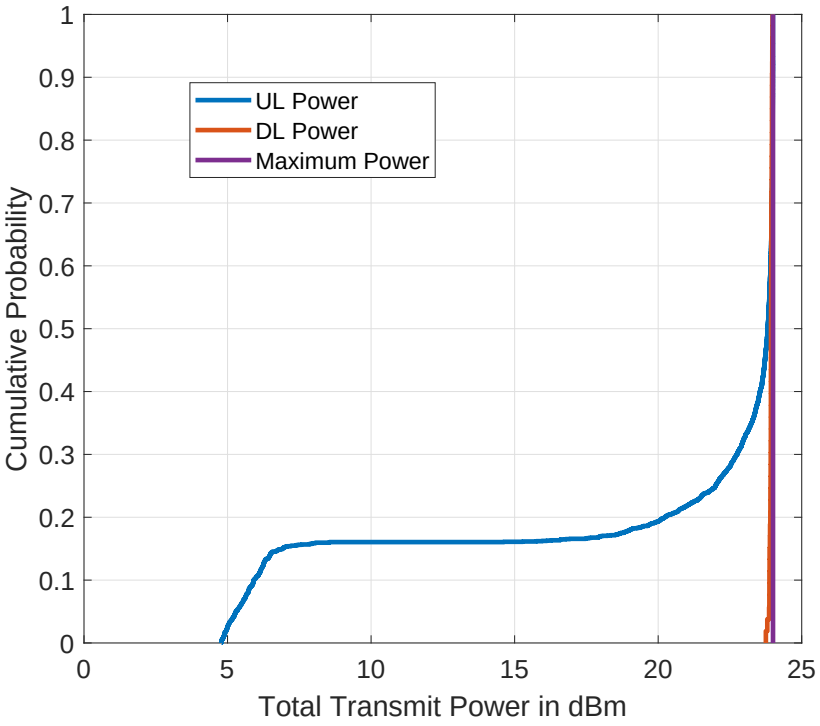

Figure 5.4 Total power expended by the UEs and the BS

We furthermore look at how this deviation from maximum power affects UE performance in the network. Figure 5.5 has a CDF plot with the corresponding UE throughputs. We notice that the ranges for the throughput values are almost identical, with a minimum close to 1.2 Mbps and a maximum equal to the demand of 2 Mbps. The median value is also identical for the two algorithms at around 1.93 Mbps. Nonetheless, the box for the case of power allocation is slightly shifted upwards and smaller. This indicates a higher range of values for these UEs. Power allocation produced slightly better performance for the UEs with less power being expended.

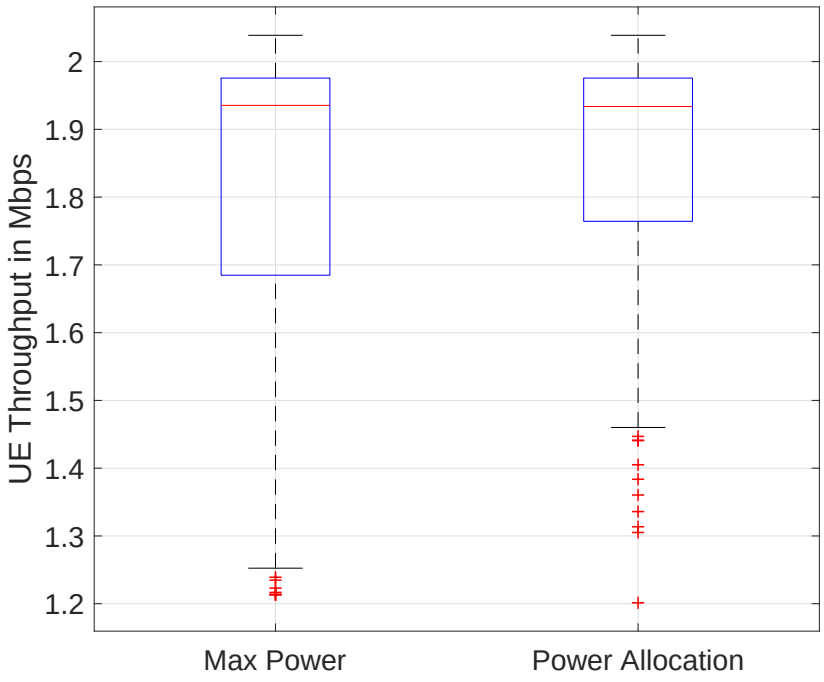

Figure 5.5 Effect of power allocation on UE performance

5.4.4 Effect of Low Self-Interference Cancellation

We want to study the performance of our algorithm in case of relatively low SIC. The SIC value is lowered to 10^8. The rest of the parameters remain unchanged from the previous section. Following the uplink UE SINR equation, the value of the SIC affects the performance of uplink UEs. We use bag plots [64] to assess the SINR values attained by uplink UEs as a function of their transmission powers on the RBs. Figures 5.6a and 5.6b show the results, with and without power allocation, respectively.

The inner bag (dark blue) in Fig. 5.6a is thinner than that corresponding to the algorithm runs without power allocation (shown in Fig. 5.6b). This implies that the power spread is smaller in the case of power allocation. Furthermore, the SINR spread favors the case of the latter as well. Power allocation helped increase the SINR values of the worst performing UEs. The lowest UE SINR value in the case of power allocation is -15 dB compared to -20 dB for the case without. Finally, the bag in Fig. 5.6a slopes upwards. This means that the SINR increases as the power expenditure increases. This is not true for the case where maximum power is used, where sometimes the expenditure of uplink power does not necessarily translate into better SINR.

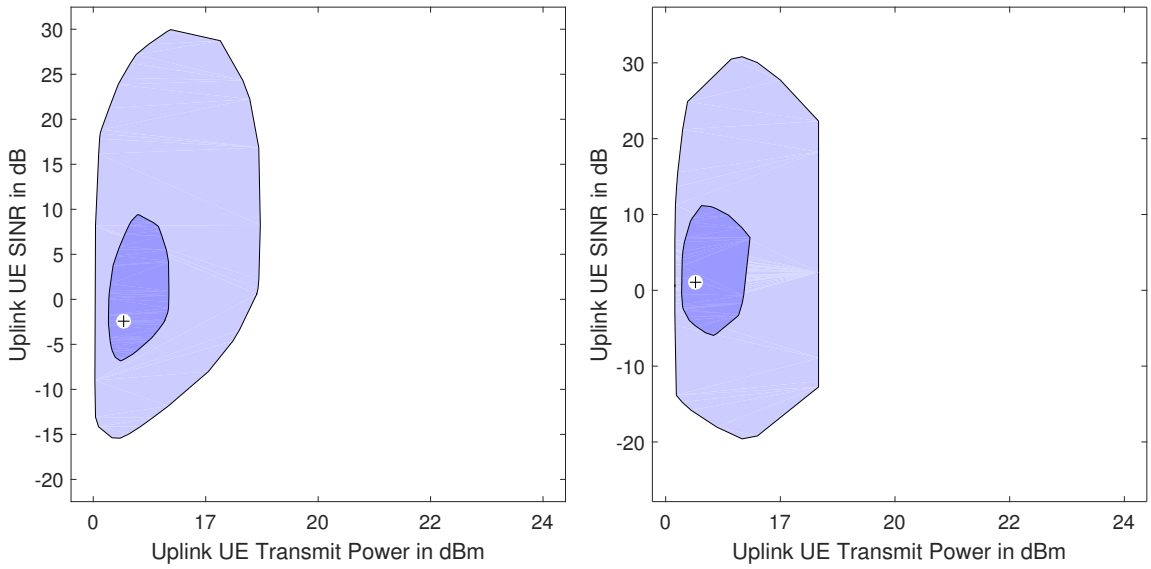

(a) With Power Allocation (b) Maximum Power

Figure 5.6 Effect of power allocation on UE performance in the case of low SIC

5.5 Conclusion

In this chapter, we presented our optimal full-duplex Priority Based algorithm for scheduling and power allocation in full-duplex wireless networks. We sought to fairly schedule the resources while appropriately allocating power to the UEs. Our algorithm is queue-aware and takes dynamic traffic arrivals into account. Additionally, it enforces fairness among the UEs without any cost in the system's performance. Finally, optimally allocating power on the RBs decreased expenditure and helped improve radio conditions for the worst faring UEs.

Chapter 6

Distributed Approach to Power Allocation

6.1 Introduction

As illustrated in this thesis thus far, and as a result of self-interference, uplink user equipment (UEs) in a full-duplex network suffer a degradation in performance with an increase in the power on the downlink. Furthermore, and due to the presence of intra-cell co-channel interference, downlink UEs in the network would suffer a degradation in performance as a result of an increase in the power on the uplink. UEs on the uplink and the base station (BS) on the downlink are competitors with contradicting objectives. This makes a selfish game theoretic approach that pits the UEs and the BS as competing players well suited for power allocation in full-duplex wireless networks. In this chapter, we propose three non-cooperative games to help tackle the intricate task of allocating power to scheduled pairs of UEs, with objectives varying from improving UE performance to reducing power expenditure. The games have two sets of players: the UEs on the uplink, and the BS on the downlink. We use a special class of games–known as super-modular games–to draft different player utilities with different objectives. Via a set of exhaustive simulations, we assess the significance of power allocation in full-duplex networks, and determine both its gains and limitations.

6.2 Framework for Scheduling and Power Allocation

We propose three games for power allocation in full-duplex wireless networks. First, the scheduler will allocate the resources to pairs of uplink-downlink UEs with the assumption of constant powers. The latter are chosen to be feasible within the power constraints. For

this task, we use the full-duplex Proportional Fair algorithm we proposed in Chapter 3. Afterwards, our game theoretic proposals are used to calculate the transmit power on every allocated resource block (RB).

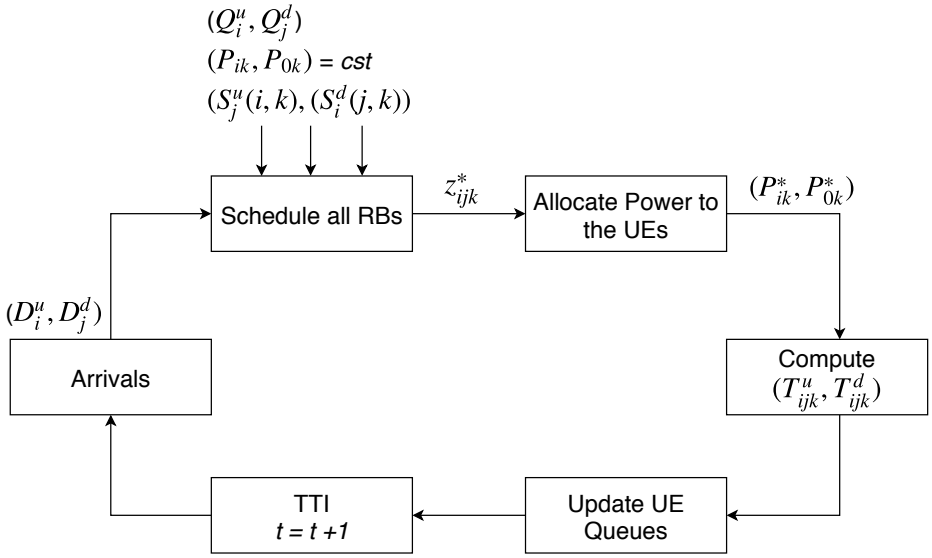

Figure 6.1 Scheduling and power allocation framework

Knowing the UE radio conditions and their queue statuses, we obtain an optimal resource allocation matrix z_{ijk}^* with fixed uplink and downlink power values. Afterwards, the power allocation problem takes this matrix as input, and computes the power levels on the uplink and the downlink. The UE SINR values are recomputed using the optimal power values, and the number of bits each UE can transmit (T_{ijk}^u), or receive (T_{ijk}^d), is calculated. The UE queues Q_i^u and Q_j^d are then appropriately deducted depending on the resources each UE was allocated. At the beginning of the next TTI, new arrivals are added to the UE queues, and the UE demands D_i^u and D_j^d are updated.

6.3 Non-Cooperative Games for Power Allocation

In the context of game theory and power allocation, the authors in [45] were the first to introduce the idea of using game theory to enhance the profitability full-duplex operations. Their article surveys possible applications and implementations of game theory in relation to scheduling and power allocation in different full-duplex network scenarios. In [40], the authors use a game theoretic approach for radio resource allocation in full-duplex wireless networks. They couple their algorithm with a water-filling based power allocation problem and iterate till a Nash equilibrium is achieved. They show that their proposal is profitable

with respect to half-duplex networks. In our work, the focus is on power allocation rather than scheduling. We aim to explore different objectives with focus on multiple aspects of performance optimization. We compare between our different proposals highlighting the gains and limitations of each.

Non-Cooperative game theory models the interactions between players competing for a common resource. Contrary to our proposal in Chapter 5, this distributed approach does not necessitate any central authority or signaling between the players. Following the SINR formulas for uplink and downlink UEs (Equations 3.1 and 3.2), an increase in the power of an uplink UE will increase its SINR but at the same time cause added interference on its paired downlink UE. Vice-versa, an increase in the transmit power at the BS, would increase the SINR of the receiving downlink UE, but cause added interference on the paired uplink UE. UEs on the uplink and the BS on the downlink, *i.e.,* the decision makers, are playing for contradicting objectives. Hence, non-cooperative game theory is well adapted to power allocation in full-duplex wireless networks. We summarize our contributions in this chapter as follows:

(a) We propose a greedy game for power allocation, where the uplink players and the BS on the downlink seek to maximize UE SINR.

(b) We propose an interference aware game, in which the players mind the interferences they generate onto the system.

(c) We propose an energy efficient game. The players in this game vary their transmit powers with respect to the interferences they generate.

(d) Via a set of exhaustive simulations, we compare and contrast between our proposals, highlighting their advantages, as well as their shortcomings.

6.3.1 Game Formulation

We define a set of multi-player games $\mathcal{G}$ between the BS (coined player 0) and the $|\mathcal{I}|$ uplink UEs. In particular, on every alloted RB k, the uplink UEs will compete with the BS. The formulation of this non-cooperative game $\mathcal{G} = \langle M, S_0 \times \prod_i S_i, U \rangle$ can be described as follows:

- A finite set of players $M = (BS, UE\,i)$ paired on the same RB k. The game is engaged between the BS and the uplink UEs for all the RBs.

- The action of a given player is the amount of power allocated on RB k, the strategy chosen by the BS is then $\boldsymbol{P}_0 = (P_{01}, ..., P_{0|\mathcal{K}|})$ and the strategy chosen by any uplink

UE i is $\boldsymbol{P}_i = (P_{i1}, ..., P_{i|\mathcal{K}|})$. A *strategy profile* $\boldsymbol{P} = (\boldsymbol{P}_0, \boldsymbol{P}_1, ..., \boldsymbol{P}_{|\mathcal{I}|})$ specifies the strategies of all players.

- For the BS, the space of pure strategies is S_0 given by what follows:

$$S_0 = \{\boldsymbol{P}_0 \in \mathbb{R}^{|\mathcal{K}|}, \text{ such as } \sum_{k \in \mathcal{K}} P_{0k} \leq p_0^{max} \text{ and } P_{0k} \geq p_0^{min}, \forall k \in \mathcal{K}\}$$

- For each uplink UE i, the space of pure strategies is S_i given by what follows:

$$S_i = \{\boldsymbol{P}_i \in \mathbb{R}^{|\mathcal{K}|}, \text{ such as } \sum_{k \in \mathcal{K}} P_{ik} \leq p_i^{max} \text{ and } P_{ik} \geq p_i^{min}, \forall k \in \mathcal{K}^i\},$$

  where $\mathcal{K}^i$ is the set of RBs alloted to UE i and $S = S_0 \times S_1 \times ... \times S_{|\mathcal{I}|}$ is the set of all strategies;

- A set of utility functions $U = (U_0, U_{i \in \mathcal{I}})$ that quantify players' profit for a given strategy profile.

Note that an uplink player i will not transmit on an RB it was not allocated.

6.3.2 Best Response

In a non-cooperative game, a valid solution is one where all players adhere to a Nash equilibrium, which is a profile of strategies in which no player will profit from deviating its strategy unilaterally. A Nash equilibrium is a static concept that often abstracts away the question of how it is reached. Thus, the main challenge in non-cooperative game theory is to devise practical algorithms to reach such an equilibrium. The simplest example of such algorithms are repeated best response dynamics. Following these dynamics, each player selects the best (locally optimal) response to other players' strategies, until convergence.

6.4 The Greedy Game

We define the greedy game $\mathcal{G}^g$. The objective of this game is to maximize UE SINR values. Both the UEs on the uplink and the BS on the downlink will aim to increase the UE SINR values. Their decisions are taken individually and independent of any factors. Let $j(i, k)$ be a reference to downlink UE j paired with uplink UE i on RB k as a result of scheduling. For simplicity, in the remainder of this chapter we use $j = j(i, k)$.

The utility of any uplink UE $i \in \mathcal{I}$ only encompasses its own SINR. It is formulated as follows:

$$U_i^g = \sum_{k \in \mathcal{K}^i} \log(\frac{P_{ik}|h_{ik}^u|^2}{N_{0k} + \frac{P_{0k}}{SIC}}), \tag{6.1}$$

where $\mathcal{K}^i$ is the set of RBs scheduled to UE i. The utility of the BS encompasses the SINR of both uplink and downlink UEs :

$$U_0^g = \sum_{k \in \mathcal{K}} (\log(\frac{P_{ik}|h_{ik}^u|^2}{N_{0k} + \frac{P_{0k}}{SIC}}) + \log(\frac{P_{0k}|h_{jk}^d|^2}{N_{jk} + P_{ik}|h_{ij,k}|^2})) \tag{6.2}$$

For any uplink UE i, U_i^g is concave in P_{ik} (logarithmic function) and continuous in P_{0k}, $\forall k \in \mathcal{K}$. For the BS, U_0^g is concave in P_{0k} since

$$\frac{\partial^2 U_0^g}{\partial P_{0k}^2} = -\frac{SIC \cdot N_{0k} \times (SIC \cdot N_{0k} + 2P_{0k})}{P_{0k}^2 \times (N_{0k} \cdot SIC + P_{0k})^2} < 0, \tag{6.3}$$

and continuous in P_{ik}, $\forall$ k $\in \mathcal{K}$. Hence, as all strategy spaces are compact, a Nash equilibrium exists for this game.

6.4.1 Computing a Nash Equilibrium

As the utility functions are strictly concave, the Nash equilibrium is the solution of the following optimization problems:

$$\max_{\boldsymbol{P}_\gamma} \; U_\gamma^g(\boldsymbol{P}_\gamma, \boldsymbol{P}_{-\gamma}) \tag{6.4a}$$

$$\text{subject to} \quad \sum_{k \in \mathcal{K}} P_{\gamma k} \leq p_\gamma^{max}, \tag{6.4b}$$

$$P_{\gamma k} \geq p_\gamma^{min}, \; \forall k \in \mathcal{K}. \tag{6.4c}$$

p_γ^{max} (resp. p_γ^{min}) is the maximal (resp. minimal) power limit on the uplink for $\gamma \in \mathcal{I}$ and on the downlink for $\gamma = 0$. As the optimization problems in (6.4) are nonlinear and convex, the Karush-Kuhn-Tucker (KKT) conditions are sufficient to determine the optimal case (i.e. the Nash equilibrium) [65].

The KKT conditions associated with $P_{ik}, \forall k \in \mathcal{K}$ for uplink UE $i \in \mathcal{I}$ gives what follows:

$$\frac{1}{P_{ik}^*} - \mu = 0, \; \forall k \in \mathcal{K} \tag{6.5a}$$

$$\mu \times (p_i^{max} - \sum_{k \in \mathcal{K}} P_{ik}^*) = 0 \tag{6.5b}$$

$$P_{ik}^* \geq p_i^{min}, \ \forall k \in \mathcal{K}^i \tag{6.5c}$$

$$\mu \geq 0, \tag{6.5d}$$

$$\sum_{k \in \mathcal{K}} P_{ik}^* \leq p_i^{max}, \tag{6.5e}$$

where μ is the Lagrange multiplier associated with the constraint (6.4b). We deduce from (6.5a) that μ cannot be null and hence all P_{ik} are equal. Further, according to (6.5b), $\sum_{k \in \mathcal{K}} P_{ik} = p_i^{max}$ and finally $P_{ik} = max(p_i^{min}, \frac{p_i^{max}}{K^i})$ if RB k is allocated to UE i and 0 otherwise. The KKT conditions associated with $P_{0k}, \forall k \in \mathcal{K}$ for the BS gives what follows:

$$\frac{1}{P_{0k}^*} - \frac{1}{N_{0k} \cdot SIC + P_{0k}^*} - \mu + \alpha_k = 0, \ \forall k \in \mathcal{K} \tag{6.6a}$$

$$\mu \times (p_0^{max} - \sum_{k \in \mathcal{K}} P_{0k}^*) = 0 \tag{6.6b}$$

$$\alpha_k \times (p_0^{min} - P_{0k}^*) = 0, \ \forall k \in \mathcal{K} \tag{6.6c}$$

$$\mu \geq 0 \tag{6.6d}$$

$$\alpha_k \geq 0, \ \forall k \in \mathcal{K} \geq 0, \tag{6.6e}$$

$$\sum_{k \in \mathcal{K}} P_{0k}^* \leq p_0^{max}, \tag{6.6f}$$

$$P_{0k}^* \geq p_0^{min}, \ \forall k \in \mathcal{K}. \tag{6.6g}$$

where μ and $\alpha_k, \forall k \in \mathcal{K}$, are the Lagrange multiplier associated with the constraints (6.4b) and (6.4c) respectively. We deduce from (6.6a) that μ cannot be null and therefore the BS will allocate greedily all available power as

$$\sum_{k \in \mathcal{K}} P_{0k}^* = p_0^{max} \tag{6.7}$$

Further, we need to distinguish two cases where $\alpha_k, \forall k \in \mathcal{K}$ are either null or not.

1. If $\alpha_k = 0, \forall k \in \mathcal{K}$, we need to solve the following second order equation: $\frac{a_k}{P_{0k}^* \times (a_k + P_{0k}^*)} = \mu, \ \forall k \in \mathcal{K}$, where $a_k = N_{0k} \cdot SIC$ which gives a single realistic solution (positive power value) $P_{0k}^* = \frac{a_k \cdot (\sqrt{1 + \frac{4}{a_k \mu}} - 1)}{2}$. As the value of power levels is still dependent on the Lagrangian variable μ (the a_k are constant and known), we have recourse to (6.7) to obtain it and compute the numerical values of $P_{0k}^*, \forall k \in \mathcal{K}$ accordingly.

2. If $\alpha_k \neq 0$, $P_{0k}^* = p_0^{min}, \forall k \in \mathcal{K}$ according to (6.6c). Further, in conjunction with (6.7), maximal and minimal thresholds should verify $\frac{p_0^{max}}{K} = p_0^{min}$.

6.4.2 Best Response Algorithm

A best response algorithm, illustrated in Algorithm 6, is used in this case to reach a Nash equilibrium. After the RBs are allocated, the uplink UEs and the BS take turn maximizing their utilities until the power values on the RBs no longer change. The resulting power allocation scheme is used in performance assessments. p^u and p^d are matrices containing all the power values on the RBs on the uplink and the downlink, respectively.

Algorithm 6 Scheduling and Power Allocation Algorithm for the Greedy Game

Requires: Maximum tolerance $\epsilon \geq 0$.
Input: UE radio conditions, channel states, initial power settings p_0^u and p_0^d
for TTI t=1,...,T
    Step 1: Scheduling
    RBs are allocated following G_t^1
    Step 2: Power Allocation
    repeat:
        Solve (6.5) in the uplink $\forall\ i \in \mathcal{I}$
        Update p_n^u
        Solve (6.6) in the downlink for the BS
        Update p_n^d
        $\delta^d = \left\| p_n^d - p_{n-1}^d \right\|$, $\delta^u = \left\| p_n^u - p_{n-1}^u \right\|$
        $n \leftarrow n + 1$
    until $\delta^d \leq \epsilon$ and $\delta^u \leq \epsilon$
end for

6.5 The Interference Aware Game

We define $\mathcal{G}^c$ as the interference aware collaborative game. As the name suggests, our objective in this game is for power allocation to be interference aware. Since the game is non-cooperative, it is necessary that each player is aware of the interferences they generate. If these interferences are not accounted for in the utilities, each player will seek to maximize its own gains independently, and consequently, increase its transmit power to the maximum (as with the greedy game). This would generate maximum interference in the network and could inadvertently degrade UE performance. The utility of every uplink UE i is thereafter defined as:

$$U_i^c = \sum_{k \in \mathcal{K}^i} \log\left(\frac{P_{ik}|h_{ik}^u|^2}{N_{0k} + \frac{P_{0k}}{SIC} + P_{ik}|h_{ij,k}|^2}\right). \tag{6.8}$$

As for the BS:

$$U_0^c = \sum_{k \in \mathcal{K}} \log(\frac{P_{0k}|h_{jk}^d|^2}{N_{jk} + P_{ik}|h_{ij,k}|^2 + \frac{P_{0k}}{SIC}}). \tag{6.9}$$

The SINR values for the UEs are thus inherently included in the utilities. Additionally, the co-channel interference, which degrades the performance of downlink UEs, is now also affecting the utility of uplink UEs. The self-interference, which degrades the performance of uplink UEs, is now also affecting the utilities relating to downlink UEs. As such, we can seek to improve UE performance, while at the same time account for the resulting interferences. Via our simulations, we show that our proposed utilities converge to an efficient Nash equilibrium which improves UE performance in terms of throughput.

6.5.1 A Super-modular Game

The convergence of a repeated best response algorithm is not guaranteed in general. For this game, we are in presence of a type of games called super-modular, where a best response algorithm permits attaining NEs. In what follows, we introduce a formal definition of super-modular games and prove that our interference aware game belongs to the latter class. According to [66], any game $\mathcal{G}$ is super-modular if for any player $\gamma \in M$:

1. The strategy space S_γ is a compact sub-lattice of $\mathbb{R}^{|\mathcal{K}|}$;
2. The objective function is super-modular, that is $\frac{\partial^2 U_0}{\partial P_0 \partial P_i} \geq 0$ and $\frac{\partial^2 U_i}{\partial P_i \partial P_0} \geq 0 \; \forall i \in \mathcal{I}$, $\forall \boldsymbol{P} \in S$, and $\forall k \in \mathcal{K}$.

In [66, 67], proof is given for the following two results in a super-modular game:

- If each player γ either initially uses its lowest or largest policy in S_γ, then a best response algorithm converges monotonically to a Nash equilibrium.
- If we start with a feasible policy, then the sequence of best responses monotonically converges to a Nash equilibrium: it monotonically increases in all components in the case of maximization in a super-modular game.

Proposition 6.5.1 *Game $\mathcal{G}^c \langle M, S_0 \times \prod_i S_i, U^c \rangle$ is a super-modular game.*

Proof: To prove the super-modularity of the game, we need to verify the aforementioned conditions. First, the strategy space S_γ is obviously a compact convex set of $\mathbb{R}^{|\mathcal{K}|}$. Hence, it suffices to verify the super-modularity of the objective function U_γ^c of any player γ as there are no constraint policies for $\mathcal{G}^c$. For any uplink UE i, we have:

$$\frac{\partial^2 U_i^c}{\partial P_{ik} \partial P_{0k}} = \frac{\frac{|h_{ij,k}|^2}{SIC}}{(N_{0k} + \frac{P_{0k}}{SIC} + P_{ik}|h_{ij,k}|^2)^2} \geq 0, \quad \forall i \in \mathcal{I}, \forall k \in \mathcal{K}.$$

And for the BS, we have what follows:

$$\frac{\partial^2 U_0^c}{\partial P_{0k}\partial P_{ik}} = \frac{\frac{|h_{ij,k}|^2}{SIC}}{(N_{jk} + \frac{P_{0k}}{SIC} + P_{ik}|h_{ij,k}|^2)^2} \geq 0, \quad \forall i \in \mathcal{I}, \forall k \in \mathcal{K}.$$

□

6.5.2 Computing a Nash Equilibrium

As we proved that we are in presence of a super-modular game, we implement a best response algorithm to reach its pure Nash equilibrium. At the convergence of the best response algorithm, a Nash equilibrium is the solution of the following two optimization problems:

$$\max_{\boldsymbol{P}_\gamma} U_\gamma^c(\boldsymbol{P}_\gamma, \boldsymbol{P}_{-\gamma}) \tag{6.10a}$$

$$\text{subject to} \quad \sum_{k\in\mathcal{K}} P_{\gamma k} \leq p_\gamma^{max}, \tag{6.10b}$$

$$P_{\gamma k} \geq p_\gamma^{min}, \ \forall k \in \mathcal{K}. \tag{6.10c}$$

where p_γ^{max} (resp. p_γ^{min}) is the maximal (resp. minimal) power limit on the uplink for $\gamma \in \mathcal{I}$ and on the downlink for $\gamma = 0$. As the optimization problems in (6.10) are convex, the Karush-Kuhn-Tucker (KKT) conditions enable determining a global optimal (*i.e.,* the Nash equilibrium at convergence) [65]. The KKT conditions associated with $P_{\gamma k}, \forall k \in \mathcal{K}$ give:

$$\frac{1}{P_{\gamma k}^*} - \frac{1}{b_{\gamma k} + P_{\gamma k}^*} = \lambda_\gamma, \ \forall k \in \mathcal{K} \tag{6.11a}$$

$$\lambda_\gamma \times (p_\gamma^{max} - \sum_{k\in\mathcal{K}} P_{\gamma k}^*) = 0 \tag{6.11b}$$

$$P_{\gamma k}^* \geq p_\gamma^{min}, \ \forall k \in \mathcal{K} \tag{6.11c}$$

$$\lambda_\gamma \geq 0, \tag{6.11d}$$

$$\sum_{k\in\mathcal{K}} P_{\gamma k}^* \leq p_\gamma^{max}. \tag{6.11e}$$

where λ_γ is the KKT multiplier associated with the constraint (6.10b), and

$$b_{\gamma k} = \begin{cases} \frac{N_{0k} + \frac{P_{0k}^*}{SIC}}{|h_{ij,k}|^2}, \gamma = i \in \mathcal{I} \\ SIC \times (N_{jk} + P_{ik}^*|h_{ij,k}|^2), \gamma = 0 \end{cases} \tag{6.12}$$

We deduce from (6.11a) that λ_γ cannot be null. As such, all $P^*_{\gamma k}$ are the solution of a second order equation that gives $P^*_{\gamma k} = \frac{b_{\gamma k} \cdot (\sqrt{1+\frac{4}{b_{\gamma k}\lambda_\gamma}}-1)}{2}$, where λ_γ can be computed numerically owing to $\sum_{k \in \mathcal{K}} P^*_{\gamma k} = p^{max}_\gamma$. Finally, in respect with constraint (6.11c), we have what follows for the BS:

$$P^*_{0k} = \max(p^{min}_0, \frac{SIC \times (N_{jk} + P^*_{ik}|h_{ij,k}|^2)}{2} \cdot (\sqrt{1 + \frac{4}{SIC \times (N_{jk} + P^*_{ik}|h_{ij,k}|^2)\lambda_0}} - 1)), \tag{6.13}$$

and for any uplink UE i:

$$P^*_{ik} = \max(p^{min}_i, \frac{N_{0k} + \frac{P^*_{0k}}{SIC}}{2|h_{ij,k}|^2} \cdot (\sqrt{1 + \frac{4}{\frac{N_{0k}+\frac{P^*_{0k}}{SIC}}{|h_{ij,k}|^2}\lambda_i}} - 1)). \tag{6.14}$$

6.5.3 Best Response Algorithm

Algorithm 7 has the pseudo-code for the scheduling and power allocation algorithm.

Algorithm 7 Scheduling and Power Allocation Algorithm for the Interference-Aware Game

Requires: Maximum tolerance $\epsilon \geq 0$.
Input: UE radio conditions, channel states, initial power settings p^u_0 and p^d_0
for TTI t=1,...,T
    Step 1: Scheduling
    RBs are allocated following G^1_t
    Step 2: Power Allocation
    repeat:
        Solve (6.10) in the uplink $\forall\ i \in \mathcal{I}$
        Update p^u_n
        Solve (6.10) in the downlink for the BS
        Update p^d_n
        $\delta^d = \left\| p^d_n - p^d_{n-1} \right\|$, $\delta^u = \left\| p^u_n - p^u_{n-1} \right\|$
        $n \leftarrow n + 1$
    until $\delta^d \leq \epsilon$ and $\delta^u \leq \epsilon$
end for

Every TTI, and following the scheduling step, the UEs on the uplink and the BS on the downlink take turns allocating powers on the RBs until a convergence is reached. Typically, the algorithm will reach a Nash equilibrium for the power allocation step in 3 to 4 iterations.

6.6 The Energy Efficient Game

Our objective in this game is to avoid power wastage as much as feasible. Our energy efficiency objective represents a benefit-to-cost ratio, where the benefit is represented by the SINR of the UEs and the cost by the interferences generated by them. To this end, any player γ weights its SINR by the interference it creates. Accordingly, for the energy efficient game $\mathcal{G}^e$, the utility of every uplink UE i becomes:

$$U_i^e = \frac{\sum_{k\in\mathcal{K}^i} \log \frac{P_{ik}|h_{ik}^u|^2}{N_{0k}+\frac{P_{0k}}{SIC}}}{\sum_{k\in\mathcal{K}^i} P_{ik}|h_{ij,k}|^2} \tag{6.15}$$

As for the BS:

$$U_0^e = \frac{\sum_{k\in\mathcal{K}} \log \frac{P_{0k}|h_{0k}|^2}{N_{jk}+P_{ik}|h_{ij,k}|^2}}{\sum_{k\in\mathcal{K}} \frac{P_{0k}}{SIC}} \tag{6.16}$$

Proposition 6.6.1 *Game $\mathcal{G}^e \langle M, S_0 \times \prod_i S_i, U^e \rangle$ is a super-modular game.*

Proof: To prove the super-modularity of the game, we need to verify the conditions discussed in the previous section. First, the strategy space S_γ is obviously a compact convex set of $\mathbb{R}^{|\mathcal{K}|}$. Hence, it suffices to verify the super-modularity of the objective function U_γ^e of any player γ as there are no constraint policies for $\mathcal{G}^e$. Hence, for any uplink UE i, we have :

$$\frac{\partial^2 U_i^e}{\partial P_{ik}\partial P_{0k}} = \frac{|h_{ij,k}|^2}{(\sum_{k\in\mathcal{K}} P_{ik}|h_{ij,k}|^2)^2(SIC\times N_{0k}+P_{0k})} \geq 0, \quad \forall i\in\mathcal{I}, \forall k\in\mathcal{K}.$$

And for the BS, we have what follows:

$$\frac{\partial^2 U_0^e}{\partial P_{0k}\partial P_{ik}} = \frac{|h_{ij,k}|^2}{SIC\times(N_{jk}+P_{ik}|h_{ij,k}|^2)(\sum_{k\in\mathcal{K}}\frac{P_{0k}}{SIC})^2} \geq 0, \quad \forall i\in\mathcal{I}, \forall k\in\mathcal{K}.$$

□

6.6.1 Computing the Nash Equilibrium

As we proved that we are in presence of a super-modular game, we implement a best response algorithm to reach its pure Nash equilibrium. A Nash equilibrium is the solution of the following optimization problems:

$$\max_{\boldsymbol{P}_\gamma} \; U_\gamma^e(\boldsymbol{P}_\gamma, \boldsymbol{P}_{-\gamma}) \tag{6.17a}$$

$$\text{Subject to} \quad \sum_{k\in\mathcal{K}} P_{\gamma k} \leq p_\gamma^{max}, \tag{6.17b}$$

$$P_{\gamma k} \geq p_\gamma^{min}, \; \forall k \in \mathcal{K}. \tag{6.17c}$$

where p_γ^{max} (resp. p_γ^{min}) is the maximal (resp. minimal) power limit on the uplink for $\gamma \in \mathcal{I}$ and on the downlink for $\gamma = 0$.

6.6.2 Dinkelbach Approach

The problems presented above cannot be solved in a straightforward manner as they are non-convex. However, as they are fractional problems, an optimal solution is obtained by iteratively solving the parametrized convex problems, according to the Dinkelbach method. For each uplink UE i, the problem is rewritten as follows:

$$\max_{\boldsymbol{P}_{ik}} \; F(\lambda_i) = \sum_{k\in\mathcal{K}^i} \log \frac{P_{ik}|h_{ik}^u|^2}{N_{0k} + \frac{P_{0k}}{SIC}} - \lambda_i \sum_{k\in\mathcal{K}^i} P_{ik}|h_{ij,k}|^2 \tag{6.18a}$$

$$\text{Subject to} \quad \sum_{k\in\mathcal{K}^i} P_{ik} \leq p_i^{max}, \tag{6.18b}$$

$$P_{ik} \geq p_i^{min}, \; \forall k \in \mathcal{K}^i. \tag{6.18c}$$

And for the BS on the downlink, it can be rewritten as follows:

$$\max_{\boldsymbol{P}_{0k}} \; F(\lambda_0) = \sum_{k\in\mathcal{K}} \log \frac{P_{0k}|h_{0k}|^2}{N_{jk} + P_{ik}|h_{ij,k}|^2} - \lambda_0 \sum_{k\in\mathcal{K}} \frac{P_{0k}}{SIC} \tag{6.19a}$$

$$\text{Subject to} \quad \sum_{k\in\mathcal{K}} P_{0k} \leq p_0^{max}, \tag{6.19b}$$

$$P_{0k} \geq p_0^{min}, \; \forall k \in \mathcal{K}. \tag{6.19c}$$

The values of λ_0 and λ_i can be calculated by iteration. The problems in (6.18) and (6.19) are first solved for large values of λ_i and λ_0, respectively. Afterwards, λ is calculated assuming that the objective functions found in (6.18a) and (6.19a) are equal to zero. The problems in

(6.18) and (6.19) are solved and the steps are repeated until the values of λ_i and λ_0 satisfy the conditions $F(\lambda_i)$= 0, and $F(\lambda_0)$= 0, respectively. This process is illustrated in Algorithm 8.

Algorithm 8 Calculating λ_γ

Define: number of iterations n
Set: λ_γ= $\mathcal{M}$ a sufficiently large value
    Repeat:
        Solve the problem in (6.18) for γ=i
        Solve the problem in (6.19) for γ=0
        Compute λ_γ such as $F(\lambda_\gamma)$=0
        $n \leftarrow n + 1$
    Until $F(\lambda_\gamma)$=0

6.6.3 Best Response

Similarly to the game before, a best response algorithm is used to reach a Nash equilibrium. Uplink players and the BS take turns solving the Dinkelbach problem for their locally optimal powers, until convergence is reached wherein the power levels on the RBs no longer change. This is illustrated in Algorithm 9.

Algorithm 9 Scheduling and Power Allocation Algorithm for the Energy Efficient Game

Requires: Maximum tolerance $\epsilon \geq 0$.
Input: UE radio conditions, channel states, initial power settings p_0^u and p_0^d
for TTI t=1,...,T
    Step 1: Scheduling
    RBs are allocated following G_t^1
    Step 2: Power Allocation
    repeat:
        Using Algorithm 8 get the value of $\lambda_i \; \forall \; i$
        Solve (6.18) in the uplink $\forall \; i \in \mathcal{I}$
        Update p_n^u
        Using Algorithm 8 get the value of λ_0
        Solve (6.19) in the downlink for the BS
        Update p_n^d
        δ^d=$\left\| p_n^d - p_{n-1}^d \right\|$, δ^u=$\left\| p_n^u - p_{n-1}^u \right\|$
        $n \leftarrow n + 1$
    until $\delta^d \leq \epsilon$ and $\delta^u \leq \epsilon$
end for

6.7 Simulations and Results

6.7.1 Simulation Parameters

We seek via our different simulation scenarios to address gains attributed to our game theoretic proposals. The simulation parameters we used are presented in Table 6.1.

Table 6.1 Simulation parameters for distributed power allocation

Parameter	Value
Cell Specifications	Single-Cell, 120-1000 m Radius
Number of RBs	60
SIC Value	10^{11}
Number of UEs	20 UEs: 10 downlink, 10 uplink
Demand Throughput	4 Mbps

6.7.2 Power Consumption

The Greedy Game

Allocating power on the RBs using the greedy game results in maximum power consumption. On the downlink, the power per RB is equal to the maximum available power divided by the total number of available resources. On the uplink, the transmit power on each RB is equal to the maximum UE transmit power divided by the number of resources allocated to a certain UE.

Figure 6.2 has a CDF plot with the results. The transmit powers on the RBs in the downlink is approximately 6.2 dBm, and for the uplink it ranges between 8 and 24 dBm.

The Interference Aware game

Similarly, allocating power on the RBs using the interference aware game also leads to maximum power usage. Nonetheless, the power is not equally divided on the RBs as before. Figure 6.3 has a CDF plot of the power allocated per RB on the uplink and the downlink. On the downlink, the power on the RBs varies between 4 and 8 dBm, and on the uplink it varies between 4 and 24 dBm. This variation comes as a result of including the generated interferences in the corresponding player utilities. This will also result in better throughput values for the UEs as we later on illustrate.

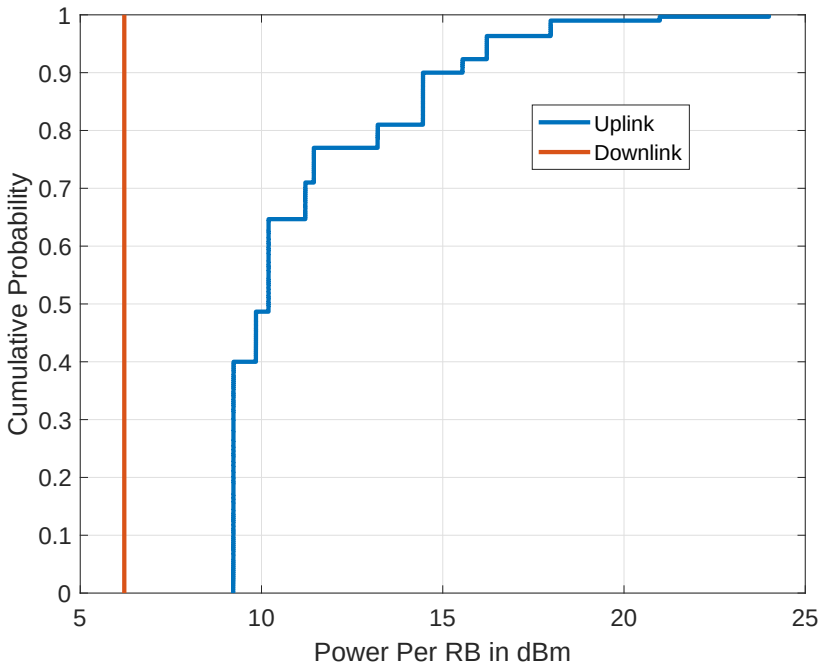

Figure 6.2 Power consumption per RB for the greedy game

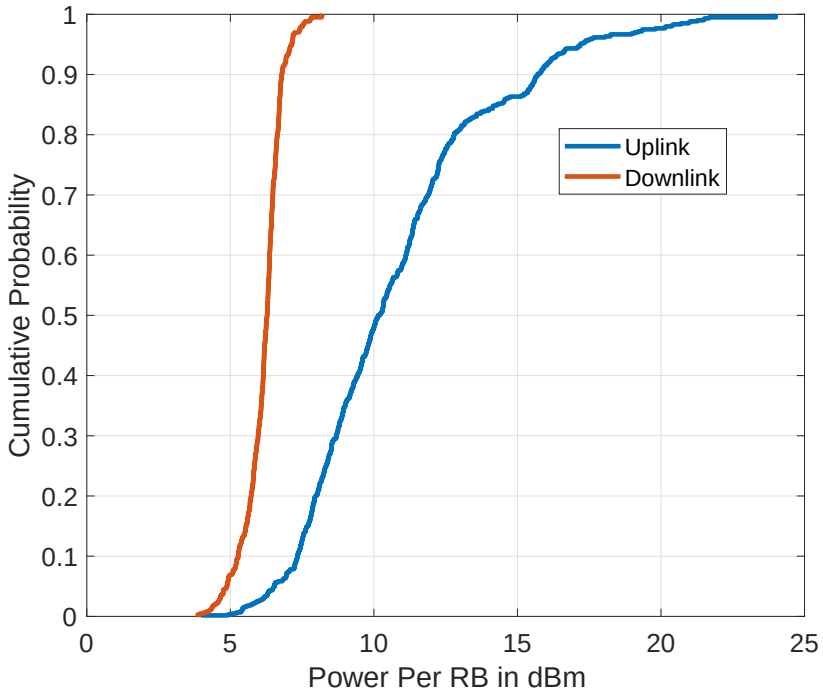

Figure 6.3 Power consumption per RB for the interference aware game

The Energy Efficient Game

In the case of the energy efficient game, neither the UEs on the uplink, nor the BS on the downlink consume maximum power. In fact, in the majority of the cases, the power assigned

on each RB defaults to the minimum allowed power. Figure 6.4 has a CDF plot with the results. For both the uplink and the downlink, and in the majority of the cases, the power allocated on the RBs is close to 6 dBm, around the default minimum value allowed for this simulation.

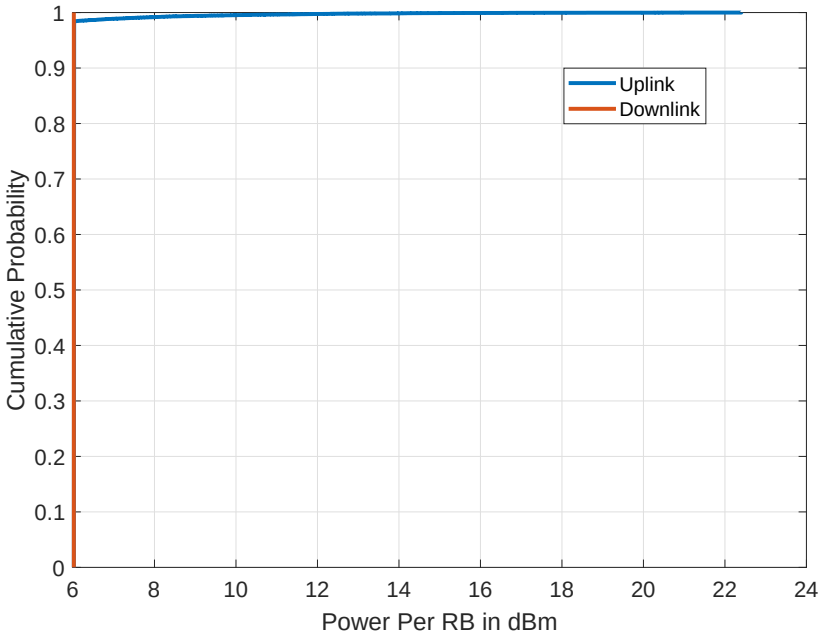

Figure 6.4 Power consumption per RB for the energy efficient game

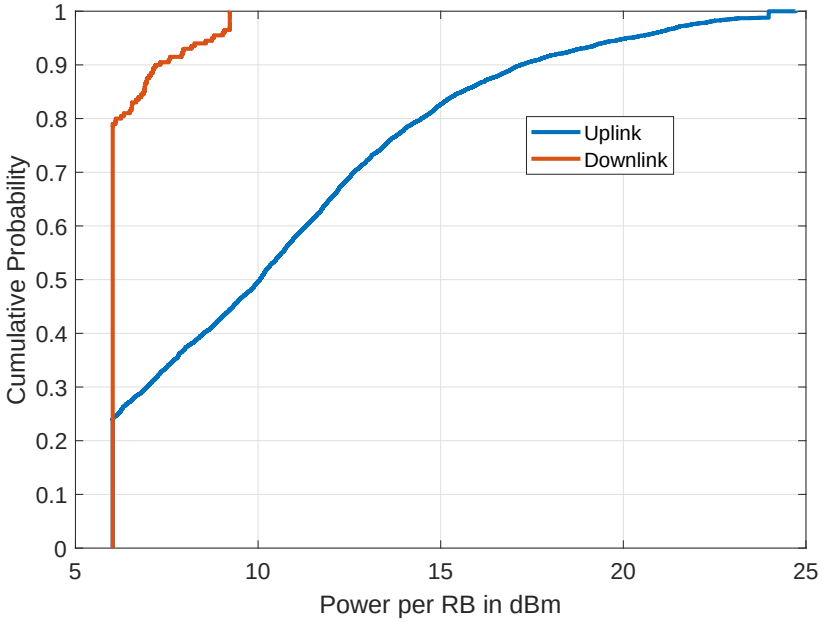

Figure 6.5 Power consumption per RB for the energy efficient game in case of a large cell

Nonetheless, the lower power limit is not the only factor in the allocation process. For example, if we increase the cell radius to 1 km, the game will result in higher power values on the RBs in order to improve the player utilities. This can be seen in Fig. 6.5. In this case, the power is significantly increased. This is due to two main reasons. First, to compensate the SINR losses resulting from increased BS-UE distances, and second in response to the now decreased UE-UE interferences as a result of the cell size increase. The power per RB on the uplink now has a median value at 10 dBm and can reach up to 24 dBm. On the downlink, about 20% of the UEs now transmit at a power larger than the minimum value.

6.7.3 Performance Evaluation in Terms of UE Throughput

We assess the performance of our proposed power allocation algorithms in terms of resulting UE throughput. We simulate the power allocation proposals alongside the full-duplex Proportional Fair scheduling algorithm. The cell radius considered in this simulation is 120 m. The results can be seen in Fig. 6.6.

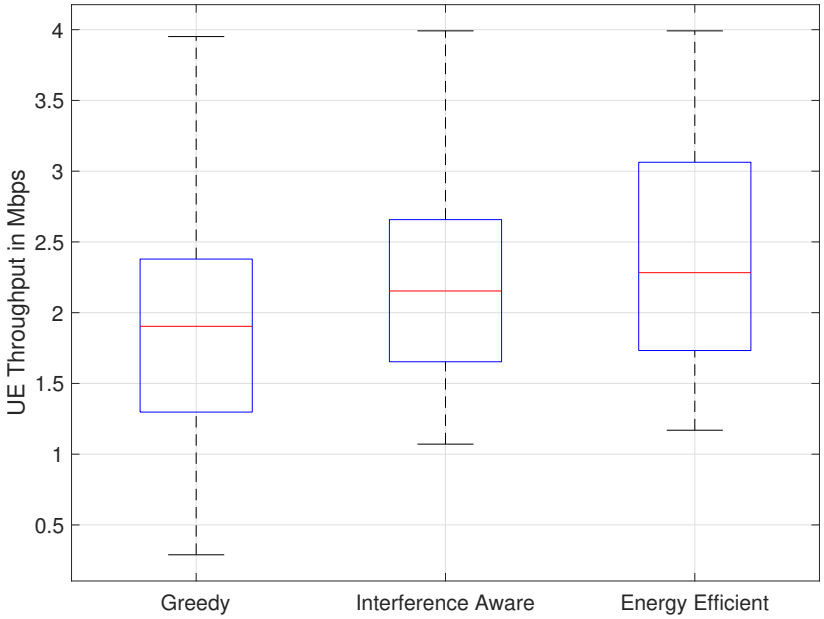

Figure 6.6 Effect of power allocation on UE throughput, case of small cell

The greedy game, the interference aware game, and the energy efficient game are all plotted. Comparing between the greedy game and the interference aware game, it is evident that better results are produced when the players mind the interferences they generate. The interference aware game has a higher maximum throughput value of 4 Mbps and a higher minimum value as well (1.1 Mbps compared to 0.25 Mbps for the greedy game). Nonetheless, it is clear that both algorithms waste power. The simulations for the energy efficient game

produce good results with lower power consumption. In comparison, the greedy game had around 25% of the UEs with throughput values less than 1.3 Mbps, about the minimum recorded throughput value for the energy efficient game.

Nonetheless, the relevance of one game over the other might change depending on the scenario at hand. In what follows, we increase the cell radius to 1 km, and note the resulting UE throughput values for each of the games. The results can be seen in Fig. 6.7. The minimum power per RB is set to 6 dBm.

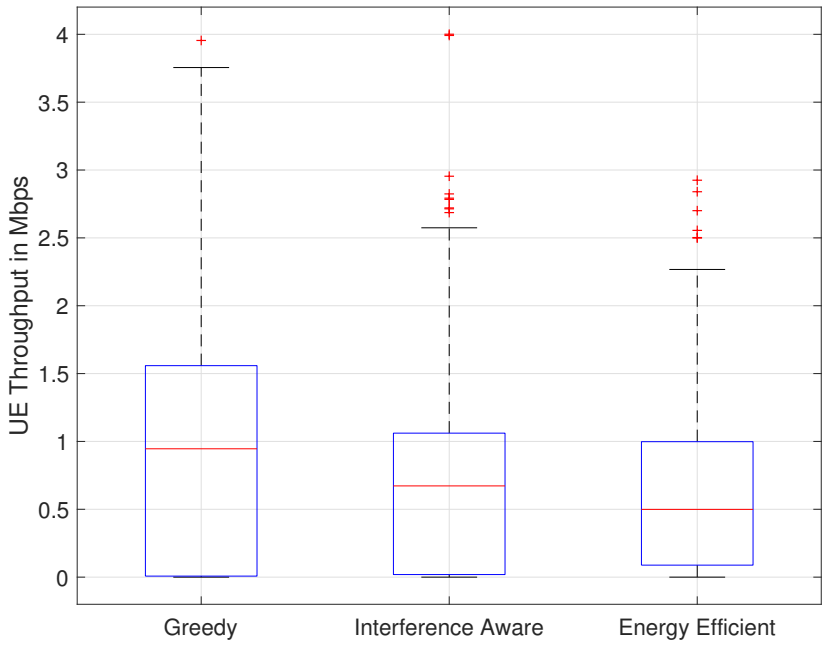

Figure 6.7 Effect of power allocation on UE throughput, case of large cell

An increase in cell size decreases inter-UE interference and lowers the SINR at UEs far away from the BS. An increase in UE power per RB would most benefit the UEs as it would improve their SINR, without affecting other UEs as much as before. As a result, the greedy game now produces the best performance in terms of UE throughput values. It produces a higher median value at about 1 Mbps, compared to 0.65 and 0.5 Mbps for the other two games, and it has much more UEs attaining throughput values close to the demand of 4 Mbps as well.

6.7.4 Performance Evaluation in Terms of Average UE Waiting Delay

As our queue model is non full-buffer, we are able to compute the average UE waiting delay using Little's formula. We calculate the latter across multiple simulation runs for full-duplex Proportional Fair alongside each of our power allocation proposals. We also compute the

average waiting delay for the full-duplex Max Sum-Rate algorithm simulated using the greedy game, and for half-duplex Proportional Fair using maximum power allocation as well. In this simulation, the cell has a radius of 120m. The results can be seen in the CDF plot of Fig. 6.8.

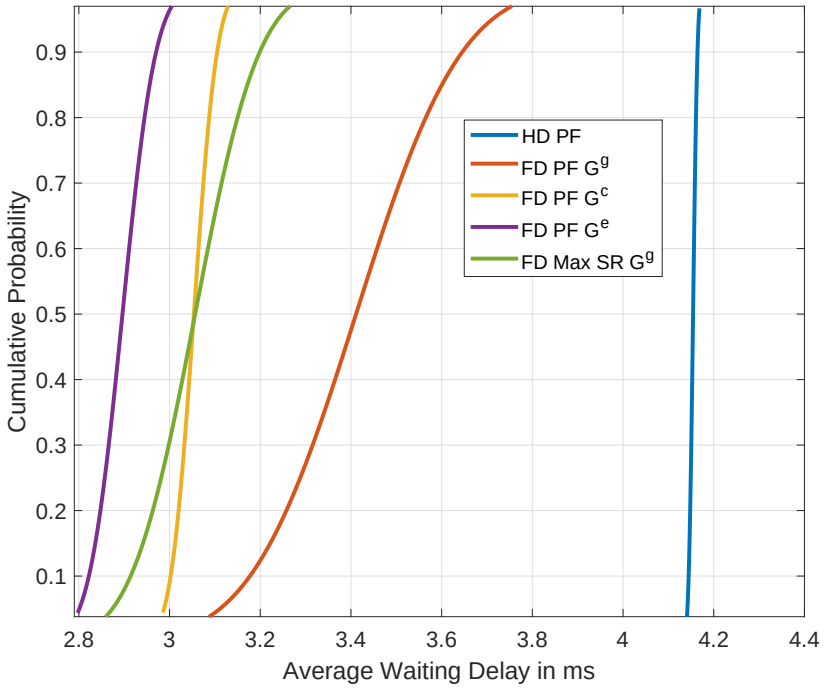

Figure 6.8 Effect of power allocation on UE waiting delay, case of small cell

As with the UE throughput values, the half-duplex algorithm produce the worst waiting delays with averages exceeding 4.16 ms. The greedy game produces average UE waiting delays between 3.1 and 3.75 ms, the interference aware game between 3 and 3.1 ms, and the energy efficient game between 2.8 and 3 ms. On the other hand, the greedy Max Sum-Rate algorithm results in average UE waiting delays ranging between 2.9 and 3.3 ms. As with throughput, the fairness imposed by Proportional Fairness scheduling will come at a cost in network and UE performances. Nonetheless, in this case both the interference aware and the energy efficient game were able to outperform or at least match the performance of greedy scheduling.

We now repeat the same simulation, albeit with the cell radius increased to 1 km. Fig. 6.9 has CDF plot with the resulting average UE waiting delays. Similar to the results seen in the previous section, the performances of the games are flipped. While half-duplex Proportional Fair still produces the largest average waiting delay (about 5 ms), the greedy game now actually produces the lowest waiting delay with average values between 3.95 and 4.85 ms. In this case, the greedy game produces lower waiting delays than the greedy Max Sum-Rate

scheduler. This can be traced back to several factors, primarily the ability of full-duplex Proportional Fair to further exploit the effects of multi-user diversity in a dynamic arrivals scenario.

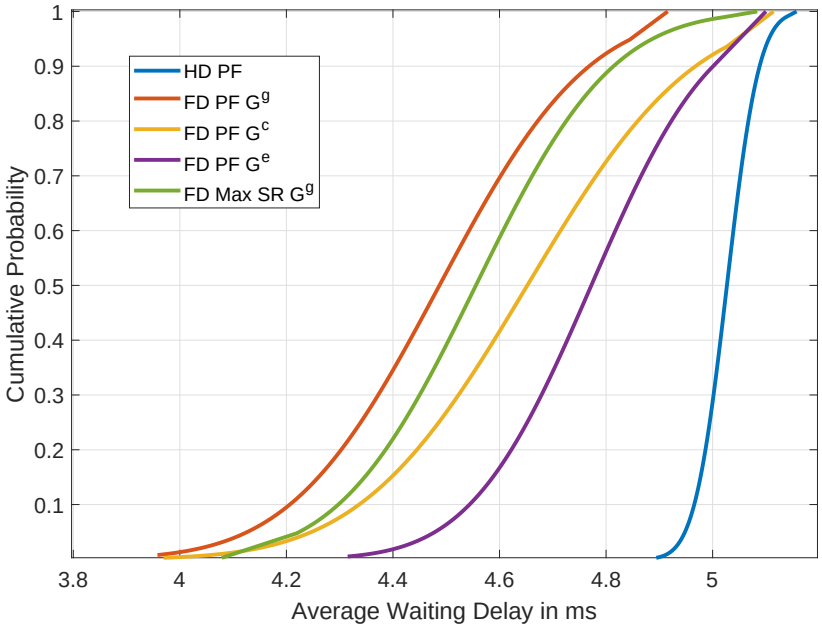

Figure 6.9 Effect of power allocation on UE waiting delay, case of large cell

6.7.5 The Price of Anarchy

The price of anarchy [68] is a game theory concept which measures how the efficiency of a system degrades due to the selfish behavior of its players. We study the price of anarchy in the case of the interference aware game. In this non-cooperative game proposal the uplink UEs and the BS on the downlink will each seek to maximize their own utilities. This is done in turn until a Nash equilibrium is achieved. A more global approach would be to maximize the sum of the uplink and downlink utilities. This problem can be written as follows:

$$\max_{\boldsymbol{P}_\gamma} \sum_{i\in\mathcal{I}}\sum_{j\in\mathcal{D}}\sum_{k\in\mathcal{K}}\left(\log\left(\frac{P_{ik}|h^u_{ik}|^2}{N_{0k}+\frac{P_{0k}}{SIC}+P_{ik}|h_{ij,k}|^2}\right)+\log\left(\frac{P_{0k}|h^d_{jk}|^2}{N_{jk}+P_{ik}|h_{ij,k}|^2+\frac{P_{0k}}{SIC}}\right)\right) \quad (6.20a)$$

$$\text{subject to} \quad \sum_{k\in\mathcal{K}} P_{\gamma k} \leq p^{max}_{\gamma}, \quad (6.20b)$$

$$P_{\gamma k} \geq p^{min}_{\gamma}, \ \forall k \in \mathcal{K}, \quad (6.20c)$$

where (6.20a) is the objective of this problem: to maximize the sum of the player utilities. (6.20b) and (6.20c) are the power constraints for the BS on the downlink and the UEs on the uplink, for $\gamma = 0$ and $\gamma = i$, respectively.

In what follows we compare the resulting objective value from the sum of maximizing the separate utilities (distributed approach) vs. the maximization of the sum of utilities *i.e.,* the global optimal (centralized approach). Figure 6.10 has a CDF plot of the ratio of the sum of objective values generated by maximizing the player utilities separately divided by the result yielded by the global problem.

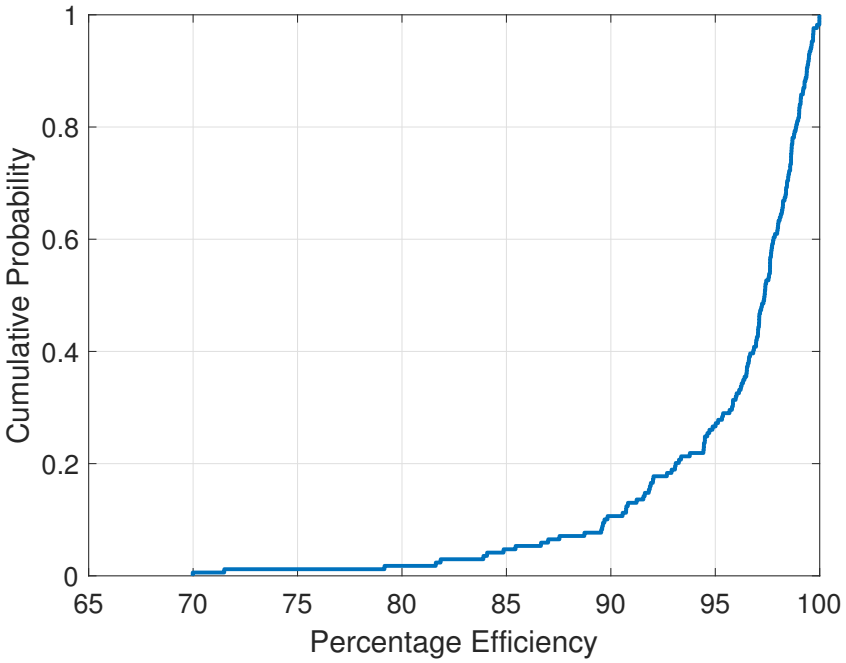

Figure 6.10 The price of anarchy for the interference aware game

In more than 80% of the cases, the selfishness of the cooperative game costs less than 7% in objective efficiency. In some rare cases, the selfish approach achieves less than 80% of the result achieved by the global objective. Nonetheless, this disparity in objectives does not yield better throughput results for the global optimal problem. As the uplink and downlink transmission are intertwined, an increase in the uplink UE power will negatively impacts its paired downlink UE and vice versa.

6.8 Conclusion

In this chapter, we put forward a game theoretic framework for power allocation in full-duplex wireless networks. Unlike the centralized approach to power allocation, this distributed

approach does not require a central authority or any signaling. Coupled with our scheduling proposals, we proposed several non-cooperative games for power allocation. These games are played between the UEs on the uplink and the BS downlink. The first of these games is greedy. In it, each player seeks to maximize its radio conditions individually. The second game is interference aware, wherein players take their generated interferences into account. And our third proposal, the energy efficient game, aims to better utilize the available power while combating the full-duplex interferences. Via a set of simulations we showed that the relevance of each game depends in fact on the scenario at hand. The energy efficient game saves power and is most viable in small cell scenarios, whilst the greedy game delivers the most in terms of performance when it comes to large cell scenarios.

Chapter 7

Scheduling and Power Allocation in Full-Duplex Multi-Cellular Networks

7.1 Introduction

In this chapter, we explore the challenges of scheduling and power allocation in the context of multi-cellular full-duplex wireless networks. This is a more realistic setting than the single cell scenario, and it better envisions how full-duplex wireless communications could eventually be implemented. We propose an optimal joint scheduling and power allocation problem for full-duplex wireless networks. Because of its mathematical intractability, we decouple the problem and solve for scheduling first, and for power allocation second. We consider both indoor and outdoor scenarios and show that the gains of multi-cellular full-duplex wireless networks, with respect to their half-duplex counterparts, are situational. Furthermore, we highlight the importance of inter-cell cooperation when it comes to scheduling resources and show that depending on the scenario at hand, interference mitigation from inter-cell cooperation can improve the performance of UEs in terms of throughput. Finally, we show that power allocation can improve UE throughput with its efficiency being tied to the deployment scenario.

7.2 Full-Duplex Multi-Cell Interferences

The presence of multi-cells greatly increases the interference problems in a full-duplex wireless network. Consider the scenario illustrated in Fig. 7.1 below, where we have two adjacent cells following our network model. The base stations (BSs) are the full-duplex

nodes, and the user equipment (UEs) are half-duplex. Each BS will schedule pairs of uplink-downlink UEs on the available radio resources.

As a result, each uplink UE in the first cell will experience interferences from three sources:

1. I1: Self-interference at the BS due to its transmission towards a downlink UE on the same resource block (RB).
2. I2: Co-channel interference resulting from uplink UEs in neighboring cells using the same RB.
3. I3: Inter-cell interference from neighboring cell BSs transmitting on the same RB.

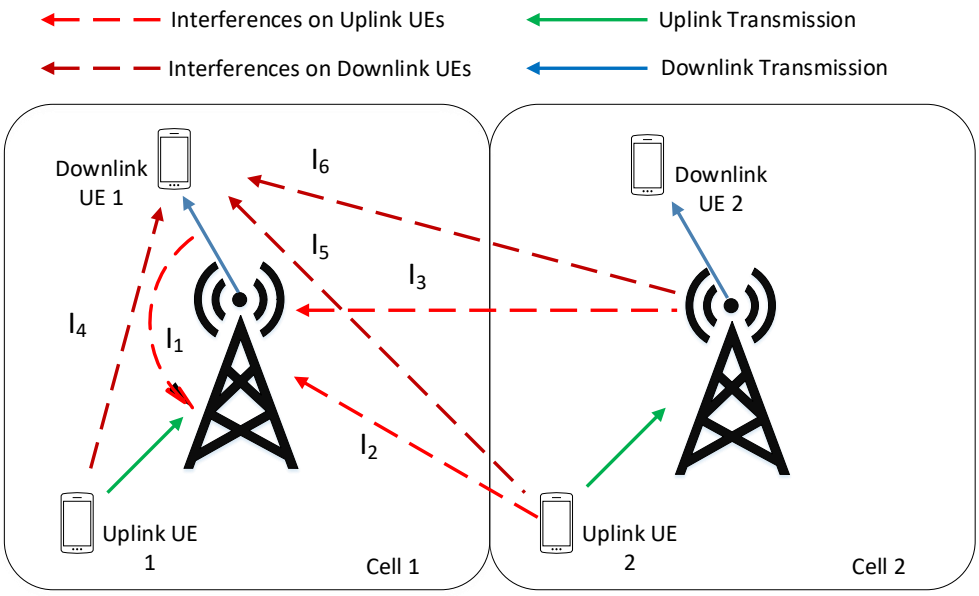

Figure 7.1 Inter-cell interferences in a multi-cell scenario

A Downlink UE in the first cell also experience interferences from three different sources:

1. I4: Intra-cell co-channel interference from its paired uplink UE using the same RB.
2. I5: Co-channel interference resulting from uplink UEs in neighboring cells using the same RB.
3. I6: Inter-cell interference from neighboring cell BSs transmitting on the same RB.

7.3 SINR Calculation

7.3.1 Notations

In order to accommodate the presence of a multi-cell scenario, a different set of notations are used. They can be seen in Table 7.1 below, where b belongs to the set of BSs $\mathcal{B}$.

Table 7.1 Notation summary

Notation	Definition
$S^u(i,j,k,b)$	SINR of uplink UE i on RB k in the pair (i,j) associated with BS b
$S^d(i,j,k,b)$	SINR of downlink UE j on RB k in the pair (i,j) associated with BS b
P^u_{ik}	Transmit power of uplink UE i on RB k
P^d_{bk}	Transmit power of BS b on RB k
h^u_{ibk}	Channel between i and BS b on RB k
$h^s_{b'bk}$	Channel between BSs b' and b on RB k
h_{ijk}	Inter-UE channel between i and j on RB k
h^d_{bjk}	Channel between BS b and downlink UE j on RB k
SIC	Self-interference cancellation factor
N^u_{bk}	Noise power at BS b on RB k
N^d_{jk}	Noise power at j on RB k

7.3.2 Interference Calculation

The full-duplex interferences on a UE transmitting or receiving on an RB k are calculated as follows.

- The self-interference experienced by every uplink UE, on RB k, at its corresponding BS is written as:
$$I_1 = \frac{P^d_{bk}}{SIC}. \tag{7.1}$$
- The interference on an uplink UE from all uplink UEs i' using the same RB:
$$I_2 = \sum_{i' \in \mathcal{I} \setminus i} (P^u_{i'k} |h^u_{i'bk}|^2 \sum_{j \in \mathcal{D}} Z_{i'jk}), \tag{7.2}$$
where $Z_{i'jk}$ is a global resource allocation variable that conditions that uplink UE i' is indeed transmitting on RB k.

- The interference on an uplink UE from all BSs transmitting on the downlink using the same RB k:

$$I_3 = \sum_{b' \in B \setminus b} P^d_{b'k} |h^s_{b'bk}|^2. \tag{7.3}$$

- The interference on a downlink UE from all uplink UEs i' using the same RB k:

$$I_4 + I_5 = \sum_{i' \in \mathcal{I}} (P^u_{i'k} |h_{i'jk}|^2 \sum_{j \in \mathcal{D}} Z_{i'jk}). \tag{7.4}$$

- The interference on a downlink UE from all BSs transmitting on the same RB k:

$$I_6 = \sum_{b' \in B \setminus b} P^d_{b'k} |h^d_{b'jk}|^2. \tag{7.5}$$

7.3.3 SINR formulation

As a result, The SINR for an uplink UE i paired with a downlink UE j on RB k and associated with BS b is written as:

$$S^u(i,j,k,b) = \frac{P^u_{ik} |h^u_{ibk}|^2}{N^u_{bk} + \frac{P^d_{bk}}{SIC} + \sum_{b' \in B \setminus b} P^d_{b'k} |h^s_{b'bk}|^2 + \sum_{i' \in \mathcal{I} \setminus i} (P^u_{i'k} |h^u_{i'bk}|^2 \sum_{j \in \mathcal{D}} Z_{i'jk})}, \tag{7.6}$$

For a downlink UE j paired with an uplink UE i on RB k and associated with BS b, the SINR becomes:

$$S^d(i,j,k,b) = \frac{P^d_{bk} |h^d_{bjk}|^2}{N^d_{jk} + \sum_{i' \in \mathcal{I}} (P^u_{i'k} |h_{i'jk}|^2 \sum_{j \in \mathcal{D}} Z_{i'jk}) + \sum_{b' \in B \setminus b} P^d_{b'k} |h^d_{b'jk}|^2}. \tag{7.7}$$

7.4 Multi-Cell Deployment Scenarios

In our work, we consider both indoor and outdoor cell scenarios. In what follows, we highlight the specifics of these scenarios.

Indoor Scenario

We consider the indoor cell scenario illustrated in Fig. 7.2 below. Seven indoor cells are present in this network. The distance from the central cell BS to all other BSs is constant. Each cell has 10 randomly distributed UEs.

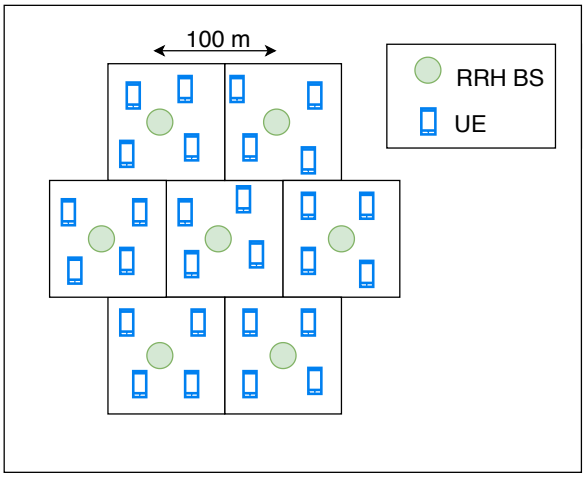

Figure 7.2 Indoor deployment scenario

The parameters used for this scenario are stated in Table 7.2 below. The path loss model used is based on 3GPP simulation recommendations for an RRH cell environment [69]. Additionally a penetration loss of 20 dB between cells due to walls is assumed. The path loss model used for BS-to-BS channels is the same one used for UE-to-UE channels with the justification that the BSs have no significant height advantages in the case of indoor cells.

The probability of line of sight is given by (d is the distance in m):

$$P_{LOS} = \begin{cases} 1, & \text{if d} \leq 18 \\ \exp(-(d-18)/27), & \text{if 18} < \text{d} < 37 \\ 0.5, & \text{if d} \geq 37 \end{cases} \tag{7.8}$$

Table 7.2 Path loss model for the indoor cells

Parameter (d in m, f_c in GHz)	**Value**
Shadowing	Log-normal with σ = 3 dB if LOS, 4 dB otherwise
Fast Fading	Exponential with unit parameter
LOS path loss within a cell in dB	32.8 + 20$\log_{10}(f_c)$ + 16.9$\log_{10}$(d)
NLOS path loss within a cell in dB	11.5 + 20$\log_{10}(f_c)$ + 43.3$\log_{10}$(d)
Path loss between two cells in dB	11.5 + 20$\log_{10}(f_c)$ + 43.3 $\log_{10}$(d)
Penetration loss	Due to boundary: 20 dB, within a cell: 0 dB

Outdoor Scenarios

The outdoor scenarios we consider in this chapter are illustrated in Fig. 7.3 below.

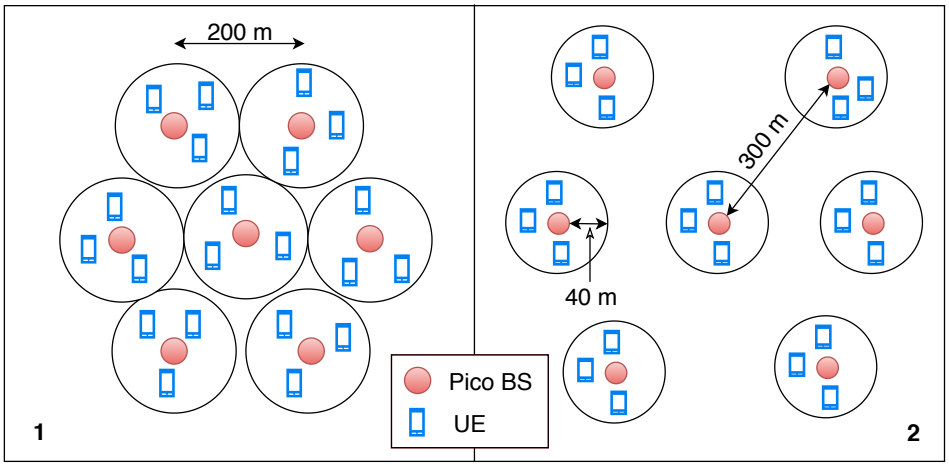

Figure 7.3 First (left) and second (right) outdoor deployment scenarios

There are no physical barriers between the cells in the outdoor scenarios. 10 UEs are randomly dropped in each cell. In the second outdoor deployment, the distribution of the UEs is closer to their corresponding BSs. This means the average distance between a UE and its inter-cell interferers is increased. The path loss model used for both scenarios, as given by 3GPP simulation standards [70], can be seen in Table 7.3. The probability of line of sight in this case is given by (d is the distance in km):

$$P_{LOS} = 0.5 - \min(0.5, 5\exp(-0.156/d)) + \min(0.5, 5\exp(-d/0.03)). \tag{7.9}$$

Table 7.3 Path loss model for the outdoor cells

Parameter (d in km)	**Value**
Shadowing inside the cell	Log-normal with σ = 3 dB if LOS, 4 dB otherwise
Shadowing between the cells	Log-normal with σ = 6 dB
Fast Fading	Exponential with unit parameter
BS-to-BS LOS path loss	if d $<$ 2/3 km then 98.4 + 20$\log_{10}(d)$, else 101.9 + 40$\log_{10}(d)$
BS-to-BS NLOS path loss	169.36 + 40$\log_{10}(d)$
BS-to-UE LOS path loss	103.8 + 20.9$\log_{10}(d)$
BS-to-UE NLOS path loss	145.4 + 37.5$\log_{10}(d)$
UE-to-UE path loss	if d $<$ 50 m then 98.45 + 20$\log_{10}(d)$, else 175.78 + 40$\log_{10}(d)$
Penetration loss	0 dB

7.5 Optimal Approach to Scheduling and Power Allocation in a Multi-Cell Setting

We propose an optimal algorithm for scheduling and power allocation in a multi-cellular full-duplex wireless network. Our objective is to maximize the logarithmic sum of the signal-to-interference-plus-noise-ratios (SINR) of the scheduled pairs of user equipment (UEs). This is a fairness oriented allocation as proclaimed in [71, 72]. We define the UE pair-RB-base station (BS) allocation variable z_{ijkb}, $\forall i \in \mathcal{I}, \forall j \in \mathcal{D}, \forall k \in \mathcal{K}, \forall b \in \mathcal{B}$. It is equal to one if uplink UE i is paired with downlink UE j on RB k, whilst associated with BS b. It is equal to zero otherwise. As explained in the following chapter, there is no inherent advantage of allowing the formation of pairs across the boundaries of different cells. As such, each BS has its unique set of UEs i and j and subsequently, unique possible UE pairings. Reuse-1 is assumed for the radio resource allocation process. As such, each BS has access to all the RBs. The scheduling and power allocation problem problem can be thereafter formulated as follows:

($\mathcal{P}^t_{mc}$)

$$\underset{z_{ijkb},P^d_{bk},P^u_{ik}}{\text{Maximize}} \quad \sum_{b\in\mathcal{B}}\sum_{k\in\mathcal{K}}\sum_{i\in\mathcal{I}}\sum_{j\in\mathcal{D}} z_{ijkb}(\log(S^u(i,j,k,b)) + \log(S^d(i,j,k,b))) \tag{7.10a}$$

$$\text{Subject to} \quad \sum_{i\in\mathcal{I}}\sum_{j\in\mathcal{D}} z_{ijkb} \leq 1,\ \forall k \in \mathcal{K},\ \forall b \in \mathcal{B}, \tag{7.10b}$$

$$\sum_{k\in\mathcal{K}}\sum_{j\in\mathcal{D}} z_{ijkb}T^u_{ijk} \leq D^u_i,\ \forall i \in \mathcal{I}, \forall b \in \mathcal{B}, \tag{7.10c}$$

$$\sum_{k\in\mathcal{K}}\sum_{i\in\mathcal{I}} z_{ijkb}T^d_{ijk} \leq D^d_j,\ \forall j \in \mathcal{D}, \forall b \in \mathcal{B}, \tag{7.10d}$$

$$\sum_{k\in\mathcal{K}} P^d_{bk} \leq p_0^{max},\ \forall b \in \mathcal{B}, \tag{7.10e}$$

$$\sum_{k\in\mathcal{K}} P^u_{ik} \leq p_i^{max},\ \forall i \in \mathcal{I}, \tag{7.10f}$$

$$P^u_{ik} \geq p_i^{min},\ \forall i \in \mathcal{I},\ \forall k \in \mathcal{K}^i, \tag{7.10g}$$

$$P^d_{bk} \geq p_0^{min},\ \forall k \in \mathcal{K},\ \forall b \in \mathcal{B}, \tag{7.10h}$$

$$z_{ijkb} \in \{0,1\},\ \forall i \in \mathcal{I}, \forall j \in \mathcal{D}, \forall k \in \mathcal{K}, \forall b \in \mathcal{B} \tag{7.10i}$$

This problem belongs to the category of mixed integer non-linear programming (MINLP). Because of the high number of variables, it is already intractable and can become impossibly complex as the number of UEs, RBs, and BSs increases. As such, we follow the same approach we used in Chapters 5 and 6, wherein the problem is divided into two: (a) a scheduling problem, followed by (b) a power allocation problem.

7.5.1 Single Cell Scheduling

In each time slot, every BS schedules its radio resources independently. With the exception of the central cell, the cells are oblivious of their surroundings and do not account for inter-cell interferences. As such, the SINR formulas introduced in Chapter 3 are used. The central cell allocates its resources based on feedback from the surrounding cells on how they each distributed their own resources. The SINR values in this case are calculated using the equations presented in this chapter. The assumption of single scheduling is essential to obtain a tractable problem as well. If each of the seven cells (as discussed in our deployment scenarios) has 10 UEs, a total of $(25)^7$ or more than 6×10^9 possible scenarios exist for the allocation of each RB. This makes the problem hard to solve in a centralized manner. The problem in its current form–as single cell scheduling–is a simple ILP problem and can be solved efficiently using any optimization software such as CVX [63]. For the purpose of scheduling, constant powers within the feasible constraints are assumed. In addition, the BS is assumed to have complete channel state information (CSI) including all the UE-to-UE channels. The single cell scheduling problem can thereafter be written as follows:

$$\underset{z_{ijk}}{\text{Maximize}} \quad \sum_{k\in\mathcal{K}}\sum_{i\in\mathcal{I}}\sum_{j\in\mathcal{D}} z_{ijk}(\log(S_j^u(i,k)) + \log(S_i^d(j,k))) \tag{7.11a}$$

$$\text{Subject to} \quad \sum_{i\in\mathcal{I}}\sum_{j\in\mathcal{D}} z_{ijk} \leq 1,\ \forall k \in \mathcal{K}, \tag{7.11b}$$

$$\sum_{k\in\mathcal{K}}\sum_{j\in\mathcal{D}} z_{ijk}T_{ijk}^u \leq D_i^u,\ \forall i \in \mathcal{I}, \tag{7.11c}$$

$$\sum_{k\in\mathcal{K}}\sum_{i\in\mathcal{I}} z_{ijk}T_{ijk}^d \leq D_j^d,\ \forall j \in \mathcal{D}, \tag{7.11d}$$

$$z_{ijk} \in \{0,1\},\ \forall i \in \mathcal{I}, \forall j \in \mathcal{D}, \forall k \in \mathcal{K}. \tag{7.11e}$$

With the exception of the central cell which allocates its resources following:

$$\underset{z_{ijk}}{\text{Maximize}} \quad \sum_{k\in\mathcal{K}}\sum_{i\in\mathcal{I}}\sum_{j\in\mathcal{D}} z_{ijk}(\log(S^u(i,j,k,1)) + \log(S^d(i,j,k,1))) \tag{7.12}$$

Subject to (7.11b) to (7.11e)

7.5.2 Multi-Cell Power Allocation

The power is allocated on all the RBs for all the cells conjointly, by an assumed central unit, after the radio resources have been allocated by each cell independently. The power

allocation problem can thereafter be written as follows:

$$\underset{P_{bk},P_{ik}}{\text{Maximize}} \quad \sum_{b\in\mathcal{B}}\sum_{k\in\mathcal{K}}\sum_{i\in\mathcal{I}}\sum_{j\in\mathcal{D}} z^*_{ijkb}(\log(S^u(i,j,k,b)) + \log(S^d(i,j,k,b))) \tag{7.13}$$

$$\text{Subject to} \quad \text{(7.10e) to (7.10i)}$$

The aim is to use power allocation to minimize the interferences generated from full-duplex operation and single cell scheduling. Whilst this problem is still of the MINLP category, it is now tractable and can be efficiently solved for each TTI using geometric programming [73].

7.6 Simulations and Results

7.6.1 Simulation Parameters

The simulation parameters used for this chapter are presented in Table 7.4 below. In the following simulations, the performance assessment is done for the central cell UEs only. Unless specified otherwise, the central cell will take its scheduling decision based on feedback from the surrounding cells on how they each allocated their resources. In the comparison between half-duplex and full-duplex scheduling, maximum power allocation is assumed for both.

Table 7.4 Simulation parameters for multi-cell scheduling

Parameter	**Value**
Number of RBs	50
SIC Value	10^{11}
Number of UEs	10 UEs per cell: 5 UL, 5 DL
Demand Throughput	4 Mbps

7.6.2 Indoor Deployment Scenario

UE Performance

We first aim to assess the profitability of full-duplex wireless communications with respect to their half-duplex counterparts. For the considered scenario, we simulate the proposed scheduling algorithm for both full-duplex and half-duplex scheduling. The results can be seen in the CDF plot of Fig. 7.4. The mean UE throughput value for half-duplex UEs is

always less than 2 Mbps. In comparison, the mean UE throughput value for full-duplex UEs is between 3.3 and 4 Mbps. The latter achieve almost double the throughput values.

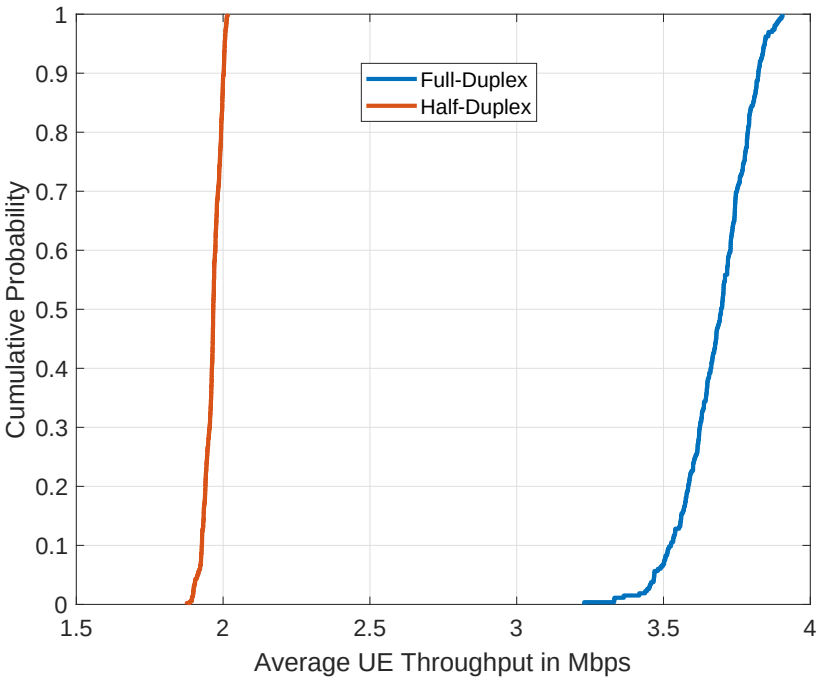

Figure 7.4 Central cell UE throughput values for the indoor scenario

Cell Cooperation

Additionally, we explore the gains resulting from relaying interference information to the central cell. We repeat the simulation of our algorithm, albeit with the central cell being unaware of the scheduling decisions of the surrounding cells (scheduling for the central cell is done following the problem in 7.11). Figure 7.5 has box plots showing the achieved efficiency ratios for both half-duplex and full-duplex scheduling. We define the latter as the ratio of the total throughput achieved by central cell UEs when such inter-cell information is not relayed to the cell, to the total UE throughput achieved when such information is in fact relayed to the central cell.

Depending on how the UEs are dropped inside the cell, the lack of relayed information to the central cell could cost up to 12% in its throughput efficiency in the case of full-duplex communications. Half-duplex communications are also affected by the absence of cell cooperation. Except for a few outliers, the maximum loss in efficiency for half-duplex is about 14%. This difference will not make half-duplex communications more profitable than their full-duplex counterparts even in the lack of cell cooperation. Nonetheless, based on these results, we can expect significant gains for full-duplex communications if the

scheduling was to be done for all cells at the same time ($i.e.$, a centralized global approach to scheduling). A further study on how cell border UEs benefit from this cooperation showed that their performances do not vary any differently when compared with the rest of the UEs in the cell. In the aforementioned scenario, the intra-cell co-channel interference and the inter-UE distance will play a more important role in regards to a UE's radio conditions than the distance separating it from the BS.

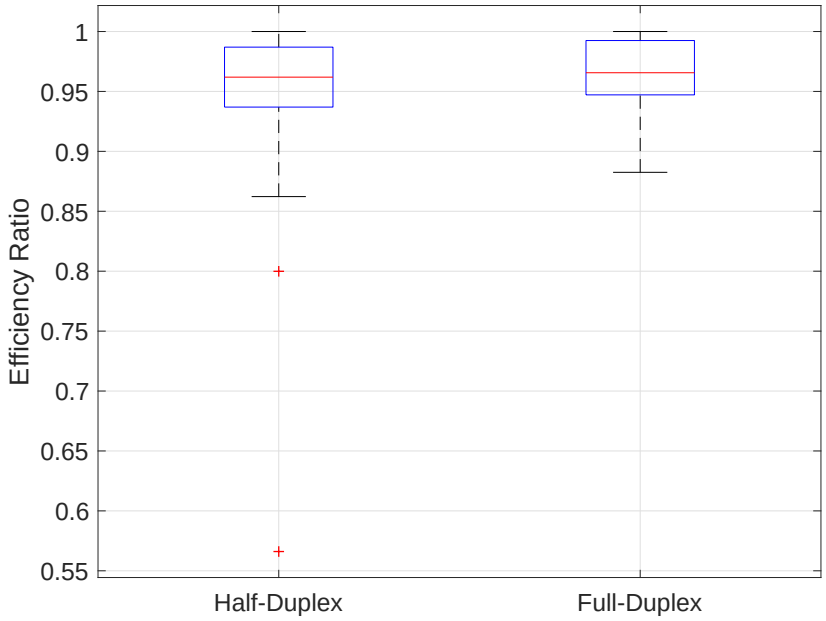

Figure 7.5 Effect of inter-cell cooperation on UE performances for the indoor scenario

7.6.3 Outdoor Scenarios

First Outdoor Scenario

We now consider the first outdoor deployment scenario illustrated by Fig. 7.3. The distance separating the central BS from all others is 200 m. Without any barriers separating the cells, the inter-cell interference affecting the UEs is enormous.

Figure 7.6a shows that in this scenario, cell cooperation is vital. More than 30% of the central cell's efficiency in terms of total throughput could be lost as a result of independent single cell scheduling, with a median efficiency loss of about 12%. Nonetheless, the gains of full-duplex communications are lost in this scenario. Figure 7.6b shows that full-duplex communications are no longer profitable with respect to their half-duplex counterparts. About 95% of the time, half-duplex UEs will attain higher average throughput values.

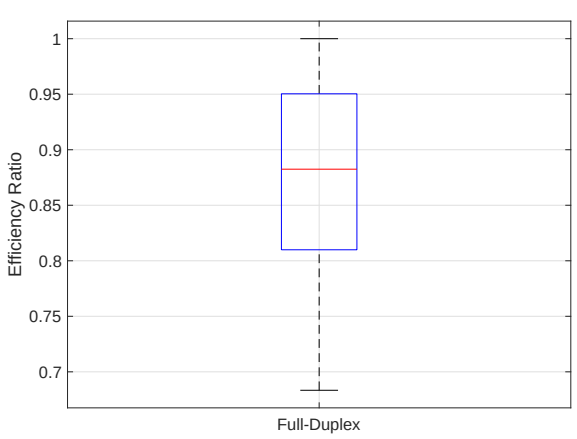

(a) Effect of inter-cell cooperation

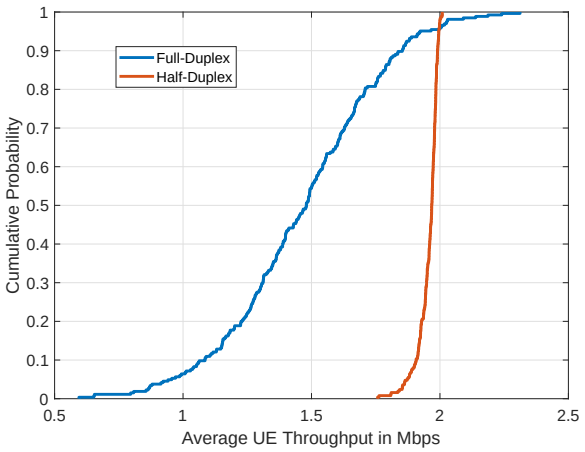

(b) Average UE throughput

Figure 7.6 Results for the first outdoor scenario

Second Outdoor Scenario

As the previous outdoor scenario produces no gains from full-duplex communications, we consider a second scenario wherein the UEs remain in close vicinity of the BSs. This case is illustrated in Fig. 7.3 as the second outdoor scenario. The simulation parameters remain as stated in the previous section. Figure 7.7 has a CDF plot illustrating the resulting average UE throughputs.

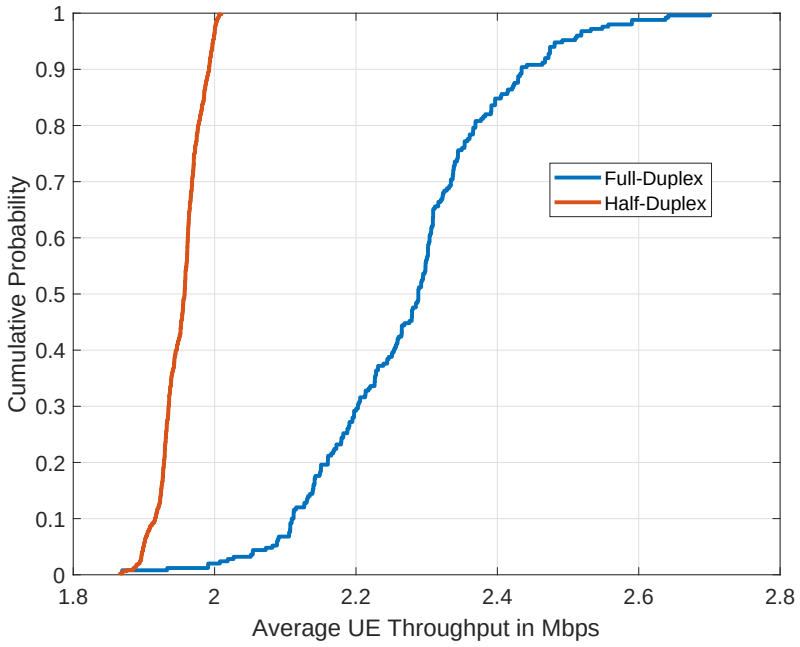

Figure 7.7 Central cell UE throughput values for the second outdoor scenario

Though not as profitable as the indoor deployment scenario, it is evident that the full-duplex gains are retrieved. The average UE throughput values for the full-duplex algorithm ranges between 1.9 Mbps to slightly over 2.6 Mbps. It registers a median around 2.3 Mbps. The half-duplex algorithm on the other hand has average UE throughput values between 1.9 Mbps and 2 Mbps with a median value of 1.97 Mbps. Half-duplex central cell UEs manage on average about 15% less than their full-duplex counterparts in terms of total throughput.

Furthermore, we assess the importance of inter-cell cooperation in this scenario as well. The box plots in Fig. 7.8 have the efficiency ratio of the total throughput achieved without cell cooperation to that achieved with it, for the central cell, for both full-duplex and half-duplex scheduling.

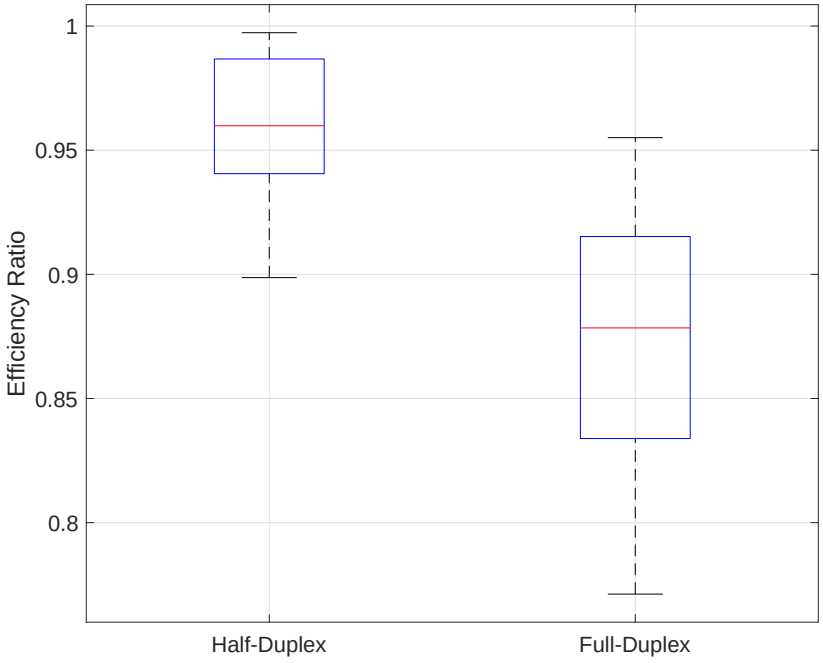

Figure 7.8 Effect of cell cooperation on UE performances for the second outdoor scenario

In the case of full-duplex communications, up to 27% of the cell's throughput could be lost due to the lack of such cooperation. For the half-duplex case, a maximum of 10% in efficiency is lost. Even in a worst case scenario, full-duplex communications would still bring profit with respect to their half-duplex counterparts. Nonetheless, these gains could be limited in case no cell cooperation exists.

7.6.4 Power Allocation for the Indoor Scenario

We first consider the indoor deployment scenario. We simulate the proposed scheduling algorithm both with and without power allocation. In the absence of power allocation, equal maximum power is assumed. On the uplink, each UE will transmit with the maximum power equally divided among the RBs it got. On the downlink, each BS will transmit on all the RBs with the same power (total power divided by the number of RBs). Figure 7.9 has a CDF plot with the resulting average UE throughput values per simulation. Though limited due to the well mitigated inter-cell interferences, the benefits of power allocation on UE throughput can be seen. On average, power allocation UEs have a higher minimum average throughput (3.45 to 3.23 Mbps) and higher maximum as well (3.95 to 3.9 Mbps). A general increase in the average UE throughput values can be noted. As much as 10% in total throughput gain for the central cell could be achieved as a result of power allocation.

7.6.5 Power Allocation for the Second Outdoor Scenario

We consider the second outdoor deployment scenario. Similar to before, we simulate our scheduling algorithm with and without power allocation. Equal maximum power is considered in the case of the latter. Figure 7.10 has a CDF plot with the results. As in the indoor scenario, power allocation provides an increase in the average UE throughput values. The median average UE throughput value for the case with power allocation is about 2.45 Mbps compared to 2.3 Mbps without power allocation. Up to 25% in total central cell throughput could be gained as a result of power allocation. The outdoor scenario exhibits higher inter-cell interferences and as a result, stands to benefit more from power allocation.

Case of Low SIC

We repeat the simulation for the same outdoor deployment scenario albeit with the self-interference cancellation (SIC) factor lowered to 10^8. Following the SINR formulas, this will degrade the performance of uplink UEs in the network. Figure 7.11 has box plots with the results. Power allocation improves the performance of uplink UEs in the central cell. Without power allocation, these UEs achieve a median throughput of about 0.5 Mbps and a maximum of 3.5 Mbps (barring some outliers). Well over 75% of the uplink UEs would achieve a throughput less than 1.5 Mbps. On the other hand, power allocated uplink UEs achieve a median of about 1.4 Mbps with half of the UEs achieving a throughput above 1.5 Mbps. Power allocation better adapts the UEs to the challenges the network could experience.

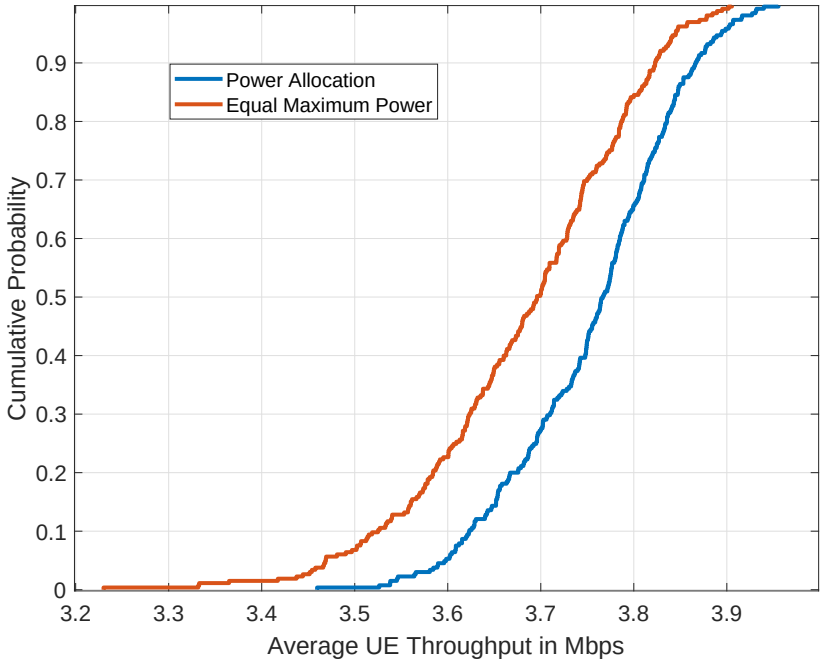

Figure 7.9 Effect of power allocation on UE throughputs for the indoor scenario

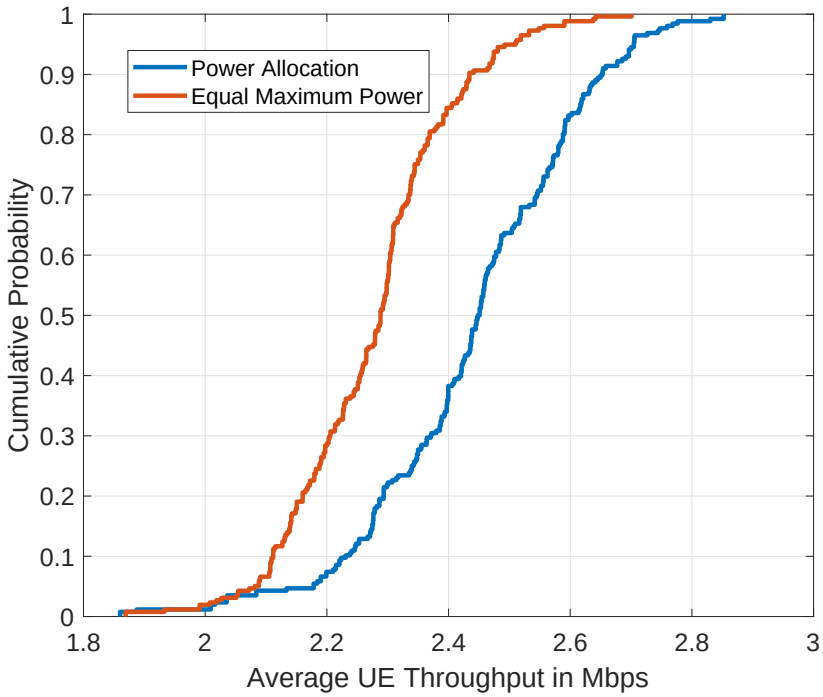

Figure 7.10 Effect of power allocation on UE throughputs for the outdoor scenario

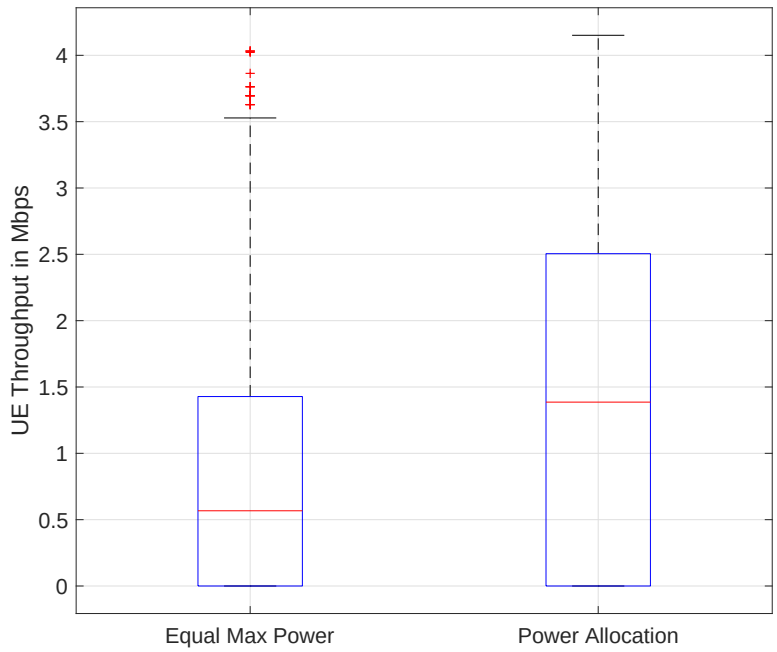

Figure 7.11 Effect of low SIC on uplink UE performances

7.7 Conclusion

In this chapter, we presented a scheduling and power allocation algorithm for full-duplex wireless networks in a multi-cell setting. We considered both indoor and outdoor deployments and showed that the profitability of multi-cellular full-duplex communications is tied to the inter-cell interference mitigation that the deployment scenario provides. Additionally, we highlighted the importance of cell cooperation when it comes to scheduling resources and showed that independent single cell scheduling could prove costly in terms of network efficiency. Finally, we showed that power allocation stands to improve UE throughput values with varying degrees of success depending on the deployment scenario.

Chapter 8

Conclusion, Discussion, and Perspectives

With the ever growing demand for faster, stronger, and better wireless network connections, full-duplex wireless communications have the means to become the next big telecommunications breakthrough. In this thesis, we explored the possible gains of full-duplex wireless communications with respect to the current half-duplex technology in place. We proposed several greedy and fair scheduling algorithms along with both centralized and decentralized approaches to power control. Generally, we presented a complete study of scheduling and power allocation in full-duplex wireless networks, as we sought to fill in the gaps in the state-of-the-art where necessary.

In our work, we considered a full-duplex wireless network where the base station (BS) is full-duplex capable and the user equipment (UEs) remain half-duplex. Our aim was to keep the complexities of implementing full-duplex technologies away from the user terminals. We began our work in Chapter 3, where we proposed global optimal problems for scheduling in both full-duplex and hybrid full-duplex/half-duplex wireless networks. Using this global problem, we presented greedy scheduling algorithms based on traditional Max-SINR scheduling, and fair scheduling algorithms based on traditional Proportional Fair scheduling. We showed that in comparison to their half-duplex counterparts, almost double the throughput values could be achieved with full-duplex communications. Current radio resource allocation schemes, designed for half-duplex networks, benefit from orthogonal downlink and uplink channels which can be optimized independently. In contrast, in the context of full-duplex wireless communications, the optimization of scheduling and power allocation has to be done jointly for the uplink and the downlink because of the concept of pairing and the generated full-duplex interferences. Consequently, it was not possible to apply any traditional half-duplex scheduling or power allocation algorithms to full-duplex networks in a straightforward manner.

In Chapter 4, we assessed the importance of complete channel state information (CSI) for

extracting gains from full-duplex wireless networks. Specifically, we focused on the inter-UE channels. No current wireless network protocols count for such channels and estimating them is expected to be a hurdle in front of practical implementations of full-duplex wireless networks. After showing that partial information about inter-UE channels is sufficient to achieve significant gains from full-duplex wireless communications, we proposed a reinforcement learning approach to scheduling capable of learning how to best allocate resources without any information on the inter-UE channels. We showed that our proposal can match greedy scheduling with complete CSI at a cost of 10% or less in total network efficiency.

Moving forward to power allocation, in Chapter 5 we proposed a centralized optimal approach to scheduling and power allocation in full-duplex wireless networks. Our approach to the joint task was fairness oriented and introduced a pair priority based on current and historic UE performances. Because the joint optimization problem was mathematically intractable, we separated the problem into two and solved for scheduling and power allocation independently. We showed via simulations that our proposal improves UE performance and saves on power expenditure, where about 50% of the uplink UEs in the network transmitted at powers levels lower than the maximum available.

In Chapter 6, we proposed a distributed approach to power allocation. The latter was based in game theoretics. We used non-cooperative game theory to model power allocation as a super-modular game with the BS and the UEs set as competing players. We put forward multiple games with objectives varying from maximizing UE SINR to improving the network's energy efficiency, and subsequently showed that the relevance of each of our proposals depends on the scenario at hand.

In Chapter 7, we addressed scheduling and power allocation in a multi-cell full-duplex wireless network. We considered both indoor and outdoor deployment scenarios and showed that the gains of full-duplex wireless communications, with respect to their half-duplex counterparts, will depend on the interference mitigation utilities available. We studied the effects that cell cooperation has on UE performance, and showed that depending on the network scenario, gains of up to 43%–in terms of cell throughput–stand to be made from the latter.

8.1 Further Discussion on the Profitability of Full-Duplex

Practical implementation of full-duplex networks will eventually hinge on their profitability with respect to current and future half-duplex wireless communications. In this section, we discuss the potential gains of full-duplex wireless communications beyond what we presented

in the course of this thesis, and we elaborate on how they fare vs. competitive half-duplex technologies designed for throughput enhancement.

Added Gains of Full-Duplex Wireless Networks

The gains of full-duplex wireless networks extend beyond increased UE throughput, added capacity, and reduced waiting delays. A classic issue for typical Wi-Fi networks is the hidden terminal problem (Fig. 8.1), wherein two nodes transmitting to one access point cannot hear each other's transmissions resulting in collisions. With the access point being full-duplex, every node in the network will be able to hear the access point's transmission to the rest of the nodes, largely avoiding the hidden terminal problem as a result. In [9], the author shows that full-duplex communications reduce packet losses due to hidden terminals by up to 88%, whilst improving the throughput on the downlink by 110%.

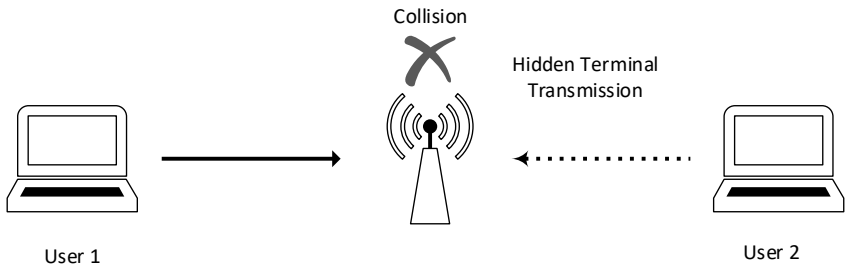

Figure 8.1 The hidden terminal problem

Gains With Respect to Half-Duplex MIMO

One recurring question in the context of full-duplex wireless communications is whether the profit they bring with respect to half-duplex communications is absolute. Multiple input multiple output (MIMO) technology can immensely improve the throughput of traditional half-duplex networks. If the transmission in a certain case is in only one direction, we can expect MIMO to outperform full-duplex communications, as it doubles the throughput of that direction. In that case, implementing a MIMO network could prove to be not only more profitable, but more feasible as well as it is already tested. In the case of bidirectional communications, it again comes down to how well full-duplex networks deal with the resulting interference problems. Full-duplex nodes can use full UE power on each antenna. In comparison, a half-duplex MIMO node has to share the UE power between its multiple antennas. As [9] attests, if the SIC technologies are good enough, and in the presence of sufficient channel knowledge, full-duplex communications will be more profitable than MIMO at high SINR values. As MIMO is being superseded by the more lucrative Massive

MIMO [74], full-duplex technologies need to be able to well mitigate their interference problems in order to compete.

8.2 Perspectives in Relation to Resource Management in Full-Duplex Networks

In this section, we discuss multiple perspectives in relation to radio resource management in full-duplex wireless networks. Specifically, we discuss proposals on how inter-UE channels could be estimated and explore axes regarding different UE pairing scenarios in full-duplex wireless networks.

Estimation of Inter-UE Channels

As discussed in this thesis, estimating inter-UE channels is an added requirement in the context of full-duplex wireless communications. The scheduler needs information on all the UE-to-UE channels in order to efficiently allocate resources and maximize full-duplex gains. However, no current wireless network protocols count for relaying such channel information from the UEs to the BS. In Chapter 4, we introduced a reinforcement learning approach to scheduling in order to circumvent the need for such inter-UE channel information. Nonetheless, estimating these channels would allow the most optimal allocation of radio resources. The authors in [36] and others in the state-of-the-art suggest using sounding reference signals (SRSs) to estimate and relay such information to the BS. After implementing neighbor discovery at the UEs to determine the strongest interferers, the uplink SRS can be used by the UEs to estimate the channels to those interferers. While such an approach could indeed be functional, it would still be challenging to distinguish between different UEs on the SRS, causing thus added complexities. Furthermore, identifying only the strongest interferes might not be a sufficient approximation. Irregardless, partial estimation of the inter-UE channels could be enough to extract gains with respect to traditional half-duplex scheduling, but those gains would not be as clear when compared to half-duplex MIMO and other multiplexing technologies.

On Pair Association in Multi-Cell Full-Duplex Wireless Networks

During our work on multi-cell full-duplex wireless networks, we assessed the significance of pair association. The idea was that instead of the current single UE association–which usually associates each UE with the nearest BS–we implement pair association, wherein pairs of uplink-downlink UEs are associated to the BSs they best perform on. This scenario

is illustrated in Fig. 8.2 below, where the first pair which includes a UE that otherwise would have been associated to the BS in the second cell, is associated to the BS in the first.

The scheduler might choose to do this if the co-channel interference between the two UEs in this pair is low enough to generate better radio conditions for the pair as a whole when it is associated to the first BS, despite the second downlink UE being closer to the second BS. We evaluated the performance of such a network and compared it to the case of single UE association. In the case where all the resources are used in adjacent cells (reuse-1), such an approach produces no gains. In fact, in some of our simulations it actually costs the network in terms of total throughput. Nonetheless, in the case where all the immediate interfering cells do not use the same frequency resources, pair association could in fact improve the performance of full-duplex networks. For the second outdoor scenario introduced in the previous chapter, up to 10% increase in total network throughput is achievable via pair association.

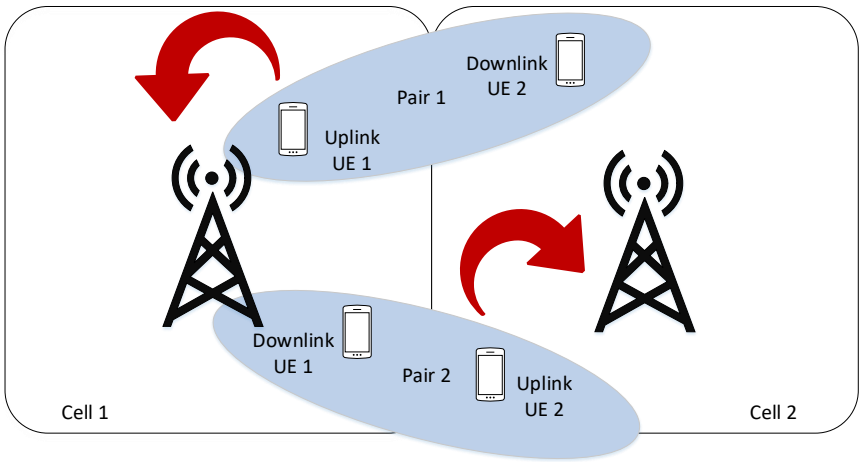

Figure 8.2 Pair association in a multi-cell scenario

Another interesting approach to UE association in full-duplex wireless networks consists of decoupling the uplink-downlink UEs and associating each with a different BS. In this case, the first uplink UE and the second downlink UE (seen in Fig. 8.2) would still be paired together albeit with each associated to a different BS. With each UE receiving from or transmitting to the closest BS, the SINR of each UE can be expected to improve. Nonetheless, such an approach would not be without its complications. A central unit would have to be in charge of the pairing and the scheduling. An extensive signaling overhead could be incurred.

On Future Works in Full-Duplex Wireless Networks

As this dissertation comes to a conclusion, our work on full-duplex wireless communication continues. Pending the time left for our work on this subject, we aim to explore the following:

1. In Chapter 4, we introduced a reinforcement learning approach to scheduling in full-duplex wireless networks. It would be interesting to adapt this algorithm to the multi-cell setting. Practically speaking, not much change would be required. The algorithm would still allocate resources to pairs of UEs based on select probabilities and afterwards, update the allocation probabilities based on how many bits were transmitted and received by the UE pairs on the RBs they were allocated. An added advantage for the learning approach in a multi-cell setting is that not only would it not require information on the inter-UE channels, it would also not require knowledge of the UEs' inter-cell interferers. What remains is to assess how quickly and how efficiently can the algorithm allocate the radio resources and whether it would incur a large cost in terms of total network throughput.

2. In Chapter 6, we used game theoretics for power allocation in full-duplex wireless networks. In [40], the authors used game theoretics for radio resource allocation in full-duplex wireless networks and implemented a water filling algorithm for power allocation. An interesting idea is to use game theory to jointly schedule the RBs and allocate power on them. Traditionally, jointly addressing scheduling and power allocation results in mathematically intractable problems. However, non-cooperative game theory can be used to address both scheduling and power allocation at the same time. The main challenge would be with identifying the players of the games designed for scheduling and power allocation. In the case of power allocation, it made sense for the UEs on the uplink and the BS on the downlink to be competing players. After all, raising the power on the uplink degrades the performance of UEs on the downlink and vice-versa. Nonetheless, this is not valid for scheduling the RBs. Uplink and downlink UEs are paired on shared resources. In this case, they are no longer competitors. One approach is to pit uplink UEs vs. uplink UEs and downlink UEs vs. downlink UEs. The end game would be to select the uplink and downlink UEs with the best radio conditions on each RB and pair them together. However, the best performing uplink UE and the best performing downlink UE might not always form a good pairing. For instance, they could be situated close to each other causing degradation in performance for the downlink UE. Another approach would be to list all possible UE pairings as the players of the scheduling game. The scheduling game would then be played between

pairs of UEs to decide which pairs get what RBs. Afterwards, a power allocation game, similar to our proposals, can be used to allocate powers to the scheduled UEs.

3. In the context of the multi-cellular networks introduced in Chapter 7, a distributed approach to power allocation presents a challenging and interesting approach. In our proposal, a central unit decides how to allocate the power on all the scheduled RBs for the entire system in one shot. As with all centralized approaches, this is expected to cause a signaling and processing burden. An alternative is to follow an iterative distributed approach to power allocation. Each BS would solve the power allocation problem individually and the BSs would take turn resolving the problem based on the results of their counterparts, until a convergence is reached. A stopping criterion $e.g.$, when the total network throughput no longer improves, might be needed.

Finally, when our work on full-duplex wireless communications started in 2016, there were high hopes for 5G inclusion. Research in the domain boomed and countless approaches to radio resource management in various scenarios of full-duplex implementations saw light. Nonetheless, last year with the 3GPP 5G release 15 [75] made public, it was evident that operators were not as excited for full-duplex wireless. Nowadays, full-duplex wireless communications are spoken of in the context of 6G [76] with small hopes for introduction in the final 5G release in 2021. It is not definitive that 6G will in fact include full-duplex, but at least another decade of research will certainly pave way for practical implementation.

Bibliography

[1] C. V. Mobile, "Cisco visual networking index: global mobile data traffic forecast update, 2017–2022 white paper," 2017.

[2] A. Grami, *Introduction to Digital Communications*. Academic Press, 2015.

[3] E. EN300175, "Digital enhanced cordless telecommunications (dect)," *Common Interface (CI)*, 2004.

[4] J. G. Andrews, A. Ghosh, and R. Muhamed, *Fundamentals of WiMAX: understanding broadband wireless networking*. Pearson Education, 2007.

[5] M. Mouly, M.-B. Pautet, and T. Foreword By-Haug, *The GSM system for mobile communications*. Telecom publishing, 1992.

[6] E. Dahlman, B. Gudmundson, M. Nilsson, and A. Skold, "Umts/imt-2000 based on wideband cdma," *IEEE Communications magazine*, vol. 36, no. 9, pp. 70–80, 1998.

[7] A. Goldsmith, *Wireless communications*. Cambridge university press, 2005.

[8] J. I. Choi, M. Jain, K. Srinivasan, P. Levis, and S. Katti, "Achieving single channel, full duplex wireless communication," in *Proceedings of the sixteenth annual international conference on Mobile computing and networking*. ACM, 2010, pp. 1–12.

[9] M. Jain, "Single channel full-duplex wireless radios," *Stanford University*.

[10] C. D. Nwankwo, L. Zhang, A. Quddus, M. A. Imran, and R. Tafazolli, "A survey of self-interference management techniques for single frequency full duplex systems," *IEEE Access*, vol. 6, pp. 30 242–30 268, 2017.

[11] O. Osterb, "Scheduling and capacity estimation in lte," pp. 63–70, 2011.

[12] R. V. Rasmussen and M. A. Trick, "Round robin scheduling–a survey," *European Journal of Operational Research*, vol. 188, no. 3, pp. 617–636, 2008.

[13] T. Park, O.-S. Shin, and K. B. Lee, "Proportional fair scheduling for wireless communication with multiple transmit and receive antennas," in *2003 IEEE 58th Vehicular Technology Conference, 2003. VTC 2003-Fall*, vol. 3. IEEE, 2003, pp. 1573–1577.

[14] S. Hong, J. Brand, J. I. Choi, M. Jain, J. Mehlman, S. Katti, and P. Levis, "Applications of self-interference cancellation in 5g and beyond," *IEEE Communications Magazine*, vol. 52, no. 2, pp. 114–121, 2014.

[15] A. Sabharwal, P. Schniter, D. Guo, D. W. Bliss, S. Rangarajan, and R. Wichman, "In-band full-duplex wireless: Challenges and opportunities." *IEEE Journal on Selected Areas in Communications*, vol. 32, no. 9, pp. 1637–1652, 2014.

[16] H. Zhao, J. Wang, and Y. Tang, "Performance analysis of rf self-interference cancellation in broadband full duplex systems," in *2016 IEEE International Conference on Communications Workshops (ICC)*, May 2016, pp. 175–179.

[17] Z. He, S. Shao, Y. Shen, C. Qing, and Y. Tang, "Performance analysis of rf self-interference cancellation in full-duplex wireless communications," *IEEE Wireless Communications Letters*, vol. 3, no. 4, pp. 405–408, Aug 2014.

[18] S. Khaledian, F. Farzami, B. Smida, and D. Erricolo, "Inherent self-interference cancellation at 900 mhz for in-band full-duplex applications," in *2018 IEEE 19th Wireless and Microwave Technology Conference (WAMICON)*, April 2018, pp. 1–4.

[19] H. Nawaz, . Gürbüz, and I. Tekin, "2.4 ghz dual polarised monostatic antenna with simple two-tap rf self-interference cancellation (rf-sic) circuitry," *Electronics Letters*, vol. 55, no. 6, pp. 299–300, 2019.

[20] Y. Kurzo, A. Burg, and A. Balatsoukas-Stimming, "Design and implementation of a neural network aided self-interference cancellation scheme for full-duplex radios," in *2018 52nd Asilomar Conference on Signals, Systems, and Computers*, Oct 2018, pp. 589–593.

[21] D. Bharadia, E. McMilin, and S. Katti, "Full duplex radios," in *ACM SIGCOMM Computer Communication Review*, vol. 43, no. 4. ACM, 2013, pp. 375–386.

[22] M. G. Sarret, G. Berardinelli, N. H. Mahmood, and P. Mogensen, "Can full duplex boost throughput and delay of 5g ultra-dense small cell networks?" in *2016 IEEE 83rd Vehicular Technology Conference (VTC Spring)*. IEEE, 2016, pp. 1–5.

[23] L. Song, Y. Li, and Z. Han, "Resource allocation in full-duplex communications for future wireless networks," *IEEE Wireless Communications*, vol. 22, no. 4, pp. 88–96, 2015.

[24] J. Marasevic, J. Zhou, H. Krishnaswamy, Y. Zhong, and G. Zussman, "Resource allocation and rate gains in practical full-duplex systems," *IEEE/ACM Transactions on Networking (TON)*, vol. 25, no. 1, pp. 292–305, 2017.

[25] G. Agrawal, S. Aniruddhan, and R. K. Ganti, "A compact mixer-first receiver with gt;24 db self-interference cancellation for full-duplex radios," *IEEE Microwave and Wireless Components Letters*, vol. 26, no. 12, pp. 1005–1007, Dec 2016.

[26] A. C. Cirik, K. Rikkinen, and M. Latva-aho, "Joint subcarrier and power allocation for sum-rate maximization in ofdma full-duplex systems," in *2015 IEEE 81st Vehicular Technology Conference (VTC Spring)*. IEEE, 2015, pp. 1–5.

[27] S. Goyal, P. Liu, S. S. Panwar, R. A. DiFazio, R. Yang, and E. Bala, "Full duplex cellular systems: will doubling interference prevent doubling capacity?" *IEEE Communications Magazine*, vol. 53, no. 5, pp. 121–127, 2015.

[28] J. M. B. da Silva, Y. Xu, G. Fodor, and C. Fischione, "Distributed spectral efficiency maximization in full-duplex cellular networks," in *2016 IEEE International Conference on Communications Workshops (ICC)*. IEEE, 2016, pp. 80–86.

[29] C. Nam, C. Joo, and S. Bahk, "Joint subcarrier assignment and power allocation in full-duplex ofdma networks," *IEEE Transactions on Wireless Communications*, vol. 14, no. 6, pp. 3108–3119, 2015.

[30] P. Tehrani, F. Lahouti, and M. Zorzi, "Resource allocation in ofdma networks with half-duplex and imperfect full-duplex users," in *2016 IEEE International Conference on Communications (ICC)*. IEEE, 2016, pp. 1–6.

[31] B. Di, S. Bayat, L. Song, Y. Li, and Z. Han, "Joint user pairing, subchannel, and power allocation in full-duplex multi-user ofdma networks," *IEEE Transactions on Wireless Communications*, vol. 15, no. 12, pp. 8260–8272, 2016.

[32] C. Nam, C. Joo, and S. Bahk, "Radio resource allocation with inter-node interference in full-duplex ofdma networks," in *2015 IEEE International Conference on Communications (ICC)*. IEEE, 2015, pp. 3885–3890.

[33] Q. Gao, G. Chen, L. Liao, and Y. Hua, "Full-duplex cooperative transmission scheduling in fast-fading mimo relaying wireless networks," in *2014 International Conference on Computing Networking and Communications (ICNC)*. IEEE, 2014, pp. 771–775.

[34] Y. Sun, D. W. K. Ng, and R. Schober, "Multi-objective optimization for power efficient full-duplex wireless communication systems," in *2015 IEEE Global Communications Conference (GLOBECOM)*. IEEE, 2015, pp. 1–6.

[35] M. M. Shaikh and M. C. Aguayo-Torres, "Analysis of coverage and binary rate in a hybrid/full duplex heterogeneous cellular network under various association criteria," *Wireless Personal Communications*, pp. 1–14.

[36] S. Goyal, P. Liu, and S. S. Panwar, "User selection and power allocation in full-duplex multicell networks," *IEEE Transactions on Vehicular Technology*, vol. 66, no. 3, pp. 2408–2422, March 2017.

[37] Y. Sun, D. W. K. Ng, Z. Ding, and R. Schober, "Optimal joint power and subcarrier allocation for full-duplex multicarrier non-orthogonal multiple access systems," *IEEE Transactions on Communications*, vol. 65, no. 3, pp. 1077–1091, 2017.

[38] B. Liu, Y. Wei, Y. Xue, and H. Lei, "Resource allocation in full-duplex ofdma wireless networks with interactive service," in *2015 International Conference on Wireless Communications Signal Processing (WCSP)*, Oct 2015, pp. 1–6.

[39] E. Park, J. Bae, H. Ju, and Y. Han, "Resource allocation for full-duplex systems with imperfect co-channel interference estimation," *IEEE Transactions on Wireless Communications*, vol. PP, pp. 1–1, 03 2019.

[40] M. Al-Imari, M. Ghoraishi, P. Xiao, and R. Tafazolli, "Game theory based radio resource allocation for full-duplex systems," in *2015 IEEE Vehicular Technology Conference*.

[41] T. T. Tran, V. N. Ha, L. B. Le, and A. Girard, "Uplink/downlink matching based resource allocation for full-duplex ofdma wireless cellular networks," in *2017 IEEE Wireless Communications and Networking Conference (WCNC)*. IEEE, 2017, pp. 1–6.

[42] F. Wu and D. Liu, "Power control and inter-node interference cancellation in full-duplex networks with residual self-interference," *Wireless Personal Communications*, pp. 1–18, 2019.

[43] X. Zhang, T. Chang, Y. Liu, C. Shen, and G. Zhu, "Max-min fairness user scheduling and power allocation in full-duplex ofdma systems," *IEEE Transactions on Wireless Communications*, vol. 18, no. 6, pp. 3078–3092, June 2019.

[44] A. C. Cirik, K. Rikkinen, R. Wang, and Y. Hua, "Resource allocation in full-duplex ofdma systems with partial channel state information," in *International Conference on Signal and Information Processing (ChinaSIP), 2015 IEEE China Summit*. IEEE, 2015, pp. 711–715.

[45] L. Song, Y. Li, and Z. Han, "Game-theoretic resource allocation for full-duplex communications," in *IEEE Wireless Communications*.

[46] L.-C. Wang and S. Rangapillai, "A survey on green 5g cellular networks," in *2012 International Conference on Signal Processing and Communications (SPCOM)*. IEEE, 2012, pp. 1–5.

[47] T. L. Marzetta and B. M. Hochwald, "Fast transfer of channel state information in wireless systems," *IEEE Trans. Signal Processing*, vol. 54, no. 4, pp. 1268–1278, 2006.

[48] D. E. Knuth, "Postscript about np-hard problems," *SIGACT News*, vol. 6, no. 2.

[49] J. Clausen, "Branch and bound algorithms-principles and examples," *Department of Computer Science, University of Copenhagen*, pp. 1–30, 1999.

[50] R. M. Karp, "Reducibility among combinatorial problems," in *Complexity of computer computations*. Springer, 1972, pp. 85–103.

[51] P. E. Mogensen and J. Wigard, "Cost action 231: Digital mobile radio towards future generation system, final report," in *Section 5.2: on Antenna and Frequency Diversity in Gsm. Section 5.3: Capacity Study of Frequency Hopping Gsm Network*, 1999.

[52] R. Jain, D.-M. Chiu, and W. R. Hawe, *A quantitative measure of fairness and discrimination for resource allocation in shared computer system*. Eastern Research Laboratory, Digital Equipment Corporation Hudson, MA, 1984, vol. 38.

[53] T. KIRKMAN, "Statistics to use," 1996.

[54] X. Guo, G. Trimponias, X. Wang, Z. Chen, Y. Geng, and X. Liu, "Learning-based joint configuration for cellular networks," *IEEE Internet of Things Journal*, vol. 5, no. 6, pp. 4283–4295, Dec 2018.

[55] X. Cao, R. Ma, L. Liu, H. Shi, Y. Cheng, and C. Sun, "A machine learning-based algorithm for joint scheduling and power control in wireless networks," *IEEE Internet of Things Journal*, vol. 5, no. 6, pp. 4308–4318, Dec 2018.

[56] S. Chinchali, P. Hu, T. Chu, M. Sharma, M. Bansal, R. Misra, M. Pavone, and S. Katti, "Cellular network traffic scheduling with deep reinforcement learning," in *Thirty-Second AAAI Conference on Artificial Intelligence*, 2018.

[57] J. Joung, "Machine learning-based antenna selection in wireless communications," *IEEE Communications Letters*, vol. 20, no. 11, pp. 2241–2244, 2016.

[58] C. Zhang, P. Patras, and H. Haddadi, "Deep learning in mobile and wireless networking: A survey," *IEEE Communications Surveys & Tutorials*, 2019.

[59] R. S. Sutton and A. G. Barto, "Reinforcement learning: An introduction," 2011.

[60] K. Pearson, "The problem of the random walk," *Nature*, vol. 72, no. 1867, p. 342, 1905.

[61] R. McGill, J. W. Tukey, and W. A. Larsen, "Variations of box plots," *The American Statistician*, vol. 32, no. 1, pp. 12–16, 1978.

[62] F. Kelly, "Charging and rate control for elastic traffic," *Transactions on Emerging Telecommunications Technologies*, vol. 8, no. 1, pp. 33–37, 1997.

[63] M. Grant, S. Boyd, and Y. Ye, "Cvx: Matlab software for disciplined convex programming," 2008.

[64] P. J. Rousseeuw, I. Ruts, and J. W. Tukey, "The bagplot: a bivariate boxplot," *The American Statistician*, vol. 53, no. 4, pp. 382–387, 1999.

[65] S. Boyd and L. Vandenberghe, "Convex optimization," in *Cambridge university press, 2004*.

[66] Topkis, "Equilibrium points in non-zero sum n-person sub-modular games," in *Queueing systems, vol. 21, no 3-4 (239 p.), pp. 449-475, 1995*.

[67] Yao, "S-modular games, with queueing applications," in *Queueing systems, vol. 21, no 3-4 (239 p.), pp. 449-475, 1995*.

[68] T. Roughgarden, *Selfish routing and the price of anarchy*. MIT press Cambridge, 2005, vol. 174.

[69] "Further advancements for e-utra physical layer aspects (release 9)," *3GPP TR 36.814, v.9.0.0*, Mar. 2010.

[70] E. U. T. R. Access, "Further enhancements to lte time division duplex (tdd) for downlink-uplink (dl-ul) interference management and traffic adaptation," 2012.

[71] A. L. Stolyar, "On the asymptotic optimality of the gradient scheduling algorithm for multiuser throughput allocation," *Operations research*, vol. 53, no. 1, pp. 12–25, 2005.

[72] H. Kim, K. Kim, Y. Han, and S. Yun, "A proportional fair scheduling for multicarrier transmission systems," in *IEEE 60th Vehicular Technology Conference, 2004. VTC2004-Fall. 2004*, vol. 1. IEEE, 2004, pp. 409–413.

[73] M. Chiang, C. W. Tan, D. P. Palomar, D. O'Neill, and D. Julian, "Power control by geometric programming," *Resource Allocation in Next Generation Wireless Networks*, vol. 5, pp. 289–313, 2005.

[74] S. Mumtaz, J. Rodriguez, and L. Dai, *MmWave Massive MIMO: A Paradigm for 5G*. Academic Press, 2016.

[75] "5g; procedures for the 5g system," *3GPP TS 23.502 version 15.2.0 Release 15*, June. 2018.

[76] M. Giordani, M. Polese, M. Mezzavilla, S. Rangan, and M. Zorzi, "Towards 6g networks: Use cases and technologies," 03 2019.

[77] H. Fawaz, S. Lahoud, M. E. Helou, and M. Ibrahim, "Max-sinr scheduling in full-duplex ofdma cellular networks with dynamic arrivals," in *2017 IEEE Symposium on Computers and Communications (ISCC)*, July 2017, pp. 493–498.

[78] ——, "Optimal max-sinr scheduling in full-duplex ofdma cellular networks with dynamic arrivals," in *2018 Wireless Days (WD)*, April 2018, pp. 196–201.

[79] ——, "Queue-aware scheduling in full duplex ofdma wireless networks with imperfect channel state information," in *European Wireless 2018; 24th European Wireless Conference*, May 2018, pp. 1–7.

[80] H. Fawaz, S. Lahoud, M. E. Helou, and J. Saad, "Queue-aware priority based scheduling and power allocation in full-duplex ofdma cellular networks," in *2018 25th International Conference on Telecommunications (ICT)*, June 2018, pp. 15–20.

[81] H. Fawaz, S. Lahoud, and M. E. Helou, "A queue-aware discrete scheduling simulator for full-duplex ofdma wireless networks," in *2018 International Conference on Computer and Applications (ICCA)*, Aug 2018, pp. 60–65.

[82] H. Fawaz, K.Khawam, S. Lahoud, and M. E. Helou, "A game theoretic approach for power allocation in full duplex wireless networks," in *The 2019 Annual IEEE International Symposium on Personal, Indoor and Mobile Radio Communications (IEEE PIMRC 2019)*, September 2019, pp. 1–7.

[83] H. Fawaz, K. Khawam, S. Lahoud, and M. El Helou, "A game theoretic framework for power allocation in full-duplex wireless networks," *IEEE Access*, vol. 7, pp. 174 013–174 027, 2019.

Appendix A

Our Simulator for Scheduling and Power Allocation in Full-Duplex Networks

A.1 Simulator Overview

In this section, we give a general overview of our simulator for scheduling and power allocation in full-duplex wireless networks. Figure A.1 depicts a schematic block diagram of our proposal. The simulator conveys two main tasks: (i) Scheduling and (ii) Power Allocation. Depending on the simulation scenarios, power allocation on the resource blocks (RBs) might not be necessary. As such, the simulator can output the results of the scheduling with constant powers, without going through the task of power allocation.

The scheduling task consists of forming the uplink-downlink UE pairs, and allocating the available RBs to these pairs. In addition to information on the radio channels, UE distribution in the cell, and the UEs' traffic model, a scheduling strategy is needed to indicate how the RBs will be distributed on the UE pairs. This strategy could be greedy *i.e.*, allocating the RBs to the UEs with the best radio conditions, or fair *i.e.*, allocating the RBs with the purpose of achieving equity between the UEs.

Allocating powers on the RBs can be done after the scheduling task has been performed for a certain TTI. Based on the power allocation objective, usually improving the UE SINR, the transmit powers on the RBs are updated.

Implementation wise, Algorithm 10 below illustrates how the simulator works. The scheduling decision is made, for all the available resources, each TTI. If desired, power allocation is performed post scheduling.

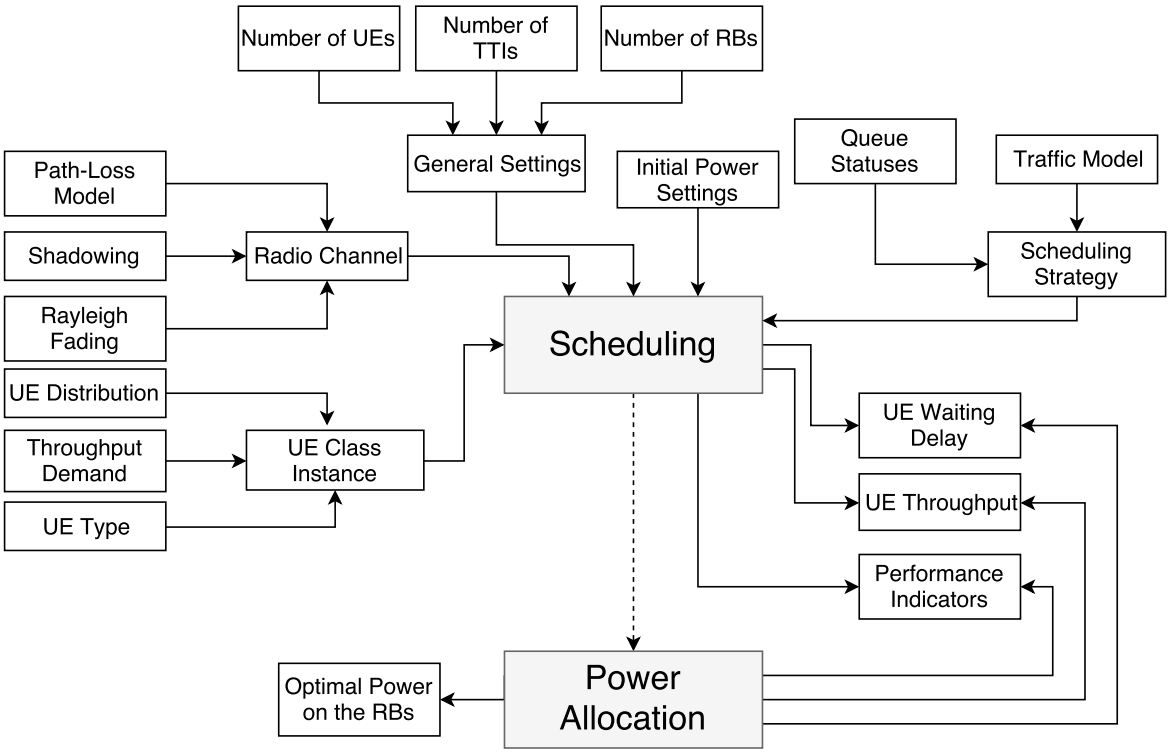

Figure A.1 Schematic block diagram of the simulator

Algorithm 10 Example Pseudo-Code

for *t=1....Number of TTIs* **do**
  for *k=1....K* **do**
    for *each UE* **do**
      Calculate UE SINR for all possible pairs.
    end
    Allocate k to pair i-j based on the scheduling objective.
  end
  Allocate power on the RBs.
  Calculate resulting UE throughputs.
end

In all cases, the resulting UE throughput values, among other metrics, are used to evaluate the performance of the network under the simulated scenarios. This permits exploring the gains and limitations of FD networks. The modularity of the simulator allows the permutation of the blocks shown in the schematic diagram changing thus specific functions and settings.

A.2 Network Model

A.2.1 Radio Model

We consider a single-cell FD-OFDMA system. This system is comprised of a full-duplex BS, and half-duplex UEs. The UEs are virtually divided into two sets: an uplink UE set, denoted by $\mathcal{I}$ and a downlink UE set, denoted by $\mathcal{D}$. The scheduling algorithms pair between uplink and downlink UEs on the RBs *k* of the set $\mathcal{K}$. This system is illustrated in Fig. A.2.

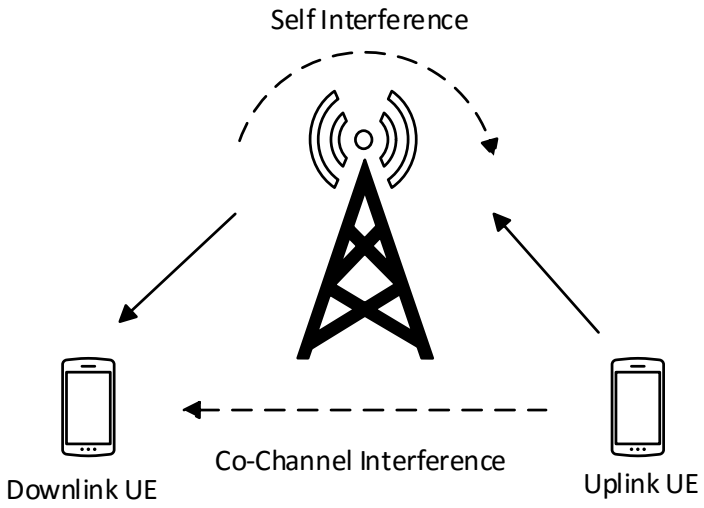

Figure A.2 Full-duplex network and interferences

The signal-to-noise and interference (SINR) ratio is calculated differently in such a network, than in legacy HD networks. Let P_{ik} denote the transmit power of the *i*th uplink UE, on the *k*th RB. P_{0k} is the transmit power of the BS on the kth RB. We denote by h^u_{ik} the channel gain from the *i*th uplink UE to the BS on RB *k*, and by and h^d_{jk} the channel gain from the BS to the *j*th downlink UE, on the kth RB. Furthermore, $h_{ij,k}$ denotes the channel gain between the *i*th uplink UE and *j*th downlink UE, on the *k*th RB. $P_{ik}|h_{ij,k}|^2$ is thus the co-channel interference on downlink UE j caused by uplink UE i, using the same RB k. The self-interference cancellation level at the BS is denoted SIC. In particular, $\frac{P_{jk}}{SIC}$ represents the residual self-interference power at the BS, on the *k*th RB. Finally, N_{0k} and N_{jk} denote the noise powers at the BS and at the *j*th downlink UE, on the *k*th RB, respectively. For an uplink UE,

$$S^u_j(i,k) = \frac{P_{ik}|h^u_{ik}|^2}{N_{0k} + \frac{P_{0k}}{SIC}}, \ i \in \mathcal{I}, \ j \in \mathcal{D}. \tag{A.1}$$

For a downlink UE,

$$S_i^d(j,k) = \frac{P_{0k}|h_{jk}^d|^2}{N_{jk} + P_{0k}|h_{ij,k}|^2},\ i \in \mathcal{I},\ j \in \mathcal{D}, \tag{A.2}$$

where $S_j^u(i,k)$ is the SINR of uplink UE i on RB k while using the same resources as UE j. Similarly, $S_i^d(j,k)$ is the SINR of downlink UE j on RB k while using the same resources as UE i.

A.2.2 Channel State Information

The state of a wireless channel is determined by the combined effect of several factors, the most pertinent of which, are the path loss, the shadowing, and the fast fading. Knowledge of the channel on a certain wireless link permits adapting the transmission to the communication channel. This is essential in achieving reliable communications, and for making efficient resource allocation decisions.

An FD-OFDMA network is concerned mainly with two types of channels: (i) BS-UE channels (ii) UE-UE channels. Currently implemented 3GPP protocols have mechanisms with which UEs can estimate BS-UE channels. UEs would periodically update the base station with this channel information. The need to estimate UE-UE channels is unique to FD networks. Knowing such channels enables a UE to distinguish the strongest interferers. This information is vital for optimal pair selection. In our work, we statistically model the radio channels as follows:

$$h_{ji,k} = G_t G_r L_p A_s A_f \tag{A.3}$$

G_t and G_r are the antenna gains at the transmitter and the receiver, respectively. L_p represents the path loss, or equivalently the mean attenuation the signal undergoes in this channel. A_s and A_f are two random variables that respectively represent the shadowing effect, and the fast fading effect. This model allows us to tune the factors affecting the different radio channels to encompass different environments such as rural or urban cells.

The simulator enables implementing different path-loss models. One implemented example is the Cost Hata Path-Loss model [51]. The path-loss (in dB), for the BS-UE channel for example, is calculated as follows. For simulating urban environments:

$$L_p|_{dB} = 46.3 + 33.9 \cdot \log_{10}(f) - 13.82 \cdot \log_{10}(h_{BS}) - a$$
$$+ (44.9 - 6.55 \cdot \log_{10}(h_{BS})) \cdot \log_{10}(d_{UE-BS}) + C_m, \tag{A.4}$$

where

$$a = (1.1 \cdot \log_{10}(f) - 0.7) \cdot h_{UE} - (1.56 \cdot \log_{10}(f) - 0.8).$$

f is the transmission frequency in *MHz*. h_{BS} is the base station antenna effective height in m. h_{UE} is the UE antenna effective height in m. d_{UE-BS} is the link distance in km. Finally, C_m is a constant equal to 3 dB for metropolitan centers, and 0 dB for medium-sized city and suburban areas.
For simulating rural environments:

$$\begin{aligned} L_p|_{dB} = {} & 69.55 + 26.16 \cdot \log_{10}(f) - 13.82 \cdot \log_{10}(h_{BS}) \\ & + (44.9 - 6.55 \cdot \log_{10}(h_{BS})) \cdot \log_{10}(d_{UE-BS}) \\ & - 4.78 \cdot (\log_{10}(f))^2 + 18.33 \cdot \log_{10}(f) - 40.94 \end{aligned} \tag{A.5}$$

Other path-loss models can also be incorporated. The log-distance path-loss model is used for calculating indoor attenuations:

$$L_p|_{dB} = L_p^0|_{dB} + 10\gamma \log_{10} \frac{d_{UE-BS}}{d_0}, \tag{A.6}$$

where d_0 is a reference distance (usually 1 *km*), and L_p^0 is the path-loss at that distance. γ is the path-loss exponent, dependent on the type of the structures.

A.2.3 Traffic Model

The simulator incorporates both full buffers for the UEs, as well as queue-awareness (Fig. A.3). In the case of queue-awareness and dynamic arrivals, each UE has a predefined throughput demand which determines the rate at which the UE will transmit or receive. A downlink UE has a queue at the BS, denoted Q_j^d. An uplink UE has a queue of bits it wants to transmit to the BS, denoted Q_i^u. UE queues are updated each TTI according to a Poisson process with a number of bits/s equal, on average, to the UE throughput demand. Once the scheduling is done for a certain TTI, the BS computes the number of bits each UE can transmit or receive, and the UE queues are deducted accordingly.

A.2.4 Performance Model

The mapping between a UE's SINR and the number of bits it can transmit/receive is done following a modulation and coding scheme (MCS). Using LTE-like configurations, we set 15 CQI values. These values use coding error rates between 1/8 and 4/5 combined with

4-QAM, 16-QAM and 64-QAM modulations. Figure A.4 maps between the UE SINR and the assigned CQI value.

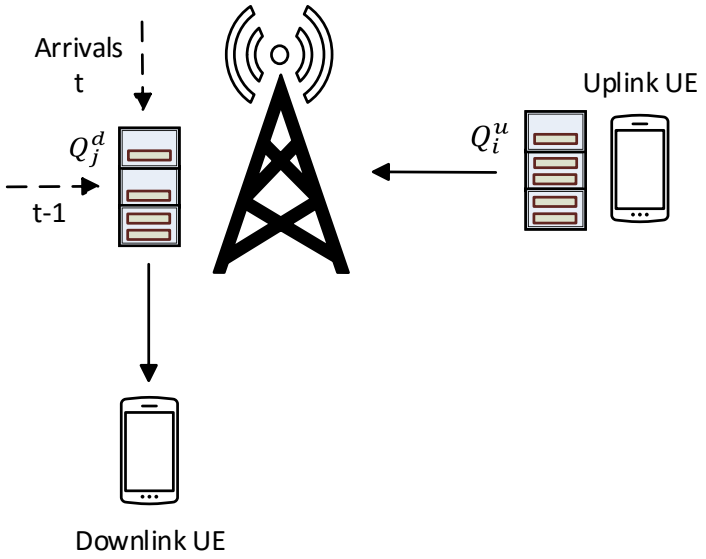

Figure A.3 Traffic model: UE pair i-j

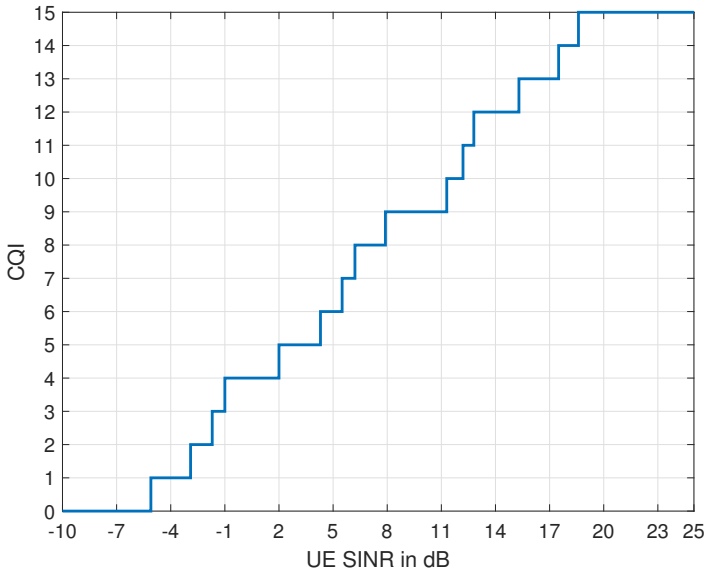

Figure A.4 CQI as a function of UE SINR

Table A.1 shows the relationship between the CQI level and the modulation and coding schemes used. Based on the MCS used, the number of bits each UE can transmit or receive on the resources allocated to it is recorded. At the end of the simulation the UE throughput is

calculated as the number of bits the UE has transmitted, divided by the simulation duration. The average delay is calculated using Little's formula as the average queue length divided by the packet arrival rate.

Table A.1 Modulation and coding scheme

CQI	Modulation	CodingRate	N°Bits/RB
0	-	-	0
1	QPSK	1/8	21
2	QPSK	1/5	33.6
3	QPSK	1/4	42
4	QPSK	1/3	55.44
5	QPSK	1/2	84
6	QPSK	2/3	111.72
7	QPSK	3/4	126
8	QPSK	4/5	134.4
9	16-QAM	1/2	168
10	16-QAM	2/3	223.44
11	16-QAM	3/4	252
12	16-QAM	4/5	268.8
13	64-QAM	2/3	336
14	64-QAM	3/4	378
15	64-QAM	4/5	307.2

A.3 Simulation Settings

Prior to the run of any scheduling algorithm, the simulator is initiated with a set of predefined settings (Seen in Fig. A.5).

```
N_UE = 20; % Number of initial active UEs
N_RB= 50; % Number of resource blocks
N_T = 10; % Number of TTIs to be simulated
N_Sim = 300; % Number of iterations
TTI_duration = 0.001; % The TTI duration in seconds
P_emitted = 0.1; % Power emitted per RB by the BS (in W)
P_UE=0.02; %Power emitted by the UEs (in W)
sigma_2 = epsilon*180000; % Background noise
BS_coordinates = [0 0];
max_delay = 8*Frame_duration; % Packet delay constraint
```

Figure A.5 Simulation Settings

Choosing the number of UEs in the network as well as the number of RBs to be allocated enables us to change the load conditions from light to heavy. Also to be set is the number of TTIs in a simulation and the duration of each. The UE and BS powers are globally set, although they can be altered from within the scheduler.

A.4 UE Class

The base station is located at the center of the simulated cell with (0,0) coordinates. The UEs are created as class instances with multiple property tags as shown in Fig. A.6. The UEs are given an ID, and for a certain simulation assigned a type: uplink or downlink. The UEs are also initialized with the throughput demand. Afterwards, a UE distribution function is called upon to determine the position of a UE inside the cell. This function enables simulating different UE distribution scenarios, with the possibility of forming UE clusters within the cell.

```
classdef UE
    properties
        ID;  %Mobile ID
        type;  %Uplink or downlink
        throughput;  %Throughput demand in (bits/s)
        coordinates;  %UE coordinates in a plane
        arrivals;  %Number of bits arriving during the current TTI
        d_BS;  %Distance between the UE and the base station
        q_k;  %Max number of bitsto tx/rx on resource block k
        sinr;  %Stores the last calculated UE SINR value
        uplinkqueue;  %Number of bits waiting for transmission
        downlinkqueue;  %Number of bits waiting for reception
        transmitted_bits;  %Number of bits already transmitted
        tx_bits;  %Number of bits transmitted in current TTI
        delay;  %Waiting delay at the beggining of the current TTI
    end
```

Figure A.6 Class UE

The remainder of the UE properties are related to the functionality of the simulator. The distance between the UE and the BS is subsequently calculated and stored. When making scheduling decisions, the simulator needs to calculate the UE SINR and the number of bits it can transmit on the RB being allocated. These property values are as such updated accordingly. After the scheduling is performed, the UE queues, also stored as properties of the class, are deducted following the resources allocated. Finally, because the simulator is queue-aware, it can compute and store performance metrics such as the waiting delay.

Appendix B

List of Publications

1. Hassan Fawaz, Samer Lahoud, Melhem El Helou, and Marc Ibrahim. "Max-SINR scheduling in Full-Duplex OFDMA cellular networks with dynamic arrivals." In 2017 IEEE Symposium on Computers and Communications (ISCC), pp. 493-498. IEEE, 2017. [77]

2. Hassan Fawaz, Samer Lahoud, Melhem El Helou, and Marc Ibrahim. "Optimal Max-SINR scheduling in full-duplex OFDMA cellular networks with dynamic arrivals." In 2018 Wireless Days (WD), pp. 196-201. IEEE, 2018. [78]

3. Hassan Fawaz, Samer Lahoud, and Melhem El Helou. "A Queue-Aware Discrete Scheduling Simulator for Full-Duplex OFDMA Wireless Networks." In 2018 International Conference on Computer and Applications (ICCA), pp. 60-65. IEEE, 2018. [79]

4. Hassan Fawaz, Samer Lahoud, Melhem El Helou, and Joe Saad. "Queue-Aware Priority Based Scheduling and Power Allocation in Full-Duplex OFDMA Cellular Networks." In 2018 25th International Conference on Telecommunications (ICT), pp. 15-20. IEEE, 2018. [80]

5. Hassan Fawaz, Samer Lahoud, Melhem El Helou, and Marc Ibrahim. "Queue-Aware Scheduling in Full Duplex OFDMA Wireless Networks with Imperfect Channel State Information." In European Wireless 2018; 24th European Wireless Conference, pp. 1-7. VDE, 2018. [81]

6. Hassan Fawaz, Kinda Khawam, Samer Lahoud, and Melhem El Helou. “A Game Theoretic Approach for Power Allocation in Full Duplex Wireless Networks”. IEEE

International Symposium on Personal, Indoor and Mobile Radio Communications (IEEE PIMRC), 2019. [82]

7. Hassan Fawaz, Kinda Khawam, Samer Lahoud and Melhem El Helou, "A Game Theoretic Framework for Power Allocation in Full-Duplex Wireless Networks," in IEEE Access, vol. 7, pp. 174013-174027, 2019. [83]

Appendix C

Résumé

C.1 Introduction et état de l'art

La prolifération des terminaux sans-fil atteint un niveau sans précédent. Qu'il s'agisse de nos téléphones mobiles, de nos ordinateurs portables ou de tout autre terminal intelligent, le besoin d'une connectivité sans-fil meilleure, plus rapide et fiable est plus urgent que jamais. Avec près de 13 milliards de terminaux mobiles et un trafic mobile mensuel estimé à 77 exabytes d'ici 2022 [1], la technologie est à peine à la hauteur. Pour les utilisateurs, l'incapacité de l'infrastructure à satisfaire la demande entraîne une perte de connectivité sur un terminal mobile ou un signal faible dans une zone surchargée. Symptômes des problèmes auxquels font face les transmissions sans-fil.

Les communications sans-fil sont confrontées à deux grands défis au fur et à mesure de leur évolution : l'atténuation des signaux et les interférences générées. En raison de la nature du support sans-fil, tout signal transmis subira une atténuation rapide, ce qui rend la distance entre l'émetteur et le récepteur un facteur important. De plus, tous les terminaux sans-fil partagent le même support et utilisent un ensemble fini et limité de ressources radio. Cela signifie que les terminaux sans-fil sont toujours en compétition pour ce support, et le partage inévitable des ressources disponibles entraînera inévitablement des interférences de signal. Le besoin croissant de capacité conduit à la réutilisation des fréquences et à la densification du déploiement des réseaux, ce qui aggrave les problèmes de brouillage hérités du passé.

Les problèmes pour les communications sans-fil n'augmentent que lorsque l'on considère la nécessité des communications bidirectionnelles. Tout terminal sans-fil doit émettre et recevoir pour fonctionner correctement. C'est ce qu'on appelle le duplexage. Néanmoins, si deux terminaux sans-fil communicants devaient utiliser la même ressource radio en même temps pour communiquer, les interférences générées rendraient impossible la réception

correcte d'un signal. En conséquence, deux mécanismes majeurs existent actuellement pour permettre le duplexage [2] :

1. Time Division Duplexing ou *TDD*, consiste à séparer les signaux transmis et reçus dans le domaine temporel. Ce dernier est décomposé en intervalles de temps d'émission (TTI), et les deux terminaux communicants se relaient pour émettre et recevoir. Si les terminaux n'émettent pas en même temps, il va de soi qu'il n'y aura pas d'interférences. Des technologies telles que DECT [3] et IEEE 802.116 WiMax [4] implémentent le TDD.

2. Frequency Division Duplexing ou *FDD*, signifie que les nœuds de chaque côté d'une liaison de communication utiliseront différentes fréquences pour envoyer et recevoir des données. Ceci empêchera les signaux d'interférer l'un sur l'autre, même si les deux terminaux émettent en même temps. Les systèmes cellulaires tels que GSM [5], CDMA2000 [6], et WiMax implémentent également FDD.

Dans une transmission TDD, un terminal sans-fil est - à un certain instant - soit en transmission, soit en réception. Dans une transmission FDD, il faut deux fois plus de ressources radio pour permettre aux nœuds d'émettre et de recevoir dans le même laps de temps. Dans les deux cas, la communication sans-fil est dite *half-duplex*, même si elle tente d'émuler ce qu'on appelle les communications *full-duplex*.

Un nœud full-duplex est un nœud qui peut émettre et recevoir sur la même ressource radio, en même temps. Si l'on met de côté tous les problèmes et toutes les limites du TDD et du FDD, l'aspect des communications en full-duplex à lui seul promet un doublement de la capacité des réseaux sans-fil. Mais aucun terminal sans-fil actuel n'est en fait un full-duplex. ***Pourquoi?*** Jusqu'à tout récemment, le terme "full-duplex sans-fil" était considéré comme un oxymore.

C.1.1 Le problème des communications full-duplex sans-fil

Probablement la phrase la plus citée dans la littérature sur les réseaux sans-fil, la caractérisation par Andrea Goldsmith des communications sans-fil full-duplex dans son livre de 2005 de Cambridge Press capture vraiment l'essence du consensus scientifique à l'époque. Goldsmith a écrit : "Il n'est généralement pas possible pour les radios de recevoir et d'émettre sur la même bande de fréquences à cause de l'interférence qui en résulte" [7]. Goldsmith a ensuite fait valoir que la séparation des liaisons montante et descendante, que ce soit dans le domaine temporel comme le TDD ou dans le domaine fréquentiel comme le FDD, était en fait le seul moyen de soutenir les communications bidirectionnelles.

Goldsmith n'avait pas tort techniquement. Considérons le modèle de réseau que nous avons utilisé dans notre travail et illustré dans la Fig. C.1 ci-dessous. Dans ce scénario, la station de base est considérée comme le nœud full-duplex. Les terminaux mobiles sont en half-duplex, c'est-à-dire qu'à un certain moment, ils émettent ou reçoivent. En même temps, un UE de liaison montante (en transmettant à la station de base) utilisera la même ressource radio qu'un UE de liaison descendante (un UE qui reçoit de la station de base). Nous disons que ces deux UE sont appariés sur la ressource. En tant que nœud full-duplex, la station de base émet et reçoit simultanément sur cette même ressource radio. Ce réseau présentera deux interférences supplémentaires majeures par rapport aux réseaux sans-fil half-duplex actuels :

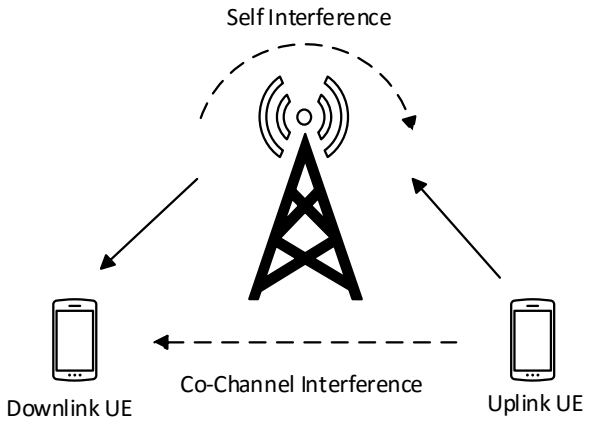

Figure C.1 Full-duplex network model and interferences

1. Auto-interference : Il s'agit du brouillage au niveau d'un nœud full-duplex, où le signal transmis sur une ressource radio donnée est plusieurs fois plus fort que le signal reçu sur cette même ressource. Ce dernier ne peut donc pas être reçu correctement. Dans le scénario susmentionné, l'auto-interférence dégrade la performance des UE sur la liaison montante.

2. Interférence intra-cellulaire co-canal : Il s'agit du brouillage résultant de l'utilisation par deux UE des mêmes ressources radio au sein d'une même cellule. Le signal d'un UE de liaison montante, généralement plusieurs fois plus puissant, interfère avec le signal reçu par un UE de liaison descendante voisin utilisant la même ressource radio. Cela entraîne une dégradation des performances de ces derniers.

Ces interférences sont dupliquées si l'on considère que les UE sont également full-duplex. Les réseaux sans-fil half-duplex souffrant déjà de problèmes d'interférence, il est évident que l'on croyait généralement que ces interférences supplémentaires rendraient simplement impossibles les communications en full-duplex. Néanmoins, comme toujours, le progrès

technologique rattrape inévitablement tout ce qui était autrefois considéré comme impossible. Pour les technologies sans-fil full-duplex, l'introduction des techniques d'annulation d'auto-interférence pour les terminaux sans-fil au début de cette décennie a marqué un tournant.

C.1.2 L'état de l'art pour l'ordonnancement et l'allocation de puissance

Dans cette section, nous présentons un aperçu général de l'état de l'art des communications sans-fil full-duplex. Nous classons ces derniers en trois catégories. La première traite du développement et de l'évolution des techniques d'annulation d'auto-interférence. Il était essentiel que ces technologies soient bien établies avant que les chercheurs n'aillent plus loin dans leurs travaux sur les technologies full-duplex. La deuxième catégorie englobe les travaux préliminaires dans le domaine qui visaient soit à suggérer différents scénarios full-duplex possibles, soit simplement à valider que des gains pourraient être tirés des communications full-duplex. La troisième catégorie de l'état de l'art, à laquelle appartient pratiquement notre travail, s'appuie sur les deux précédentes pour proposer et simuler des algorithmes d'ordonnancement et d'allocation de puissance pour les réseaux sans-fil full-duplex.

Il était important que les technologies SIC soient bien développées et testées avant tout autre travail sur le sans-fil full-duplex. Après tout, c'est le développement de ces technologies qui a rendu les communications sans-fil full-duplex possibles.

Les auteurs de [14] ont été parmi les premiers à discuter des impacts directs des techniques SIC développées sur les communications full-duplex. Ils affirment que ces technologies invalident des hypothèses de longue date concernant la conception des réseaux sans-fil, et ils donnent un aperçu de ce qui serait requis des techniques d'annulation des interférences afin de propulser les communications sans-fil full-duplex dans la réalité. Dans l'un des premiers travaux sur le full-duplex en bande pour les réseaux sans-fil, les auteurs de [15] passent en revue un ensemble de techniques SIC et abordent les principaux défis auxquels sont confrontés les réseaux sans-fil full-duplex. Les articles de [16] et [17] visaient à évaluer la performance de l'auto-ingérence dans le contexte des communications sans-fil full-duplex. Les auteurs de [16] concluent que la performance du SIC augmente à mesure que la largeur de bande du signal diminue, tandis que ceux de [17] se concentrent sur l'impact des erreurs d'amplitude et de phase sur l'efficacité des technologies de suppression des brouillages.

En outre, alors que nous suivons l'évolution de ces technologies, les articles de [18–20] suivent les derniers développements dans le domaine de la suppression des interférences. Les auteurs de [18] proposent une nouvelle technique SIC analogique pour les antennes uniques dans les systèmes full-duplex en bande. Ils montrent que leur modèle peut annuler 40 dB d'interférence sur une bande de fréquence de 35 MHz. Ils affirment qu'il suffit d'éviter la saturation du convertisseur analogique-numérique. Les auteurs de [19] se penchent sur

les applications pratiques de l'annulation d'interférence et présentent un modèle d'antenne patch avec un simple SIC à deux prises RF/analogique basé sur le domaine. Il est important de noter qu'ils attestent qu'il est possible d'atteindre des performances SIC à large bande. Enfin, les auteurs de [20] conçoivent et mettent en œuvre un système SIC assisté par réseau neuronal pour la radio full-duplex. Ils vérifient par simulations qu'ils peuvent obtenir de bons résultats de performance avec une complexité de calcul inférieure à celle des technologies existantes.

Après un consensus sur la viabilité des techniques SIC et sur le rôle que ces technologies pourraient jouer dans la faisabilité des communications par le full-duplex, la recherche dans le domaine s'est orientée vers l'exploration de ce que seraient les réseaux sans-fil full-duplex et si des obstacles autres que l'auto-interférence pourraient entraver la réalisation de gains grâce aux communications sans-fil full-duplex.

Les travaux de [22–25] portent sur l'évaluation des gains possibles des réseaux sans-fil full-duplex. Leurs auteurs étudient différentes implémentations des systèmes full-duplex, ainsi que les limites et les obstacles auxquels ils sont confrontés.

Dans le contexte de cette thèse, nous avons supposé que la technologie de mise en œuvre de l'émission et de la réception full-duplex est existante et bien testée. L'état de l'art est également bien investi dans différents scénarios de réseaux full-duplex. Notre travail s'appuie sur ces données pour proposer des algorithmes d'ordonnancement et d'allocation de puissance pour les réseaux sans-fil full-duplex.

Les technologies SIC étant maintenant bien établies dans l'état de l'art, et les technologies full-duplex étant maintenant bien motivées, ce n'était qu'une question de temps avant que les chercheurs dans le domaine du sans-fil ne s'orientent vers la conception d'algorithmes d'ordonnancement et d'allocation de puissance pour les réseaux sans-fil full-duplex. La gestion des ressources radio a toujours été le pilier de toute technologie de transmission. Pour les réseaux sans-fil full-duplex en particulier, l'enjeu était plus important. Dans ce contexte, l'ordonnancement et l'attribution de puissance ne visent pas seulement à améliorer la gestion des ressources radio, mais aussi à atténuer les interférences full-duplex. Sans un ordonnacement appropriée - capable de lutter contre les effets sur le brouillage intra-cellulaire co-canal - les communications full-duplex ne seraient pas viables.

Le tableau C.1 résume la majorité de l'état de l'art en matière d'ordonnancement et d'allocation de puissance dans les réseaux sans-fil full-duplex. Il met en évidence les scénarios de réseau full-duplex utilisés et indique si les articles référencés introduisent des algorithmes d'allocation de puissance en plus des propositions d'ordonnancement. Le tableau indique également si ces approches d'allocation de puissance sont distribuées ou centralisées. Des informations supplémentaires sur le scénario et la taille des cellules, le type de trafic et l'état de la CSI considérée sont incluses. Les cellules du tableau marquées "-" sont destinées aux cas où l'information indiquée n'est pas donnée dans les documents, ou ne peut être directement déduite.

La grande majorité des articles de l'état de l'art présentent un scénario full-duplex semblable à celui que nous avons utilisé dans notre travail. On suppose que la station de base est le nœud full-duplex et que les équipements d'utilisateur restent half-duplex. Ce scénario est celui mis en œuvre dans tous les modèles full-duplex OFDMA [30–32] cités en référence également. D'autres modèles dans les travaux connexes se concentrent sur le relais [33], MIMO [34], et même des réseaux hétérogènes [35]. Bien que ces trois derniers ne soient pas directement liés à notre travail, nous les avons étudiés en raison de l'existence d'une problématique commune lorsqu'il s'agit de traiter les problèmes et les interférences full-duplex.

Quant à l'ordonnancement, presque tous les travaux de l'état de l'art mettent en œuvre des approches gloutonnes axées sur la maximisation du débit (Max SR) ou le débit (Max TP) [33]. D'autres variations gloutonnes dans les travaux connexes incluent la maximisation de l'efficacité spectrale du réseau (Max SE) [28], et la maximisation de la somme des logarithmes des débits [36]. De plus, un ensemble d'algorithmes d'allocation de puissance est utilisée, un bon nombre d'entre eux étant basés sur une certaine forme d'optimisation. D'autres approches telles que l'Iterative Water Filling (IWF) [29], l'optimisation multi-objectifs (MOOP) [34], et le contrôle de puissance fractionnaire (FPC) [35] étaient utilisées dans certains de ces travaux.

Les scénarios multi-cellules ne sont guère mis en œuvre dans l'état de l'art. Cela s'explique principalement par l'augmentation exponentielle de la complexité qu'entraîneraient l'étude et la simulation de tels scénarios. En outre, l'existence d'interférences intercellulaires complique davantage la preuve de faisabilité et des avantages des communications sans-fil full-duplex. Comme nous le montrons plus loin dans notre travail, tous les scénarios multi-cellules ne produisent pas des gains par rapport aux communications half-duplex. Certains articles de l'état de l'art mettent en œuvre un modèle simpliste, comme dans [22], dans lequel des hypothèses irréalistes d'interférence intercellulaire sont faites. Le travail en [36] introduit le modèle multi-cellulaire le plus complet dans les travaux connexes. Les auteurs examinent des scénarios de cellules à l'intérieur et à l'extérieur et associent l'ordonnancement visant la maximisation de la somme des débits à un problème d'allocation optimale de puissance. Ils envisagent l'établissement d'un ordonnancement par cellule et l'attribution coordonnée de puissance.

Les technologies d'annulation d'auto-interférence sont une pierre angulaire des communications full-duplex. Certains articles de l'état de l'art supposent des conditions idéales [32] *i.e.,* les technologies disponibles sont capables d'annuler toute l'auto-interférence. Comme nous l'avons déjà dit, ce n'est pas tout à fait réaliste. D'autres modèles supposent des conditions quasi-idéales d'annulation du brouillage, où un petit facteur résiduel d'auto-interférence (Residual Self-Interference en anglais, RSI) est ajouté au calcul du SINR en tant que bruit. Une autre approche pour modéliser l'effet de l'auto-interférence consiste à utiliser un modèle RSI [24], où le RSI suit une fonction probabiliste telle qu'une loi gaussienne. Comme pour notre travail, la majorité des articles examinés utilisent un ensemble de facteurs d'annulation

d'interférence pour déterminer l'RSI. Dans les limites supérieures de 120 à 130 dB, ces hypothèses restent admissibles.

Table C.1 L'état de l'art en full-duplex

Publication	Type de Réseau	Ordonnancement		Allocation de Puissance		Spécifications des Cellules		
		Objectif	Q-Aware	Centralisé	Distribué	Multi-Cell	Taille (R)	SIC
Sarret *et al.*[22]	BS/UEs full-duplex	Max TP	✓	×	×	✓	Petite	Idéal
Cirik *et al.*[26]	OFDMA	Max SR	×	✓	×	×	40 m	70-110 dB
Song *et al.*[23]	BS/UEs full-duplex	Max SR	×	×	×	×	-	-
Da Silva *et al.* [28]	BS full-duplex	Max SE	×	✓	×	×	100 m	110 dB
Gao *et al.* [33]	MIMO Relay	Max TP	×	×	×	×	-	-
Sun *et al.* [34]	MU-MIMO	-	×	✓	×	×	250 m	80 dB
Tehrani *et al.*[30]	OFDMA	Max SR	×	✓	×	×	20-1000 m	130 dB
Di *et al.*[31]	OFDMA	Max SR	×	✓	×	×	-	100 dB
Nam *et al.* [32]	OFDMA	Max SR	×	✓	×	×	1 km	Idéal
Sun *et al.* [37]	MC-NOMA	Max SR	×	✓	×	×	600 m	110 dB
Goyal *et al.* [36]	BS full-duplex	Max $\log(R)$	×	✓	✓	✓	Petite	Modèle RSI
Marasevic *et al.* [24]	BS/UEs full-duplex	Max SR	×	-	-	×	×	Modèle RSI
Nam *et al.* [29]	OFDMA	Max SR	×	✓	×	×	500 m	Quasiment idéal
Liu *et al.* [38]	OFDMA	Max TP	×	×	×	×	500 m	Quasiment idéal
Park *et al.* [39]	BS full-duplex	Max SE	×	✓	×	×	100 m	Modèle RSI
Al-Imari *et al.* [40]	OFDMA	Max SR	×	✓	×	×	200 m	85 dB
Tran *et al.* [41]	OFDMA	Max SR	×	✓	×	×	250 m	120 dB
Wu *et al.* [42]	BS full-duplex	Max SR	×	✓	×	×	150 m	Modèle RSI
Shaikh *et al.* [35]	Hybrid BS	-	×	✓	×	×	Petite	Idéal
Zhang *et al.* [43]	OFDMA	Max-Min	-	✓	×	Het-Net	100 m	110 dB
Our Proposal	full-duplex BS	Multiple	✓	✓	✓	✓	Multiple	110 dB

C.2 Ordonnancement dans les réseaux sans-fil full-duplex avec CSI complète

Dans ce chapitre de thèse, nous avons présenté un algorithme mathématique optimal pour l'ordonnancement dans les réseaux sans-fil full-duplex et hybrides full-duplex/half-duplex. Notre problème d'optimisation générique tient compte des files d'attente et relève les nouveaux défis qui découlent de l'utilisation de réseaux sans-fil full-duplex : l'auto-interférence et l'interférence intra-cellulaire co-canal. Nous appliquons cette optimisation avec différents objectifs d'ordonnancement, en nous attaquant à des problèmes tels que la maximisation du SINR et l'équité entre les utilisateurs. En conséquence, nous proposons d'abord un algorithme d'ordonnancement Max-SINR full-duplex optimal et un algorithme d'ordonnancement Proportional Fair full-duplex optimal. De plus, et puisque les communications full-duplex ne sont pas toujours rentables, nous avons introduit un algorithme d'ordonnancement Max-SINR hybride optimal et un algorithme d'ordonnancement Proportional Fair optimal. Ces algorithmes commutent entre les transmissions full-duplex et half-duplex, afin d'améliorer les performances du réseau. De plus, pour éviter d'éventuels problèmes d'insolubilité avec les problèmes d'optimisation, nous avons proposé des versions heuristiques de nos algorithmes. Nous évaluons la performance de nos propositions heuristiques dans de multiples scénarios d'ordonnancement difficiles et montrons qu'elles donnent des résultats quasi optimaux. Enfin, par rapport à leurs homologues half-duplex, nous avons montré que les communications

full-duplex peuvent plus que doubler le débit du terminal mobile, tout en réduisant de moitié le délai d'attente.

C.3 Ordonnancement dans les réseaux sans-fil full-duplex sans CSI complète

Dans le chapitre 3 de la thèse, nous avons présenté notre approche de l'ordonnancement dans les réseaux sans-fil full-duplex en présence d'informations complètes sur l'état des canaux. Néanmoins, il n'existe toujours pas de moyens évidents permettant aux réseaux full-duplex d'atteindre cet état d'exhaustivité. Après tout, aucun protocole de réseau sans-fil existant n'est pris en compte pour estimer les canaux interutilisateurs ou pour déterminer comment l'information sur ces canaux pourrait être relayée à la station de base. Afin d'allouer correctement les ressources entre les paires d'équipements utilisateurs de liaison montante et descendante, le réseau a besoin d'informations exactes sur les canaux entre tous les UE, en plus de tous les canaux half-duplex traditionnels UE vers BS. Dans un réseau unique de femto cellules composé de cinq UE de liaison montante et de cinq UE de liaison descendante, la station de base devrait être continuellement mise à jour avec des informations sur un maximum de 35 canaux radio. Dix d'entre eux sont de type UE-to-BS et 25 de type UE-to-UE. Un nombre qui augmenterait considérablement dans les scénarios de macro cellules. Étant donné que l'ordonnancement se fait sur une petite échelle de temps (ms), l'ordonnancement avec CSI complet est rendu encore plus complexe par une surcharge de signalisation qui alourdit encore plus les équipements d'utilisateur. Dans ce chapitre, nous avons abordé les conséquences de l'ordonnancement dans des réseaux sans-fil full-duplex avec CSI incomplet, puis nous avons proposé un algorithme d'ordonnancement par apprentissage par renforcement qui peut allouer des ressources radio sans avoir besoin de telles informations. De plus, nous avons détaillé les principaux défis auxquels fait face une proposition d'ordonnancement par machine learning, en nous concentrant sur les effets du trafic de mémoire vide et des conditions radio dynamiques sur la performance de l'algorithme. Nous avons testé notre proposition dans de multiples scénarios d'ordonnancement allant du trafic UE aléatoire, au clustering des UE et en présence d'un faible SIC. Alors que le regroupement des terminaux dégrade les performances des UE de liaison descendante et des UE de liaison montante, nous avons illustré que notre proposition par apprentissage fonctionne toujours bien en termes de débit des terminaux et de réseau. Par conséquent, nous avons vérifié la validité de notre algorithme sans égard aux obstacles auxquels se heurte la tâche d'ordonnancement.

C.4 Allocation centralisée de puissance

Dans le chapitre 5 de la thèse, nous avons proposé une approche centralisée optimale de l'ordonnancement et de l'allocation de puissance dans les réseaux sans-fil full-duplex. Nous voulions utiliser l'allocation

de puissance parallèlement à l'ordonnancement pour surmonter les problèmes d'interférence générés par les communications sans-fil full-duplex. Étant donné que le brouillage co-canal et l'auto-interférence sont tous deux liés aux puissances de la liaison montante et de la liaison descendante, respectivement, l'attribution de puissance peut jouer un rôle important pour atténuer ces interférences. Dans cette approche centralisée, une unité centrale, $i.e.$, la station de base est supposée avoir toutes les informations nécessaires pour allouer puissance sur les ressources. Nous formulons un problème d'ordonnancement équitable et d'allocation de puissance pour les réseaux sans-fil full-duplex, en tenant compte des files d'attente. En raison de son insolubilité, nous décomposons ce problème en deux : un problème d'ordonnancement et un problème d'allocation de puissance. Nous comparons notre proposition à l'état de l'art et montrons qu'elle améliore l'équité entre les terminaux mobiles, et ce, sans impact négatif sur la performance du système.

C.5 Allocation décentralisée de puissance

Comme on l'a vu jusqu'à présent, et en raison de l'auto-interférence, les terminaux mobiles de liaison montante d'un réseau full-duplex subissent une dégradation des performances avec une augmentation de la puissance sur la liaison descendante. En outre, et en raison de la présence de brouillage intra-cellulaire co-canal, les terminaux mobiles de la liaison descendante du réseau subiraient une dégradation des performances en raison d'une augmentation de la puissance sur la liaison montante. Les équipements utilisateurs sur la liaison montante et la station de base sur la liaison descendante sont des concurrents aux objectifs contradictoires. Cela rend une approche egoiste de la théorie des jeux parfaitement adapté à l'allocation de puissance dans les réseaux sans-fil full-duplex. Dans ce chapitre de la thèse, nous avons proposé trois jeux non coopératifs pour aider à s'attaquer à la tâche complexe de l'allocation de puissance aux paires d'équipements d'utilisateur programmées, avec des objectifs allant de l'amélioration des performances des utilisateurs à la réduction des dépenses en énergie. Les jeux ont deux groupes de joueurs : les utilisateurs sur la liaison montante et la station de base sur la liaison descendante. Nous utilisons une classe spéciale de jeux, connus sous le nom de jeux super-modulaires, pour créer des utilités différentes avec des objectifs différents. En s'aidant un ensemble de simulations exhaustives, nous avons évalué l'importance de l'allocation de puissance dans les réseaux full-duplex, et déterminé ses gains et ses limites.

C.6 Ordonnancement et allocation de puissance dans les réseaux sans-fil multicellulaire

Dans ce chapitre de la thèse, nous avons exploré les défis de l'ordonnancement et de l'allocation de puissance dans le contexte des réseaux sans-fil full-duplex multicellulaires. Il s'agit d'un cadre plus réaliste que le scénario à cellule unique, et il envisage mieux la façon dont les communications

sans-fil en full-duplex pourraient être mises en œuvre. Nous avons proposé un problème optimal d'ordonnancement conjointe et d'allocation de puissance pour les réseaux sans-fil full-duplex. En raison de son insolubilité mathématique, nous avons découplé le problème et résolu d'abord le problème de l'ordonnancement, puis celui de l'attribution de la puissance. Nous avons examiné des scénarios de déploiement à l'intérieur et à l'extérieur et nous avons montré que les avantages des réseaux sans-fil full-duplex multicellulaires, par rapport à leurs équivalents half-duplex, sont situationnels. En outre, nous avons souligné l'importance de la coopération intercellulaire en matière d'ordonnancement des ressources et montré que, selon le scénario à l'étude, l'atténuation des interférences dues à la coopération intercellulaire peut améliorer les performances des équipements utilisateurs en termes de débit. Enfin, nous avons montré que l'allocation de puissance peut améliorer le rendement de l'UE, son efficacité étant liée au scénario de déploiement.

C.7 Conclusion

Avec la demande sans cesse croissante de connexions réseau sans-fil plus rapides, plus fortes et de meilleure qualité, les communications sans-fil full-duplex ont les moyens de devenir la prochaine grande percée en télécommunications. Dans cette thèse, nous avons exploré les gains possibles des communications sans-fil full-duplex par rapport à la technologie half-duplex actuelle en place. Nous avons proposé plusieurs algorithmes d'ordonnancement gourmands et équitables ainsi que des approches centralisées et décentralisées de la gestion de puissance. En général, nous avons présenté une étude complète de l'ordonnancement et de l'allocation de puissance dans les réseaux sans-fil full-duplex, alors que nous cherchions à combler les lacunes de l'état de l'art si nécessaire.

Dans notre travail, nous avons considéré un réseau sans-fil full-duplex où la station de base est compatible full-duplex et les terminaux mobiles restent half-duplex. Notre objectif était d'éviter que la complexité de la mise en œuvre des technologies full-duplex n'atteigne les terminaux des utilisateurs. Nous avons commencé notre travail au chapitre 3, où nous avons proposé des problèmes globaux optimaux pour l'ordonnancement dans les réseaux sans-fil full-duplex et hybride full-duplex et half-duplex. En utilisant ce problème global, nous avons présenté des algorithmes d'ordonnancement gourmands basés sur l'ordonnancement Max-SINR traditionnel, et des algorithmes d'ordonnancement équitable basés sur l'ordonnancement proportionnel équitable traditionnel. Nous avons montré que, par rapport à leurs homologues half-duplex, les communications en full-duplex permettent d'atteindre des valeurs de débit presque deux fois plus élevées. Les schémas actuels d'allocation des ressources radio, conçus pour les réseaux half-duplex, bénéficient de canaux de liaison descendante et montante orthogonaux qui peuvent être optimisés indépendamment. En revanche, dans le contexte des communications sans-fil en full-duplex, l'optimisation de la programmation et de l'attribution de puissance doit se faire conjointement pour la liaison montante et la liaison descendante en raison du concept de couplage et des interférences en full-duplex produites. Par conséquent, il n'a pas été possible d'appliquer les algorithmes traditionnels d'ordonnancement half-duplex ou d'allocation de

puissance aux réseaux full-duplex d'une manière simple et directe.

Au chapitre 4, nous avons évalué l'importance de l'information complète sur l'état des canaux pour extraire les gains des réseaux sans-fil full-duplex. Plus précisément, nous nous sommes concentrés sur les canaux inter-UE. Aucun protocole de réseau sans-fil actuel ne compte pour de tels canaux et on s'attend à ce que leur estimation constitue un obstacle à la mise en œuvre pratique de réseaux sans-fil en full-duplex. Après avoir démontré qu'une information partielle sur les canaux inter-UE est suffisante pour réaliser des gains significatifs avec les communications sans-fil full-duplex, nous avons proposé une approche d'apprentissage par renforcement de l'ordonnancement capable d'apprendre comment allouer au mieux les ressources sans aucune information sur les canaux inter-UE. Nous avons montré que notre proposition peut faire correspondre une ordonnancement gloutonnes avec un CSI complet à un coût de 10 % ou moins en termes d'efficacité réseau totale.

En ce qui concerne l'attribution de puissance, nous avons proposé au chapitre 5 une approche centralisée et optimale de la programmation et de l'attribution de puissance dans les réseaux sans-fil full-duplex. Notre approche de la tâche conjointe était axée sur l'équité et a introduit une priorité de paire basée sur les performances actuelles et historiques de l'UE. Comme le problème de l'optimisation commune était mathématiquement insoluble, nous avons séparé le problème en deux et l'avons résolu pour l'ordonnancement et l'allocation de puissance indépendamment. Nous avons montré par des simulations que notre proposition améliore les performances de l'UE et permet d'économiser sur les dépenses de puissance, où environ 50 % des UE de liaison montante du réseau sont transmis à des niveaux de puissance inférieurs au maximum disponible.

Au chapitre 6, nous avons proposé une approche distribuée d'allocation de puissance. Ce dernier était basé sur la théorie des jeux. Nous avons utilisé la théorie des jeux non coopératifs pour modéliser l'allocation de puissance comme un jeu super-modulaire avec les BS et les UE comme joueurs concurrents. Nous avons proposé de multiples jeux avec des objectifs allant de la maximisation du SINR de l'UE à l'amélioration de l'efficacité énergétique du réseau, et avons ensuite montré que la pertinence de chacune de nos propositions dépend du scénario à l'étude.

Au chapitre 7, nous avons abordé l'ordonnancement et l'allocation de puissance dans un réseau sans-fil full-duplex à cellules multiples. Nous avons examiné des scénarios de déploiement à l'intérieur et à l'extérieur et avons montré que les avantages des communications sans-fil full-duplex, par rapport à leurs homologues half-duplex, dépendront des utilitaires de réduction des interférences disponibles. Nous avons étudié les effets de la coopération cellulaire sur les performances de l'UE et montré que, selon le scénario du réseau, des gains allant jusqu'à 43 % - en termes de débit cellulaire - peuvent être réalisés à partir de ce dernier.

C.8 Perspectives

Dans cette section, nous abordons les multiples perspectives de la gestion des ressources radio dans les réseaux sans-fil full-duplex. Plus précisément, nous discutons des propositions sur la façon dont

les canaux inter-UE pourraient être estimés et explorons les axes concernant les différents scénarios d'appariement UE dans les réseaux sans-fil full-duplex.

C.8.1 Estimation des canaux inter-UE

Tel que discuté dans cette thèse, l'estimation des canaux inter-UE est une exigence supplémentaire dans le contexte des communications sans-fil full-duplex. L'ordonnanceur a besoin d'informations sur tous les canaux UE-UE afin d'allouer efficacement les ressources et de maximiser les gains en full-duplex. Toutefois, aucun protocole de réseau sans-fil actuel ne permet de relayer ces informations de canal des équipements d'utilisateur à la station de base. Dans le chapitre 4 de la thèse, nous avons introduit une approche d'apprentissage de renforcement de l'ordonnancement afin de contourner le besoin d'une telle information de canal inter-UE. Néanmoins, l'estimation de ces canaux permettrait une allocation optimale des ressources radio. Les auteurs de [36] et d'autres auteurs de l'état de la technique suggèrent d'utiliser des signaux de référence de sondage (SRS) pour estimer ces informations. Après la mise en œuvre de la découverte du voisin dans les UE pour déterminer les brouilleurs les plus puissants, le SRS de la liaison montante peut être utilisé par les UE pour estimer les canaux vers ces brouilleurs. Bien qu'une telle approche puisse effectivement être fonctionnelle, il serait toujours difficile de faire la distinction entre les différents UE du SRS, ce qui entraînerait des complexités supplémentaires. De plus, le fait de n'identifier que les interférences les plus fortes pourrait ne pas être une approximation suffisante. Quoi qu'il en soit, une estimation partielle des canaux inter-UE pourrait suffire à extraire des gains par rapport à la programmation traditionnelle en half-duplex, mais ces gains ne seraient pas aussi évidents si on les compare à la technologie MIMO en half-duplex et autres technologies de multiplexage.

C.8.2 Association de paire dans les réseaux full-duplex multicellulaire

Au cours de nos travaux sur les réseaux sans-fil full-duplex multicellulaire, nous avons évalué l'importance de l'association de paires. L'idée était qu'au lieu de l'association des terminaux unique actuelle, qui associe habituellement chaque UE à la station de base la plus proche, nous mettions en place une association de paires, dans laquelle les paires des terminaux de liaison montante et descendante sont associées aux stations de base où elles fonctionnent le mieux. Ce scénario est illustré dans la figure 8.2 ci-dessous, où la première paire, qui comprend un UE qui aurait autrement été associé à la station de base dans la deuxième cellule, est associée à la station de base dans la première.

L'ordonnanceur peut choisir de le faire si le brouillage co-canal entre les deux UE de cette paire est suffisamment faible pour générer de meilleures conditions radio pour l'ensemble de la paire lorsqu'elle est associée à la première station de base, bien que la deuxième station de base de la liaison descendante soit plus proche de la seconde. Nous avons évalué la performance d'un tel réseau et

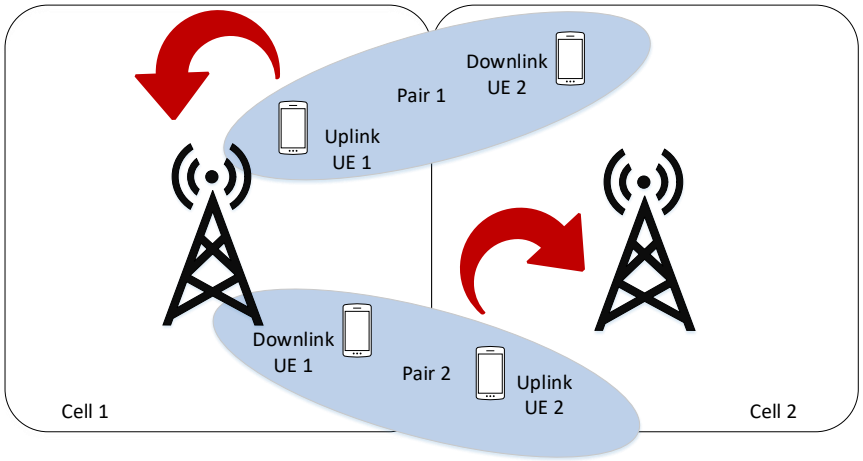

Figure C.2 Pair association in a multi-cell scenario

l'avons comparé au cas d'une association unique. Dans le cas où toutes les ressources sont utilisées dans des cellules adjacentes, une telle approche ne produit aucun gain. En fait, dans certaines de nos simulations, le coût total du réseau est calculé en fonction du débit total. Néanmoins, dans le cas où toutes les cellules brouilleuses immédiates n'utilisent pas les mêmes ressources fréquentielles, l'association de paires pourrait en fait améliorer les performances des réseaux full-duplex. Pour le deuxième scénario extérieur présenté dans le chapitre précédent, il est possible d'augmenter jusqu'à 10 % le débit total du réseau par association de paires.

Une autre approche intéressante de l'association des terminaux dans les réseaux sans-fil full-duplex consiste à découpler les UE de liaison montante et descendante et à les associer à une station de base différente. Dans ce cas, le premier UE sur la liaison montante et le second UE sur la liaison descendante (voir la Fig. C.2) seraient toujours appariés, mais chacun étant associé à une station de base différente. Avec chaque UE recevant ou transmettant de ou vers la station de base la plus proche, on peut s'attendre à ce que le SINR de chaque UE s'améliore. Néanmoins, une telle approche ne serait pas sans complications. Une unité centrale devrait être chargée de l'appariement et de l'ordonnancement. Au moins, il faudrait une signalisation aérienne importante.

C.9 Travaux Futurs

Alors que cette thèse tire à sa fin, notre travail sur la communication sans-fil full-duplex se poursuit. Nous avons l'intention d'explorer ce qui suit :

1. Au chapitre 4, nous avons introduit une approche par apprentissage par renforcement de l'ordonnan-cement dans les réseaux sans-fil full-duplex. Il serait intéressant d'adapter cet algorithme dans un contexte multicellulaire. Dans la pratique, peu de changements seraient nécessaires. L'algorithme continuerait d'allouer des ressources à des paires des terminaux en fonction de probabilités choisies, puis mettrait à jour les probabilités d'allocation en fonction

du nombre de bits transmis et reçus par les paires des terminaux sur les ressources radio qui leur ont été attribuées. Un autre avantage de l'approche d'apprentissage dans un contexte multicellulaire est que non seulement elle n'exigerait pas d'information sur les canaux inter-UE, mais elle n'exigerait pas non plus une connaissance des brouilleurs intercellulaires des UE. Il reste à évaluer la rapidité et l'efficacité avec lesquelles l'algorithme peut allouer les ressources radio et si cela entraînerait un coût élevé en termes de débit total du réseau.

2. Au chapitre 6, nous avons utilisé la théorie des jeux pour l'allocation de puissance dans les réseaux sans-fil full-duplex. Dans [40], les auteurs ont utilisé la théorie des jeux pour l'allocation des ressources radio dans les réseaux sans-fil full-duplex et ont mis en œuvre un algorithme IWF pour l'allocation de puissance. Une idée intéressante est d'utiliser la théorie des jeux pour décider conjointement de l'ordonnancement des ressources radio et leur allocation de puissance. Traditionnellement, le fait d'aborder conjointement l'ordonnancement et l'allocation de puissance entraîne des problèmes insolubles sur le plan mathématique. Cependant, la théorie des jeux non coopératifs peut être utilisée pour traiter à la fois l'ordonnancement et l'allocation de puissance. Le principal défi consisterait à identifier les joueurs des jeux conçus pour la programmation et l'allocation de puissance. Dans le cas de l'allocation de puissance, il était logique que les UE sur la liaison montante et les stations de base sur la liaison descendante soient des acteurs concurrents. Après tout, l'augmentation de la puissance sur la liaison montante dégrade la performance des équipements d'utilisateur sur la liaison descendante et vice-versa. Néanmoins, ceci n'est pas valable pour l'ordonnancement des ressources radio. Les UE de liaison montante et descendante sont appariés sur des ressources partagées. Dans ce cas, ils ne sont plus des concurrents. L'une des approches consiste à opposer les UE de liaison montante aux UE de liaison montante et les UE de liaison descendante aux UE de liaison descendante. La fin du jeu consisterait à sélectionner les UE de liaison montante et descendante présentant les meilleures conditions radio sur chaque ressources radio et à les coupler entre eux. Toutefois, l'UE la plus performante de liaison montante et l'UE la plus performante de liaison descendante peuvent ne pas toujours former un bon couple. Par exemple, ils pourraient être situés à proximité l'un de l'autre, ce qui entraînerait une dégradation des performances pour les équipements d'utilisateur de liaison descendante. Une autre approche consisterait à dresser la liste de tous les appariements UE possibles en tant que joueurs du jeu d'ordonnancement. Le jeu d'ordonnancement se jouerait alors entre les paires des terminaux pour décider quelles paires obtiennent quelles ressources radio. Par la suite, un jeu d'allocation de puissance, semblable à nos propositions, peut être utilisé pour allocation du puissance aux UE prévues.

3. Dans le contexte des réseaux multicellulaires présentés au chapitre 7, une approche distribuée de l'allocation de puissance présente un défi et une approche intéressante. Dans notre proposition, une unité centrale décide comment allouer puissance sur tous les ressources radio programmés pour l'ensemble du système en un seul coup. Comme pour toutes les approches centralisées,

on s'attend à ce que cela entraîne une charge de signalisation et de traitement. Une autre solution consiste à suivre une approche itérative allocation de puissance. Chaque station de base résoudrait individuellement le problème d'allocation de puissance et les stations de base le résoudraient à tour de rôle sur la base des résultats de leurs homologues, jusqu'à ce qu'une convergence soit atteinte. Un critère d'arrêt $par\ exemple$, lorsque le débit total du réseau ne s'améliore plus, pourrait être nécessaire.

Enfin, lorsque nos travaux sur les communications sans-fil en full-duplex ont commencé en 2016, les espoirs d'inclusion de la 5G étaient grands. La recherche dans le domaine a connu un essor considérable et d'innombrables approches de la gestion des ressources radio dans divers scénarios de mise en œuvre en full-duplex ont vu le jour. Néanmoins, l'année dernière, avec la publication de la version 15 du 3GPP 5G, il était évident que les opérateurs n'étaient pas aussi enthousiastes à l'idée de communications sans-fil full-duplex. De nos jours, on parle de communications sans-fil full-duplex dans le contexte de 6G [76] avec de faibles espoirs d'introduction dans la version finale 5G en 2021. Il n'est pas certain que la 6G inclura effectivement le full-duplex, mais au moins une autre décennie de recherche ouvrira certainement la voie à une mise en œuvre pratique.